Vegetable Oil-based Polyols and Some Novel Analytical Techniques Used in Their Development

by

Mohammad Hossein Tavassoli Kafrani

A thesis submitted in partial fulfillment of the requirements for the degree of

Doctor of Philosophy
in
Food Science and Technology

Department of Agricultural, Food and Nutritional Science
University of Alberta

Abstract

This thesis first describes the development of novel analytical methods for use in lipid transformations. It continues with the synthesis of vegetable oil-based polyols with high hydroxyl value (OHV) and low viscosity, an example of a lipid transformation. Vegetable oils are amenable to transformation into the monomers, such as polyols, which can be used for the synthesis of polyurethanes or other polymers. The use of rapid and reliable analytical methods for the measurement of critical parameters involve in lipid transformation can facilitate the development of lipid-based polyols.

Analytical methods using FTIR were developed for the determination of OHV of polyols, moisture content of vegetable oils, and to monitor the epoxidation of vegetable oils. The stoichiometric reaction of toluenesulfonyl isocyanate (TSI) with hydroxyl groups was used to develop two FTIR methods for the determination of OHV of polyols. In addition to hydroxyl groups, water can also react with TSI generating CO_2 as a product, which has distinct absorbance in FTIR spectrum. The spectral absorption of the CO_2 was used to establish a rapid and simple FTIR method for the measurement of moisture content of vegetable oils. For monitoring the epoxidation of vegetable oils, the FTIR absorptions associated with the double bonds and oxirane groups were used to develop an attenuated total reflectance (ATR) FTIR method.

The ozonolysis of vegetable oils followed by hydrogenation is another chemical route to transform vegetable oils into polyols. In this thesis, a gas chromatography coupled with flame ionization detector (GC-FID) was employed to develop an analytical method for the measurement of nonanal and oleic acid (as indications of the ozonolysis progress) during the ozonolysis process.

Finally, a new route was explored for the synthesis of vegetable oil-based polyols with high OHV and relatively low viscosity. This approach involves the epoxidation of oils, transesterification by 1,3-propanediol, and finally ring opening of the oxirane groups by 1,3-propanediol.

Preface

This work was carried out between 2012 and 2016 in Lipid Chemistry Group (LCG) at university of Alberta under supervision of Prof. Jonathan Curtis. Chapters 2, 3, and 4, are collaborative works with Prof. Frederick van de Voort, a scientist visitor from McGill University IR group.

Chapter 2 has been published as "Tavassoli-Kafrani, M. H., Curtis, J. M., van de Voort, F. R. A primary method for the determination of hydroxyl value of polyols by Fourier transform mid-infrared spectroscopy. *Journal of American Oil Chemists' Society*. 2014, *91*, 925-933".

Chapter 3 has been published as "Tavassoli-Kafrani, M. H., Curtis, J. M., van de Voort, F. R. A single-sample method to determine the hydroxyl values of polyols using mid-FTIR spectroscopy. *European Journal of Lipid Science and Technology*. 2015, *117*, 65-72".

Chapter 4 has been published as a cover article in Analytica Chemica Acta "van de Voort, F. R., Tavassoli-Kafrani, M. H., and Curtis, M. J. Stoichiometric determination of moisture in edible oils by mid-FTIR spectroscopy. *Analytica Chimica Acta*. 2016, *918*, 1-7".

In these chapters, I was responsible for performing experiments, collecting and analyzing the data, and preparing the draft manuscripts. The experimental designs and further improvement of manuscripts were collaborative works with Prof. van de Voort. I was also supervised by Prof. Curtis and he assisted in manuscripts preparations and editions.

Chapter 5 has been submitted to *European Journal of lipid Science and Technology* as "Tavassoli-Kafrani, M. H., van de Voort, F. R., Curtis, J. M. The use of ATR-FTIR Spectroscopy to Measure Changes in the Oxirane Content and Iodine Value of Vegetable Oils during Epoxidation. 2016". In this work, I designed and performed experiments, collected and analyzed

the data, and prepared manuscript under supervision and assistance of Prof. Curtis. The manuscript was further edited by Prof. van de Voort before submission.

Chapter 6 was published as "Tavassoli-Kafrani, M. H., Foley, P., Kharraz, E., Curtis, J. M. Quantification of nonanal and oleic acid formed during the ozonolysis of vegetable oil free fatty acids or fatty acid methyl esters. *Journal of the American Oil Chemists' Society*. 2016, *93*, 303-310". In this work, I was responsible to design and perform experiments, collect and analyze data, and manuscript composition. Prof. Curtis supervised me and was involved in experimental designs and manuscript preparation. Mr. Ereddad Kharraz performed preliminary experiments related to the derivatization reaction. The derivatization reaction used in this work was the idea of Dr. Patrick Foley.

Chapter 7 has been partially used for a patent application as "Curtis, J. M., Omonov, T. S., Kharraz, E., Kong, X., Tavassoli-Kafrani, M. H., Method for polyol synthesis from triacylglyceride oils. U.S. Provisional Patent Application 62/183,982, Jun 24, 2015".

In the works presented in this Chapter, I was responsible for designing and performing experiments, collecting and analyzing data, and Chapter composition under supervision of Prof. Curtis. In this Chapter, the idea of performing transesterification with 1,3-propanediol on epoxidized oil was initially proposed by Dr. Omonov.

Dedication

I would like to dedicate this work to my love, my life, my wife, Nastaran and to my parents, Ali and Soraya, for all their supports and love. Love you all.

Acknowledgements

Almost four years has passed since I came here to Canada to begin my journey, and now I would take great pleasure to thank all those who have provided me with the opportunity to learn both in my academic and personal life. All these great experiences occurred because of these generous people:

I wish to extend my wholehearted thanks to my dear supervisor, Prof. Jonathan M. Curtis. I would like to express my sincere appreciations for accepting me as your student, teaching, and guiding me over these memorable years. Thanks for all of your kind efforts to edit and revise this thesis.

Also, similar profound gratitude goes to Prof. F. R. van de Voort for his invaluable pieces of advice and endless efforts to kindly teach and guide me over these years. I am so thankful to you for teaching me about the infrared spectroscopy and the development of analytical methods as well as helping to revise and edit papers.

I am so grateful to Prof. David Bressler and Dr. Lingyun Chen, members of my supervisory committee, for their insightful advice and suggestions.

Special thanks go to Alberta Innovates Technology Futures (AITF) and department of Agricultural, Food, and Nutritional Science (AFNS) for offering scholarships that significantly helped me to accomplish this work.

I am also highly appreciative to the special people in the lipid chemistry groups;

Dr. Xaiohua Kong for her warm encouragements and valuable advice over these years also for kindly teaching me about polymers. Dear Xaiohua, you helped me a lot and I am so thankful to you.

Mr. Ereddad Kharraz for his generous technical support and friendly discussions. I will not forget your help Ereddad. I would like to thank Dr. Tolibjon Omonov and Dr. Yuan Yuan Zhao for their kind help in the lab. My precious friends; Lisa, Siew, Magdalena, and Yiran for providing a friendly and warm environment in the lab and office, thank you so much.

To my compassionate friends in Edmonton; Mohsen, Ali, Reza, and their families who made my life more enjoyable in Edmonton. Thank you so much for creating such memorable events and moments.

To my love, Nastaran who is always my haven to gain harmony and confidence, words are too limited to express how much your companionship was important in my study. To my parents and my sisters for their endless supports in my life. Thank you all.

THANK YOU ALL

HOSSEIN

Table of Contents

List of Tables

List of Figures

List of Abbreviations and Symbols

1,3-PD	1,3-propanediol
AOCS	American oil chemist's society
ASTM	American society for testing and materials
ATR	Attenuated total reflectance
CNC	Cellulose nanocrystal
CO	Canola oil
CV	Coefficient of variation
DSC	Differential scanning calorimetry
EI	Electron ionization
EO	Epoxidized oil
ESI	Electrospray ionization
FAME	Fatty acid methyl ester
FFA	Free fatty acid
FID	Flame ionization detector
FTIR	Fourier Transform infrared
GC	Gas chromatography
GPC	Gel permeation chromatography

IR	Infrared
IV	Iodine value
MAG	Monoacylglycerol
MS	Mass Spectrometry
NMR	Nuclear magnetic resonance
OHV	Hydroxyl value
OOC	Oxirane oxygen content
PLS	Partial least squares
PU	Polyurethane
RE	Relative error
TAG	Triacylglycerol
T_g	Glass transition temperature
TOF	Time of flight
TSA	Toluenesulfonyl amide
TSI	p- Toluenesulfonyl isocyanate
ΔIV	Change in iodine value

CHAPTER 1

General Introduction

1.1 Vegetable Oils as Feedstock for Bio-based Polymers

Currently, most organic polymers are produced from intermediate chemicals derived from petroleum or natural gas [1]. Fossil fuel resources are non-renewable, being depleting rapidly, and probably start diminishing within one or two generations [2]. Furthermore, the utilization of these resources releases greenhouse gases such as carbon dioxide and methane into the atmosphere which contributes to global warming. Therefore, there is an increasing demand for the polymers derived from biobased renewable materials [3,4]. Renewable raw materials can be used for the preparation of a wide variety of monomers required for polymers synthesis therefore, the use of these raw materials can considerably contributes to the sustainable development [5], a term which is defined by the united nations as "*acting responsibly to meet the needs of the present without compromising the ability of future generations to meet their own needs*" [6]. Proteins, lignocellulosic materials, carbohydrates such as starch, fats and oils are the examples of these renewable materials. From these, vegetable oils are a promising and suitable feedstock for the production of biobased polymers as explained below [7-9].

Vegetable oils include approximately 80% of the total global production of fat and oils [10]. Unlike most proteins and carbohydrates are hydrophobic and thus, suitable for the production of hydrophobic polymers which complement hydrophilic biobased polymers derived from proteins and carbohydrates. Furthermore, they can be converted into monomers with similar structure to

petrochemical-based monomers. This makes possible to produce vegetable oil-based polymers with the same desired properties to petrochemical-based polymers. Vegetable oils can be precursors for producing various building blocks for the synthesis of various polymers such as polyurethane, polyether, polyester and polyolefin [11].

The chemical structure of vegetable oils consist of glycerol esterified with three fatty acids; commonly having 12 to 22 carbon atoms and 0 to 3 carbon-carbon double bonds [12]. These unsaturated moieties provide potential reaction sites to introduce variable functional groups such as epoxy, hydroxyl, and carbonyl groups [13,14]. In addition to the double bonds, ester groups, and allylic positions are other reactive sites in vegetable oils amenable to chemical reactions [11] (Figure 1-1). For example, the ester groups could be transesterified with alcohols or reduced to aldehydes or hydroxyl groups. Another example is the oxidation of allylic positions by singlet oxygen through 'ene' reaction. This reaction leads to the formation of allylic hydroperoxides which are then reduced into hydroxyl groups [15,16].

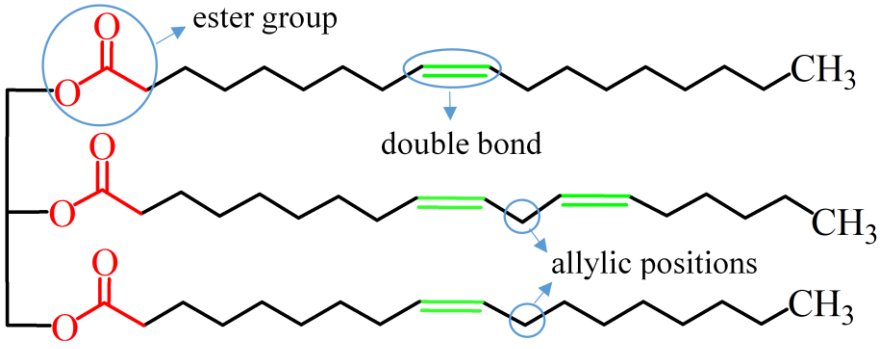

Figure 1-1 The structure of triglyceride and reactive sites.

1.2 Vegetable Oil-based Polyurethane

Polyurethane (PU) is one of the most important and versatile classes of polymeric materials with many diverse applications including in adhesives, coatings, rigid or flexible foams and sealants [17]. Polyurethanes are generally synthesized by the reaction of polyols (molecules containing two or more hydroxyl groups) with di- or polyisocyanate molecules (Eq. 1-1).

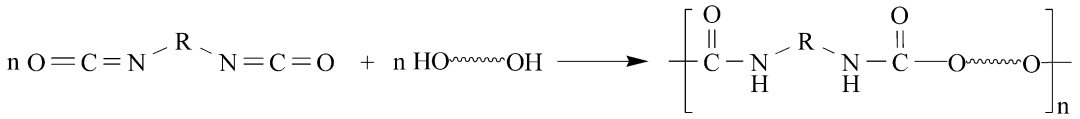

Eq. 1-1

There are few types of isocyanate compounds such as toluene diisocyanate (TDI), diphenylmethane diisocyanate (MDI), and polymeric diphenylmethane diisocyanate (PMDI) which are widely used in industry [18] therefore, the mechanical and thermal properties of the PUs greatly depend on the characteristics of the polyols [1].

The concentration of hydroxyl groups in polyols is an important parameter in making PUs. This parameter is defined as the hydroxyl value (OHV) or hydroxyl number (OHN) which is expressed as equivalent weight (mg) of potassium hydroxide for one gram sample (mgKOH/g). A higher OHV results in the formation of a PU with a higher cross-linkage density. This leads to a material with higher Young's modulus, glass transition temperature (T_g) and tensile strength [19,20]. In addition to the OHV, the positions of OH groups in polyol monomers, and the types of OH groups (primary or secondary) affect the properties of PUs. Location of hydroxyl groups at the middle of a fatty acid chain (Δ^9 or Δ^{10} and Δ^{12} or Δ^{13} carbon atoms) results in a dangling chain which is the part of the chain between end chain and the first hydroxyl group (Figure 1-2). These chains act as plasticizers in polymers and reduce the rigidity of the polymer [21]. Primary hydroxyl groups, compared to secondary ones, are ~3-3.3 times more reactive toward reaction with isocyanate [22] and because of this, the primary hydroxyl groups in polyols are often favorable in PUs synthesis.

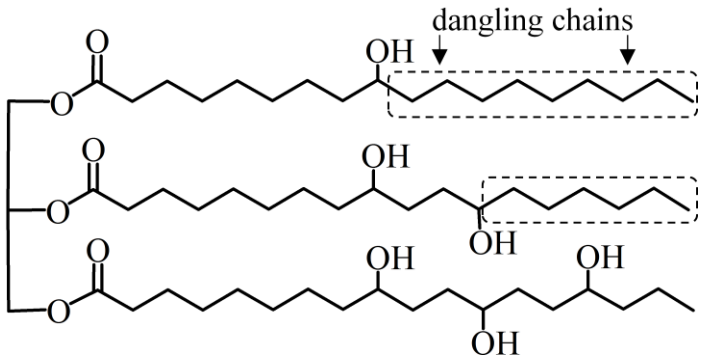

Figure 1-2 dangling chains in a vegetable oil-based polyol.

1.2.1 Vegetable Oil-based Polyol

Currently, most of the polyols used for the production of PUs are petrochemical-based but recently there is an intensive interest to find alternative biobased polyols particularly from vegetable oils [23-25]. In addition to fats and oils, other renewable materials such as lignocellulosic materials [26-28], proteins [29,30] and cardanol [31] have been also used to prepared PUs.

Vegetable oils, other than castor oil, lack hydroxyl groups. Therefore, to use them as polyol, hydroxyl groups are introduced into their structure [21]. There are several routes for the chemical transformation of vegetable oils into polyols with the most studied ones illustrated in Figure 1-3 [12]. Epoxidation of double bonds followed by ring opening [19,32], transesterification with diols or polyols [23,33], ozonolysis [34,35], hydroformylation [36], thiol-ene coupling reaction [37,38] and amidation [39,40] are the examples of such reactions. The carbon-carbon double bonds and ester groups are the two important reaction sites in vegetable oils which are used for the production of polyols [12].

1.2.1.1 Epoxidation and Ring Opening

Epoxidation of double bonds followed ring opening by proton donors is the most widely used route for the preparation of vegetable oil-based polyols [41]. In this route, vegetable oils can be epoxidized by a peracid generated *in situ* from the reaction of hydrogen peroxide and a carboxylic acid such as formic or acetic acids. The epoxidized vegetable oils rather than being used for polyol synthesis have several other applications such as reactive diluent [42], a plasticizer for polyvinyl chloride [43], and epoxy resin monomers [44].

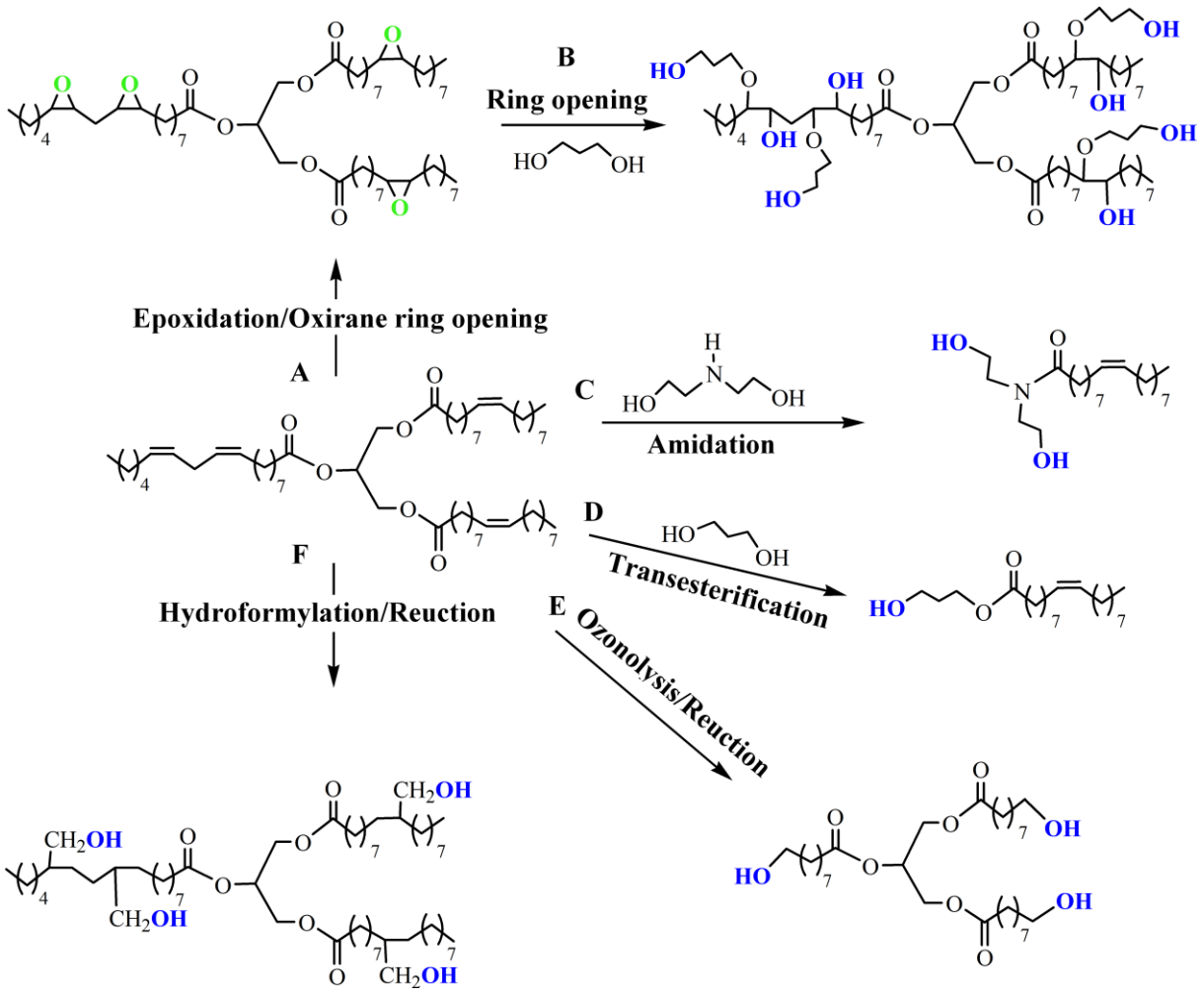

Figure 1-3 Common routes for the synthesis of polyols from vegetable oil.

Ring opening of epoxy groups (Figure 1-3B) can be performed by various proton donors such as water, alcohols, and acids. Water is the cheapest one and can open epoxy groups in the presence of acids such as formic acid, acetic acid, and perchloric acid [45,46] leading to the formation of two secondary hydroxyl groups per each epoxy group. Mono alcohols such as methanol, ethanol, n-propanol, n-butanol, and n-pentanol have also been used as ring opening reagents. Among these, methanol due to its lower price and favorable product is more popular [21]. Ring opening by these alcohols is performed in the presence of strong acids such as sulfuric acid [47-49] and results in the formation of one secondary hydroxyl group per epoxy group. In addition to mono alcohols, diols such as ethylene glycol and 1,3-propanediols can be also used to open epoxy groups. Ring opening by diols, compared to mono alcohols, has the advantage of introducing two hydroxyl groups per epoxy group. The downside is that oligomerization can take place when both hydroxyl groups present in a diol open epoxy groups. Oligomerization increases the viscosity and reduces the OHV of the resulting polyol [50] and hence is not favorable.

1.2.1.2 Transesterification/ Amidation

Transesterification and amidation of vegetable oils with diols and polyols are two other routes used in the synthesis of vegetable oil-based polyols (Figure 1-3C,D) [1]. Transesterification of vegetable oils with glycerol which results in the formation of monoglycerides is economically preferred because it can be performed in a single step process [51]. However, at high temperature, the glycerol in monoglycerides is degraded to an unsaturated compound by elimination of a water molecule. For this reason, glycerol have been replaced with more thermally stable polyols such as trimethylolpropane or pentaerythritol [52]. In the transesterification reaction, strong acids such as sulfuric acid, bases such as sodium or potassium methoxide and enzyme are used as catalysts. The efficiency of the transesterification reaction is affected by several conditions including the molar

ratio of alcohols/vegetable oil, type of catalyst, free fatty acid or water content and temperature [53].

Amidation of vegetable oils is usually performed with diethanolamine and leads to the formation of diethanol fatty amine (Figure 1-3C) [54]. Transesterification or amidation alone leads to the formation of fatty acid chains with fixed numbers of hydroxyl groups and relatively low OHV which is not favorable. Furthermore, these fatty acid chains with no hydroxyl groups in the middle (Figure 1-3C,D) act as dangling chains in PU network which reduce mechanical properties of the obtained PUs [24]. Transesterification and amidation of esters groups can be used in a combination with other reactions such as epoxidation and ring opening which are performed on double bonds. In this way, both double bonds and ester groups are used to introduce hydroxyl groups which increases OHV and reduces dangling chains of produced polyol [50].

1.2.1.3 Ozonolysis/ Reduction

The ozonolysis of vegetable oils is another route to produce polyols. Ozonolysis involves the efficient cleavage of double bonds present in fatty acids by ozone and leads to the formation of aldehyde groups, as one of the ozonolysis products, which can be reduced to primary terminal OH groups (Figure 1-3E) [34]. Polyols obtained by this method could have maximum three hydroxyl groups per molecule [11]. However, the advantage of this method is that it yields primary OH groups which are more reactive toward isocyanate compared to secondary OH groups. Furthermore, fatty acid chains with double bonds are shortened by ozone and hence no dangling chains in the resulting PUs (Figure 1-3E) [55].

1.2.1.4 Hydroformylation/ Reduction

Vegetable oil can be converted into polyols through hydroformylation/reduction route. In this route, hydroxymethyl groups are introduced into fatty acid chains at double bond positions in a two steps process. In the first step, double bonds are converted into aldehyde groups by syngas (a mixture of carbon monoxide and hydrogen) in the presence of a catalyst such as cobalt and in the second step, the aldehyde groups are reduced by hydrogen to yield hydroxyl groups [36]. In this method, each double bond can give one hydroxyl group therefore the number of hydroxyl groups in polyols obtained using this method depends on the number of double bonds present in the initial fatty acids. In this route, catalyst must be fully recovered in order to make this route commercially practical. Hydroformylation/reduction similar to the ozonolysis/ reduction, yields primary hydroxyl groups but unlike ozonolysis, these hydroxyl groups are located in side chains rather than terminal (Figure 1-3F).

1.2.2 Measurement of Critical Parameters Involved in Polyol Synthesis

In order to achieve a product with expected desired properties or develop new products, it is important to measure, monitor and control the critical parameters over the course of each process step. In this thesis, vegetable oils were transformed into polyols through epoxidation/ ring opening procedure and analytical methods were developed to measure some of the critical parameters involve in this procedure (Figure 1-4).

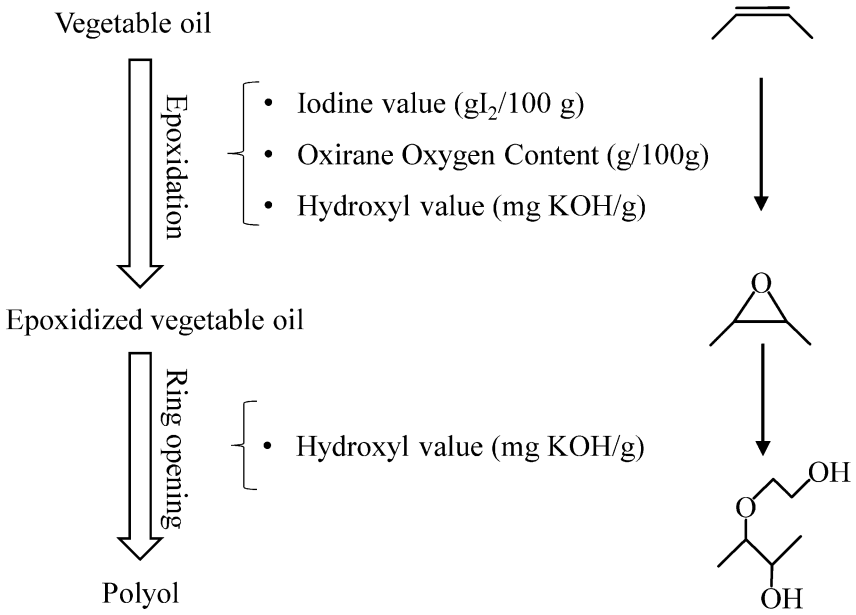

Figure 1-4 some of the critical parameters involve in the preparation of vegetable oil-based polyol through epoxidation and ring opening (by 1,3-propanediol). For simplicity, the epoxidation and ring opening are shown only for one double bond.

Efficient and powerful analytical methods for the measurement of these critical parameters are essential and could facilitate the optimization of the process and the development of new products.

1.2.2.1 Hydroxyl Value (OHV)

As mentioned earlier, the OHV of a polyol is an important parameter which dictate the properties of the corresponding PUs therefore, it should be known prior to making PU. In addition to the OHV of polyols, it is useful to know the OHV of epoxidized oil prior to the hydroxylation (Ring opening) step in the epoxidation-ring opening route. In epoxidation reaction, side reactions such as ring opening by water can occur. This results in a formation of secondary hydroxyl groups and a decrease in oxirane oxygen content (OOC) of the epoxidized oil. Therefore, measurement of the OHV of an epoxidized oil can give an estimation of such side reactions.

In the ring opening step, particularly in the case of ring opening by diols, the oligomerization and polymerization reactions occur at longer reaction times and decrease the OHV of the polyol obtained. Therefore, it is also desirable to measure the OHV over the course of the ring opening step reaction so that the reaction can be stopped after the optimum time (i.e., maximum OHV).

1.2.2.2 Oxirane Oxygen Content (OOC) and Iodine Value (IV)

The concentration of double bonds in vegetable oils is expressed as the iodine value (IV) which is defined as weight of iodine (g) absorbed by 100g oil. Similarly, the oxirane oxygen content (OOC) is defined as the weight of oxirane oxygen (g) in 100g oil. In the epoxidation reaction, double bonds are converted into oxirane groups (Figure 1-4). Therefore, it is useful to measure the changes in IV (ΔIV) and OOC (ΔOOC) over the course of the epoxidation process because it can give an indication about the conversion of double bonds into the oxirane groups. Furthermore, in order to obtain a product with the maximum OOC, the reaction must be stopped once it reaches the maximum OOC, since after that, the OOC reduces as a result of side reactions.

1.2.2.3 Water Content

Water content of a polyol is another important parameter which should be measured prior to making PU. Water present in the polyol reacts with isocyanate groups and produces carbon dioxide, which results in the formation of bubbles in PU. A water content in the range of 0.05 to 0.1% is acceptable for the majority of the polyols [56].

Water content of vegetable oils and their epoxidized oils is also an important parameter in some reactions. For example, when sodium methoxide is used as a catalyst for the transesterification of vegetable oils or epoxidized vegetable oils, the presence of water results in

the formation of soap. Also, in the ring opening step, water present in the epoxidized oil can act as a ring opening agent which results in the formation of secondary OH groups. Therefore, it is useful to measure the water content before the transesterification and ring opening reactions.

1.3 Fourier Transform Infrared Spectroscopy (FTIR)

Many current methods for the measurement of the above parameters (water content, OHV, OOC, IV) are time consuming and/or have special chemical or solvent requirements. The development of rapid and reliable methods for their measurement would facilitate the development and subsequent production and as well as quality control of polyols made from vegetable oils. Fourier Transform infrared spectroscopy (FTIR) is a suitable tool for the rapid analysis of lipids and their derivatives, as explained below.

The use of infrared spectroscopy in lipid analysis was popular between 1945 and 1965. After 1965, interest was diminished as the result of the development of new techniques such as gas chromatography and nuclear magnetic resonance spectroscopy (NMR). However, in the mid-1970s Fourier transform infrared spectroscopy (FTIR) was developed and became important in quantitative analysis [57]. Over the past two decades, the FTIR spectroscopy has gained attention for quantitative and qualitative analyses, especially in the lipids area since it is a non-destructive and rapid technique which usually requires minimum sample preparation. The infrared region covers the electromagnetic spectrum with the wavenumber between 14000 to 50 cm^{-1} and can be divided into three categories; Far-infrared from 400-50 cm^{-1}, Mid-infrared (MIR) from 4000 to 400 cm^{-1} and Near-infrared (NIR) from 14000 to 4000 cm^{-1}.

The NIR regions exhibit three weak and broad overlapping bands which are associated with the C-H overtones and combinations of vibrational modes [57]. Therefore, associating IR frequencies to the specific chemical group is difficult and usually very robust calibrations are

required for NIR data analysis. The development of these calibrations is laborious and often involves applying chemometrics and multivariable statistical techniques such as partial least squares (PLS) [58]. NIR radiation penetrates a sample more than MIR radiation and NIR bands are approximately 10-100 times less intense than MIR. These allow to use near-FTIR for direct analysis of porous samples. Also, due to relatively weak absorptions of water in NIR region, near-FTIR is suitable for the analysis of high-moisture samples [58].

Unlike the NIR, the mid-FTIR spectrum are usually comprised of resolved or partially resolved narrower bands associated with the vibration of particular functional groups present in the sample (Figure 1-5). Therefore, calibration of the mid-FTIR is generally simpler. However, the chemometric analysis may still be needed where there are overlaps in the IR absorbances. The intensity of an IR absorption in the spectrum is proportional to the concentration of the corresponding functional group in the sample. This adherence to Beer's law allows to use IR spectra in quantitative analyzes [59]. Although, both near [60-63] and mid-FTIR have been used for the analysis of edible oils, the focus here is the applications of mid-FTIR in vegetable oil analyses.

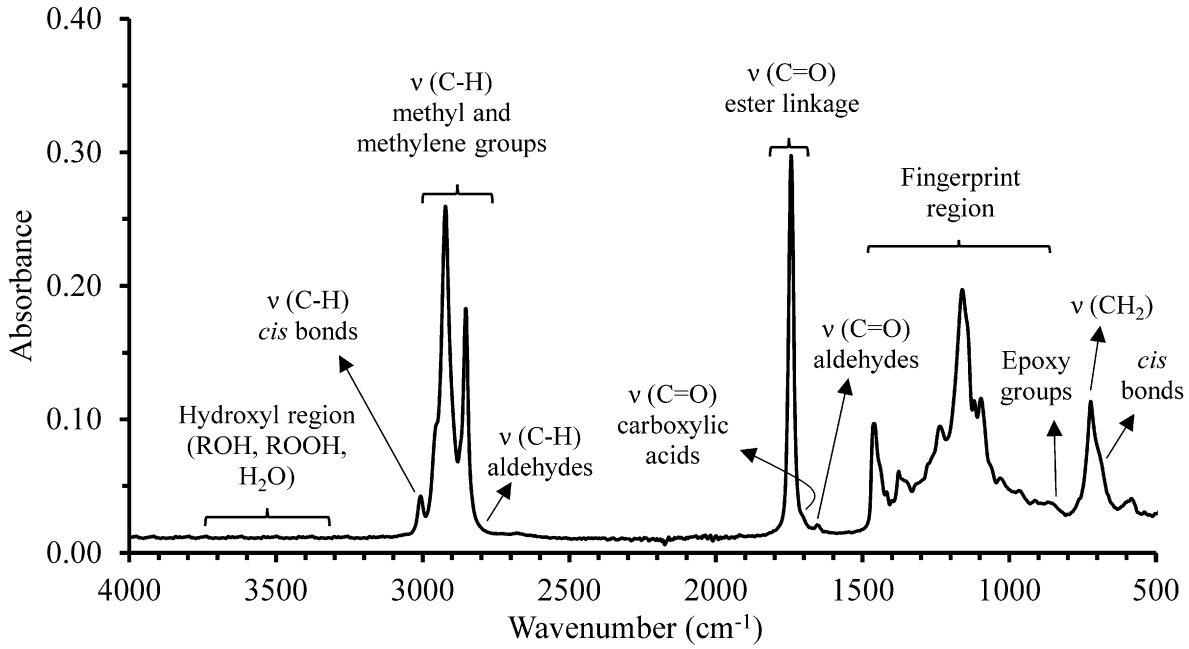

Figure 1-5 The IR spectrum of canola oil obtained by mid-FTIR indicating the absorptions associated to specific functional groups.

Mid-FTIR has been used for the quantitative determination of various parameters in vegetable oil such as iodine value [64,65], peroxide value [66], free fatty acid and *trans* content [65,67,68], phenolic content [69], phospholipids content [70], and water content [69,71]. These methods are based on the measurements of the absorption/s that are directly associated with the target compounds. Another approach for the development of quantitative FTIR methods is to use stoichiometric reactions, where the analyte reacts with a chemical reagent to produce more specific and intense absorptions in the IR spectrum [72-75]. Although this approach requires a chemical reaction step, it can provide some advantages. In particular, by choosing a stoichiometric reaction which produces signals in the FTIR regions in which few functional groups show absorptions (e. g., regions between 2700 and 1900 cm^{-1} shown in Figure 1-5), the interfering absorptions from other functional groups can be eliminated. Therefore, in this approach, the calibration is usually

easier to develop and transfer to other instruments which makes the method more general and robust.

FTIR spectroscopy is also a useful technique to monitor a reaction. To perform this, FTIR spectra of sample are collected over the course of the reaction and changes in the spectra are correlated to the formation or loss of functional groups in the reaction. FTIR have been used for monitoring degradations, oxidative stabilities, and aging of vegetable oils [76-80]. The FTIR has been also widely used for the authentication and detection of adulterants in oils [59,78,81-83].

1.4 Gas Chromatography (GC)

Gas chromatography (or gas liquid chromatography) was developed more than 50 years ago. Since then, it has been widely used in lipid analysis for the analysing compounds that can be vaporized and are chemically stable at the high temperatures used in GC [84]. GC coupled with flame ionization detector (FID) has high accuracy, very high resolution, and low limit of detection and is capable of separating mixtures and analysing their components. Whilst volatile and thermally stable compounds can be directly analyzed by the GC, non-volatile and/or thermally liable compounds such as fatty acids require sample preparation [84]. These types of compounds can be derivatized into products suitable for GC analysis by various chemical reactions. One example is transesterification of triacylglycerols (TAGs) into their corresponding fatty acid methyl esters (FAME) using boron trifluoride (BF3) in methanol [85].

1.5 Hypothesis and Objectives

It is hypothesized that;

a) FTIR spectroscopy can be employed for the development of rapid methods for the monitoring and measurement of critical parameters involved in the synthesis of vegetable oil-based polyols.

b) Representative samples can be collected from the reaction mixture during the ozonolysis of fatty acids and their methyl esters and analyzed for the nonanal (a product of oleic acid cleavage) and oleic acid contents using GC-FID.

c) Vegetable oil-based polyols with high hydroxyl value and low viscosity can be obtained by a process consisting of transesterification of an epoxidized oil by 1,3-propanediol prior to oxirane ring opening by 1,3-propanediol.

These hypotheses were tested as described in the next section (Section 1.6).

1.6 Thesis Construction

Figure 1-6 represents the overall structure of the current study. This thesis can be categorized into two major parts; development of analytical methods; and synthesis of vegetable oil-based polyols with improved properties through a new route.

Chapter 2 and 3 outline two FTIR methods developed for the measurement of OHV of polyols. Both of these methods are based on the reaction of *p*-toluenesulfonyl isocyanate with hydroxyl groups resulting in the formation of a carbamate compound. In Chapter 2, the FTIR absorbance of carbamate linkages, and in Chapter 3, the absorption of isocyanate is used to develop

FTIR method for the determination of OHV of polyols and the results are compared with those obtained by standard method (American Oil Chemists' Society, method AOCS Cd 13-60).

In Chapter 4, the absorption of CO_2, formed as a product of the reaction of *p*-toluenesulfonyl isocyanate with water, is used to develop a rapid FTIR method for the measurement of moisture content of vegetable oils. The performance of the method is compared to Karl Fischer (KF) method by analysing moisture content of oil samples prepared by gravimetrically blending various ratio of wet and dry oils.

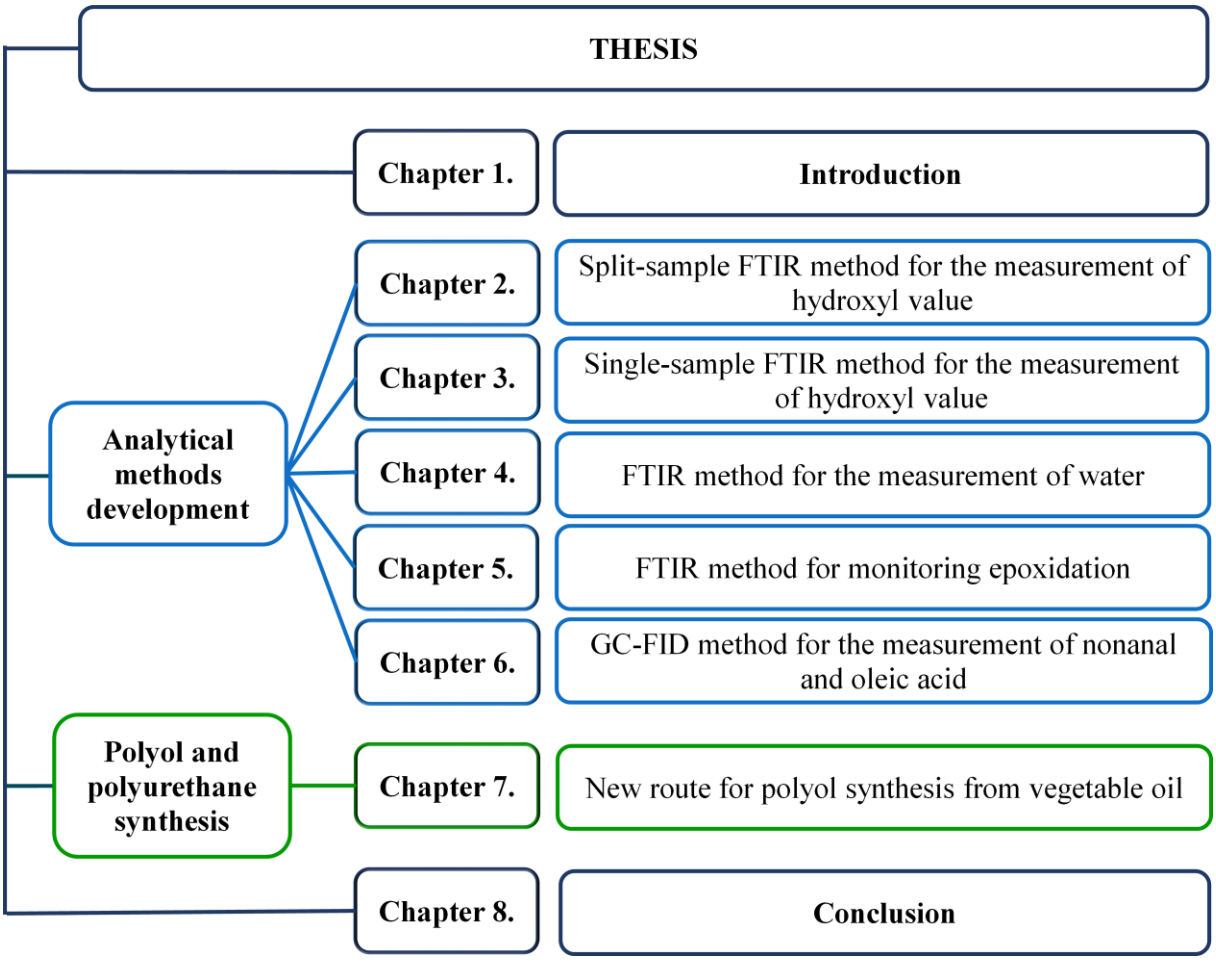

Figure 1-6 Overall construction of the thesis.

In Chapter 5, the absorptions of double bonds and epoxy groups in ATR-FTIR spectra are used to develop an ATR-FTIR method for the measurement of changes in iodine value and oxirane oxygen content, respectively, over the course of the epoxidation of vegetable oils. In this Chapter, vegetable oils including canola, camelina, and flax are epoxidized by performic acid and the changes in iodine value and oxirane oxygen content are determined by ASTM methods to compare with results from the ATR-FTIR method.

Chapter 6 outlines an analytical method for the determination of nonanal and oleic acid contents in the ozonolysis of fatty acids and their methyl esters. In this Chapter aldehydes and acids are derivatized using BF_3 in methanol then injected into a GC-FID. The products of the derivatization reaction are identified using mass spectrometry. For method validation, samples are collected from the ozonolysis mixture after certain times of reaction and subjected to standard additions of nonanal and oleic acid. The concentration of nonanal and oleic acid in these samples are determined by the GC-FID and compared to the actual added nonanal and oleic acid.

In Chapter 7, new polyols with high OHV are produced from canola and flax oils through a new route; epoxidation of vegetable oil→ transesterification with 1,3-propanediol→ ring opening by 1,3-propanediol. In this route, transesterification of the epoxidized in the presence of sodium methoxide as catalyst and acetone as a solvent is performed prior to ring opening step in order to introduce a primary hydroxyl group to fatty acid end chain and hence increase the OHV of the final polyol. In this Chapter, transesterification reaction is optimized using various ratios of catalyst, 1,3-propanediol, and acetone to epoxidized oil. The properties (such as OHV, viscosity, and oligomer content) of the polyols produced by this route are compared with the properties of polyols produced in other routes.

Chapter 8 gives the conclusion of this thesis and provides an overall discussion of the use of FTIR technique in the transformation of vegetable oils into polyols. In addition, the potential benefits of the developed analytical methods and the new route for the synthesis of polyols are discussed.

1.7 References:

[1] Pfister, D. P., Xia, Y., Larock, R. C., Recent advances in vegetable oil-based polyurethanes, *Chemsuschem*. 2011, *4*, 703-717.

[2] Gandini, A., Polymers from renewable resources: A challenge for the future of macromolecular materials, *Macromolecules*. 2008, *41*, 9491-9504.

[3] Nohra, B., Candy, L., Blanco, J. F., Guerin, C., Raoul, Y., Mouloungui, Z., From petrochemical polyurethanes to biobased polyhydroxyurethanes, *Macromolecules*. 2013, *46*, 3771-3792.

[4] Desroches, M., Escouvois, M., Auvergne, R., Caillol, S., Boutevin, B., From vegetable oils to polyurethanes: Synthetic routes to polyols and main industrial products, *Polymer Reviews*. 2012, *52*, 38-79.

[5] Vilela, C., Sousa, A. F., Fonseca, A. C., Serra, A. C., Coelho, J. F. J., Freirea, C. S. R., Silvestrea, A. J. D., The quest for sustainable polyesters–insights into the future, *Polymer Chemistry*. 2014, *5*, 3119--3141.

[6] Towards sustainable development, in our common future, ch. 2, http://www.un-documents.net/ocf-02.htm, accessed March 2016.

[7] Rouilly, A., Rigal, L., Agro-materials: A bibliographic review, *Journal of Macromolecular Science-Polymer Reviews*. 2002, *C42*, 441-479.

[8] Williams, C. K., Hillmyer, M. A., Polymers from renewable resources: A perspective for a special issue of polymer reviews, *Polymer Reviews*. 2008, *48*, 1-10.

[9] Seniha Guner, F., Yagci, Y., Tuncer Erciyes, A., Polymers from triglyceride oils, *Progress in Polymer Science*. 2006, *31*, 633-670.

[10] Metzger, J. O., Bornscheuer, U., Lipids as renewable resources: current state of chemical and biotechnological conversion and diversification, *Applied Microbiology and Biotechnology*. 2006, *71*, 13-22.

[11] Miao, S. D., Wang, P., Su, Z. G., Zhang, S. P., Vegetable-oil-based polymers as future polymeric biomaterials, *Acta Biomaterialia*. 2014, *10*, 1692-1704.

[12] Alagi, P., Hong, S. C., Vegetable oil-based polyols for sustainable polyurethanes, *Macromolecular Research*. 2015, *23*, 1079-1086.

[13] Meier, M. A. R., Metzger, J. O., Schubert, U. S., Plant oil renewable resources as green alternatives in polymer science, *Chemical Society Reviews*. 2007, *36*, 1788-1802.

[14] L. Montero de Espinosa, Meier, M. A. R., Plant oils: The perfect renewable resource for polymer science ?, *European Polymer Journal*. 2011, *47*, 837-852.

[15] de Espinosa, L. M., Ronda, J. C., Galia, M., Cadiz, V., A new route to acrylate oils: crosslinking and properties of acrylate triglycerides from high oleic sunflower oil, *Journal of Polymer Science Part a-Polymer Chemistry*. 2009, *47*, 1159-1167.

[16] Montero De Espinosa, L., Ronda, J. C., Galia, M., Cadiz, V., A straightforward strategy for the efficient synthesis of acrylate and phosphine oxide-containing vegetable oils and their crosslinked materials, *Journal of Polymer Science Part a-Polymer Chemistry*. 2009, *47*, 4051-4063.

[17] Bica, I., Anitas, E. M., Averis, L. M. E., Tensions and deformations in composites based on polyurethane elastomer and magnetorheological suspension: Effects of the magnetic field, *Journal of Industrial and Engineering Chemistry*. 2015, *28*, 86-90.

[18] More, A. S., Lebarbé, T., Maisonneuve, L., Gadenne, B., Alfos, C., Cramail, H., Novel fatty acid based di-isocyanates towards the synthesis of thermoplastic polyurethanes, *European Polymer Journal*. 2013, *49*, 823-833.

[19] Zhang, C. Q., Madbouly, S. A., Kessler, M. R., Biobased polyurethanes prepared from different vegetable oils, *Acs Applied Materials & Interfaces*. 2015, *7*, 1226-1233.

[20] Zhang, C. Q., Xia, Y., Chen, R. Q., Huh, S., Johnston, P. A., Kessler, M. R., Soy-castor oil based polyols prepared using a solvent-free and catalyst-free method and polyurethanes therefrom, *Greem Chemistry*. 2013, *15*, 1477-1484.

[21] Lligadas, G., Ronda, J. C., Galia, M., Cadiz, V., Plant oils as platform chemicals for polyurethane synthesis: Current state-of-the-art, *Biomacromolecules*. 2010, *11*, 2825-2835.

[22] Pechar, T. W., Wilkes, G. L., Zhou, B., Luo, N., Characterization of soy-based polyurethane networks prepared with different diisocyanates and their blends with petroleum-based polyols, *Journal of Applied Polymer Science*. 2007, *106*, 2350-2362.

[23] Campanella, A., Bonnaillie, L. M., Wool, R. P., Polyurethane foams from soyoil-based polyols, *Journal of Applied Polymer Science*. 2009, *112*, 2567-2578.

[24] Zlatanic, A., Lava, C., Zhang, W., Petrovic, Z. S., Effect of structure on properties of polyols and polyurethanes based on different vegetable oils, *Journal of Polymer Science Part B: Polymer Physics*. 2004, *42*, 809-819.

[25] Miao, S. D., Zhang, S. P., Su, Z. G., Wang, P., A novel vegetable oil-lactate hybrid monomer for synthesis of highT_g polyurethanes, *Journal of Polymer Science Part a-Polymer Chemistry*. 2010, *48*, 243-250.

[26] Aniceto, J. P. S., Portugal, I., Silva, C. M., Biomass-based polyols through oxypropylation reaction, *Chemsuschem*. 2012, *5*, 1358-1368.

[27] Nadji, H., Bruzzese, C., Belgacem, M. N., Benaboura, A., Gandini, A., Oxypropylation of lignins and preparation of rigid polyurethane foams from the ensuing polyols, *Macromolecular Materials and Engineering*. 2005, *290*, 1009-1016.

[28] Hu, S., Luo, X., Li, Y., Polyols and Polyurethanes from the Liquefaction of Lignocellulosic Biomass, *Chemsuschem*. 2014, *7*, 66-72.

[29] Kumar, S., Hablot, E., Moscoso, J. L. G., Obeid, W., Hatcher, P. G., DuQuette, B. M., Graiver, D., Narayan, R., Balan, V., Polyurethanes preparation using proteins obtained from microalgae, *Journal of Materials Science*. 2014, *49*, 7824-7833.

[30] Yu, F., Le, Z., Chen, P., Liu, Y., Lin, X., Ruan, R., Atmospheric pressure liquefaction of dried distillers grains (DDG) and making polyurethane foams from liquefied DDG, *Applied Biochemistry and Biotechnology*. 2008, *148*, 235-243.

[31] Suresh, K. I., Kishanprasad, V. S., Synthesis, structure, and properties of novel polyols from cardanol and developed polyurethanes, *Industrial & Engineering Chemistry Research*. 2005, *44*, 4504-4512.

[32] Gobin, M., Loulergue, P., Audic, J. L., Lemiegre, L., Synthesis and characterisation of bio-based polyester materials from vegetable oil and short to long chain dicarboxylic acids, *Industrial Crops and Products*. 2015, *70*, 213-220.

[33] Mohammed, I. A., Al-Mulla, E. A. J., Kadar, N. K. A., Ibrahim, M., Structure-property studies of thermoplastic and thermosetting polyurethanes using palm and soya oils-based polyols, *Journal of Oleo Science*. 2013, *62*, 1059-1072.

[34] Petrovic, Z. S., Zhang, W., Javni, I., Structure and properties of polyurethanes prepared from triglyceride polyols by ozonolysis, *Biomacromolecules*. 2005, *6*, 713-719.

[35] Kong, X., Narine, S. S., Physical properties of polyurethane plastic sheets produced from polyols from canola oil, *Biomacromolecules*. 2007, *8*, 2203-2209.

[36] Guo, A., Demydov, D., Zhang, W., Petrovic, Z. S., Polyols and polyurethanes from hydroformylation of soybean oil, *Journal of Polymers and the Environment*. 2002, *10*, 49-52.

[37] Caillol, S., Desroches, M., Carlotti, S., Auvergne, R., Boutevin, B., Synthesis of new polyurethanes from vegetable oil by thiol-ene coupling, *Green Materials*. 2013, *1*, 16-26.

[38] Desroches, M., Caillol, S., Lapinte, V., Auvergne, R., Boutevin, B., Synthesis of biobased polyols by thiol-ene coupling from vegetable oils, *Macromolecules*. 2011, *44*, 2489-2500.

[39] Chaudhari, A. B., Tatiya, P. D., Hedaoo, R. K., Kulkarni, R. D., Gite, V. V., Polyurethane prepared from neem oil polyesteramides for self-healing anticorrosive coatings, *Industrial & Engineering Chemistry Research*. 2013, *52*, 10189-10197.

[40] Chaudhari, A., Kuwar, A., Mahulikar, P., Hundiwale, D., Kulkarni, R., Gite, V., Development of anticorrosive two pack polyurethane coatings based on modified fatty amide of Azadirachta indica Juss oil cured at room temperature - a sustainable resource, *Rsc Advances*. 2014, *4*, 17866-17872.

[41] Galià, M., de Espinosa, L. M., Ronda, J. C., Lligadas, G., Cádiz, V., Vegetable oil-based thermosetting polymers, *European Journal of Lipid Science and Technology*. 2010, *112*, 87-96.

[42] Mustata, F., Bicu, I., Cascaval, C. N., Rheological and thermal behaviour of an epoxy resin modified with reactive diluents, *Journal of Polymer Engineering*. 1997, *17*, 491-506.

[43] Rosch, J., Mulhaupt, R., Polymers from renewable resoureces: polyester resins and blends based upon anhydride-cured epoxidized soybean oil, *Polymer Bulletin*. 1993, *31*, 679-685.

[44] Thames, S. F., Yu, H., Cationic UV-cured coatings of epoxide-containing vegetable oils, *Surface & Coatings Technology*. 1999, *115*, 208-214.

[45] Harry-O'Kuru, R. E., Carriere, C. J., Synthesis, rheological characterization, and constitutive Modeling of polyhydroxy triglycerides derived from milkweed oil, *Journal of Agricultural and Food Chemistry*. 2002, *50*, 3214-3221.

[46] Harry-O'kuru, R. E., Holser, R. A., Abbott, T. P., Weisleder, D., Synthesis and characteristics of polyhydroxy triglycerides from milkweed oil, *Industrial Crops and Products*. 2002, *15*, 51-58.

[47] Ionescu, M., Petrovic, Z. S., Wan, X., Ethoxylated soybean polyols for polyurethanes, *Journal of Polymers and the Environment*. 2007, *15*, 237-243.

[48] Lu, Y., Larock, R. C., Soybean-oil-based waterborne polyurethane dispersions: Effects of polyol functionality and hard segment content on properties, *Biomacromolecules*. 2008, *9*, 3332-3340.

[49] Javni, I., Zhang, W., Petrovic, Z. S., Effect of different isocyanates on the properties of soy-based polyurethanes, *Journal of Applied Polymer Science*. 2003, *88*, 2912-2916.

[50] Kong, X., Liu, G., Curtis, J. M., Novel polyurethane produced from canola oil based poly(ether ester) polyols: Synthesis, characterization and properties, *European Polymer Journal*. 2012, *48*, 2097-2106.

[51] Lyon, C. K., Garrett, V. H., Goldblatt, L. A., Rigid urethane foams from blown castor oils *Journal of the American Oil Chemists Society*. 1964, *41*, 23-25.

[52] Petrovic, Z. S., Fajnik, D., Preparation and properties of castor oil-based polyurethanes, *Journal of Applied Polymer Science*. 1984, *29*, 1031-1040.

[53] Schuchardt, U., Sercheli, R., Vargas, R. M., Transesterification of vegetable oils: a review, *Journal of the Brazilian Chemical Society*. 1998, *9*, 199-210.

[54] Hablot, E., Zheng, D., Bouquey, M., Averous, L., Polyurethanes based on castor oil: Kinetics, chemical, mechanical and thermal properties, *Macromolecular Materials and Engineering*. 2008, *293*, 922-929.

[55] Narine, S. S., Kong, X., Bouzidi, L., Sporns, P., Physical properties of polyurethanes produced from polyols from seed oils: I. Elastomers, *Journal of the American Oil Chemists Society*. 2007, *84*, 55-63.

[56] Ionescu, M.: The general characteristics of oligo-polyols, in: *Chemistry and technology of polyols for polyurethanes*, RAPRA Technology, United Kongdom 2005, pp. 40-47.

[57] Voort, F. R. v. d., Sedman, J., Russin, T., Lipid analysis by vibrational spectroscopy. I, *European Journal of Lipid Science and Technology*. 2001, *103*, 815-825.

[58] Subramanian, A., Rodriguez-Saona, L.: Fourier transform infrared (FTIR) spectroscopy, in: *Infrared Spectroscopy for Food Quality Analysis and Control* Ed. D. Sun, Academic Press, Amsterdam 2009, pp. 145-178.

[59] Vlachos, N., Skopelitis, Y., Psaroudaki, M., Konstantinidou, V., Chatzilazarou, A., Tegou, E., Applications of Fourier transform-infrared spectroscopy to edible oils, *Analytica Chimica Acta*. 2006, *573*, 459-465.

[60] Mba, O., Adewale, P., Dumont, M.-J., Ngadi, M., Application of near-infrared spectroscopy to characterize binary blends of palm and canola oils, *Industrial Crops and Products*. 2014, *61*, 472-478.

[61] Azizian, H., Kramer, J. K. G., A rapid method for the quantification of fatty acids in fats and oils with emphasis on trans fatty acids using Fourier transform near infrared spectroscopy (FT-NIR), *Lipids*. 2005, *40*, 855-867.

[62] Li, H., van deVoort, F. R., Sedman, J., Ismail, A. A., Rapid determination of cis and trans content, iodine value, and saponification number of edible oils by Fourier transform near-infrared spectroscopy, *Journal of the American Oil Chemists Society*. 1999, *76*, 491-497.

[63] Li, H., van de Voort, F. R., Ismail, A. A., Cox, R., Determination of peroxide value by Fourier transform near-infrared spectroscopy, *Journal of the American Oil Chemists Society*. 2000, *77*, 137-142.

[64] Hendl, O., Howell, J. A., Lowery, J., Jones, W., A rapid and simple method for the determination of iodine values using derivative Fourier transform infrared measurements, *Analytica Chimica Acta*. 2001, *427*, 75-81.

[65] Sedman, J., van de Voort, F. R., Ismail, A. A., Simultaneous determination of iodine value and trans content of fats and oils by single-bounce horizontal attenuated total reflectance Fourier transform infrared spectroscopy, *Journal of the American Oil Chemists Society*. 2000, *77*, 399-403.

[66] Yu, X., van de Voort, F. R., Sedman, J., Determination of peroxide value of edible oils by FTIR spectroscopy with the use of the spectral reconstitution technique, *Talanta*. 2007, *74*, 241-246.

[67] Yu, X., de Voort, F. R. v., Sedman, J., Gao, J.-m., A new direct Fourier transform infrared analysis of free fatty acids in edible oils using spectral reconstitution, *Analytical and bioanalytical chemistry*. 2011, *401*, 315-324.

[68] Xu, L., Zhu, X., Chen, X., Sun, D., Yu, X., Direct FTIR analysis of isolated trans fatty acids in edible oils using disposable polyethylene film, *Food Chemistry*. 2015, *185*, 503-508.

[69] Cerretani, L., Giuliani, A., Maggio, R. M., Bendini, A., Toschi, T. G., Cichelli, A., Rapid FTIR determination of water, phenolics and antioxidant activity of olive oil, *European Journal of Lipid Science and Technology*. 2010, *112*, 1150-1157.

[70] Meng, X., Pan, Q., Ding, Y., Jiang, L., Rapid determination of phospholipid content of vegetable oils by FTIR spectroscopy combined with partial least-square regression, *Food Chemistry*. 2014, *147*, 272-278.

[71] Meng, X., Sedman, J., van de Voort, F. R., Improving the determination of moisture in edible oils by FTIR spectroscopy using acetonitrile extraction, *Food Chemistry*. 2012, *135*, 722-729.

[72] Xiuzhu, Y., Qinghua, L., Daijun, S., Xiaobin, D., Tong, W., Determination of the peroxide value of edible oils by FTIR spectroscopy using polyethylene films, *Analytical Methods*. 2015, *7*, 1727-1731.

[73] Ma, K., vandeVoort, F. R., Sedman, J., Ismail, A. A., Stoichiometric determination of hydroperoxides in fats and oils by Fourier transform infrared spectroscopy, *Journal of the American Oil Chemists Society*. 1997, *74*, 897-906.

[74] Al-Alawi, A., van de Voort, F. R., Sedman, J., A new FTIR method for the analysis of low levels of FFA in refined edible oils, *Spectroscopy Letters*. 2005, *38*, 389-403.

[75] Chalasani, S. R. K., Dewasthale, S., Hablot, E., Shi, X., Graiver, D., Narayan, R., A spectroscopic method for hydroxyl value determination of polyols, *Journal of the American Oil Chemists Society*. 2013, *90*, 1787-1793.

[76] Tena, N., Aparicio, R., Garcia-Gonzalez, D. L., Thermal deterioration of virgin olive oil monitored by ATR-FTIR analysis of trans content, *Journal of Agricultural and Food Chemistry*. 2009, *57*, 9997-10003.

[77] Rohman, A., Man, Y. B. C., Application of FTIR spectroscopy for monitoring the stabilities of selected vegetable oils during thermal oxidation, *International Journal of Food Properties*. 2013, *16*, 1594-1603.

[78] Rohman, A., Man, Y. B. C., The use of Fourier transform mid infrared (FT-MIR) spectroscopy for detection and quantification of adulteration in virgin coconut oil, *Food Chemistry*. 2011, *129*, 583-588.

[79] Srivastava, Y., Semwal, A. D., A study on monitoring of frying performance and oxidative stability of virgin coconut oil (VCO) during continuous/prolonged deep fat frying process using chemical and FTIR spectroscopy, *Journal of Food Science and Technology-Mysore*. 2015, *52*, 984-991.

[80] Dreau, Y. l., Dupuy, N., Gaydou, V., Joachim, J., Kister, J., Study of jojoba oil aging by FTIR, *Analytica Chimica Acta*. 2009, *642*, 163-170.

[81] Quinones-Islas, N., Gabriela Meza-Marquez, O., Osorio-Revilla, G., Gallardo-Velazquez, T., Detection of adulterants in avocado oil by Mid-FTIR spectroscopy and multivariate analysis, *Food Research International*. 2013, *51*, 148-154.

[82] Abdul, R., Riyanto, S., Sasi, A. M., Mohd. Yusof, F., The use of FTIR spectroscopy in combination with chemometrics for the authentication of red fruit (Pandanus conoideus Lam) oil from sunflower and palm oils, *Food Bioscience*. 2014, *7*, 64-70.

[83] Zhang, Q., Liu, C., Sun, Z., Hu, X., Shen, Q., Wu, J., Authentication of edible vegetable oils adulterated with used frying oil by Fourier Transform Infrared Spectroscopy, *Food Chemistry*. 2012, *132*, 1607-1613.

[84] Escuderos, M. E., Olive oil aroma evaluation by Gas chromatographic method: A critical review, *Critical Reviews in Analytical Chemistry*. 2011, *41*, 70-80.

[85] Tao, W., Jina, L., SeongHo, C., HanSeok, K., HongGu, L., Comparative studies on derivatization methods of single or mixed fatty acids, *Food Science and Biotechnology*. 2013, *22*, 1573-1579.

CHAPTER 2

A Primary Method for the Determination of Hydroxyl Value of Polyols by Fourier Transform Mid-Infrared Spectroscopy[1]

2.1 Introduction

Polyols are the basic raw material used for the production of polyurethanes, a group of plastics that have a wide range of properties and applications. In the production of polyurethanes, the polyol hydroxyl functional groups (OH) are cross-linked with monomeric molecules containing two or more isocyanate functional groups (N=C=O). The physical and chemical properties of the plastics produced are strongly dependent on the number of OH groups available in the polyol used. Thus, it is vital to know how many OH groups are present in the polyol, a value which is known as the Hydroxyl Value (OHV). Measuring the OHV, expressed as mg KOH/g sample, is standard practice in polyol manufacturing and development since this largely dictates the properties of the polyurethane product. A number of standard procedures for the measurement of OHV have been established, with the key ones listed in Table 2-1.

With the exception of American Society for Testing and Materials (ASTM) E1899-08 and ASTM D6342-12, all of these methods use acetic anhydride as an acetylating agent in pyridine and employ essentially the same steps to obtain an OHV using duplicate test samples as follows:

[1] A version of this chapter has been published: Tavassoli-Kafrani, M. H., Curtis, M. J., and Van de Voort, F. R., *Journal of the American Oil Chemists' Society*, 2014, *91*, 925-933.

Table 2-1 Common methods used to determine OHV of polyols.

Method Title	Organization	Method	Reference
Hydroxyl Value Determination Procedure	AOCS	Cd 13-60	[1]
Standard Test Method for Hydroxyl Value of Fatty Oils and Acids	ASTM	D4274-11	[2]
Standard Test Methods for Hydroxyl Groups Using Acetic Anhydride Acetylation	ASTM	E222-10	[3]
Standard Test Method for Hydroxyl Groups Using Reaction with p-Toluenesulfonyl Isocyanate (TSI) and Potentiometric Titration with Tetrabutylammonium Hydroxide.	ASTM	E1899-08	[4]
Determination of Hydroxyl Value - Part 2: Method with catalyst	DIN	53240-2	[5]
Standard Practice for Polyurethane Raw Materials: Determining Hydroxyl Number of Polyols by Near Infrared (NIR) Spectroscopy	ASTM	D6342-12	[6]

Test sample1: Dilute the sample with pyridine and titrate with standardized KOH to determine the sample acidity:

$$RCOOH + KOH \longrightarrow \text{Sample Acidity} \qquad \text{Eq. 2-1}$$

Test sample 2: Reflux and react ROH with excess acetic anhydride in pyridine to form the ester plus acetic acid. Some residual unreacted acetic anhydride will remain.

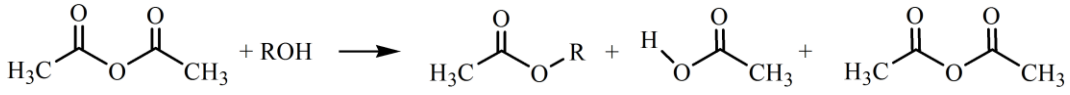

Eq. 2-2

Excess Ester Acid Residual

The residual acetic anhydride is converted into acetic acid by adding an excess of water. Then, the amount of acetic anhydride not consumed by the esterification reaction can be determined by titrating with standardized KOH solution, giving the sample titer:

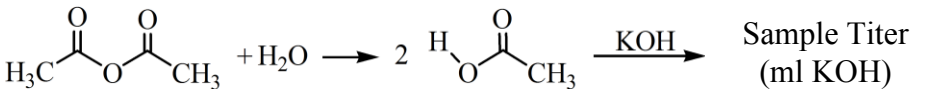

Eq. 2-3

Blank: An aliquot of the initial pyridine-acetic anhydride solution is converted to acetic acid by adding excess water and titrating with standardized KOH to obtain the blank titer:

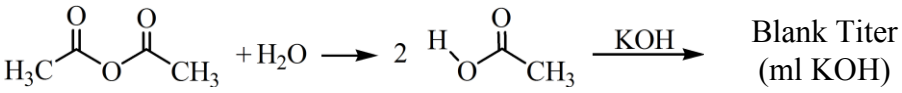

Eq. 2-4

The difference in titer between the blank and the test sample reflects the net acidity consumed by the sample, expressed in mg KOH/g of sample. However, since functional groups such as 1° or 2° amines or, more commonly, carboxylic acids also react with acetic anhydride or KOH, they can also contribute to the OHV. This effect can be corrected by titration of an unacetylated sample of the raw material using standardized acid or base, e.g., Eq. 2-1. The acetic anhydride methods given in Table 2-1 are considered quite accurate if carried out carefully, but they are time-consuming and require relatively large amounts of sample and solvents. The use of pyridine, which is both noxious and difficult to dispose of, is particularly undesirable.

ASTM E1899-08 is a newer method based on potentiometric titration of an acidic carbamate produced by reaction between OH groups and *p*-toluenesulfonyl isocyanate (TSI) as shown in Eq. 2-5:

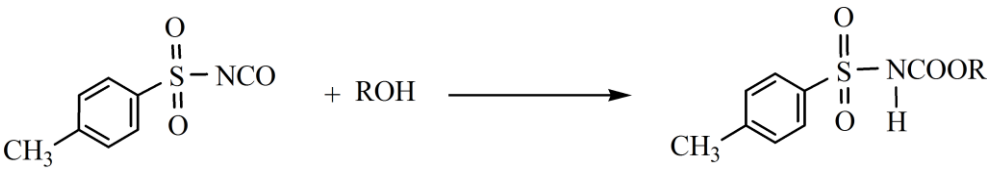

TSI Carbamate Eq. 2-5

The carbamate formed in Reaction (Eq. 2-5) is quantified by titration with tetrabutylammonium hydroxide ($Bu_4N^+OH^-$), commonly referred to as TAB:

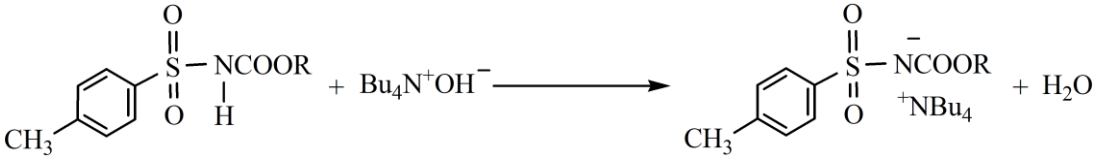

Carbamate TAB Carbamate- TAB Salt Eq. 2-6

TSI also reacts with any moisture present in the sample, producing CO_2:

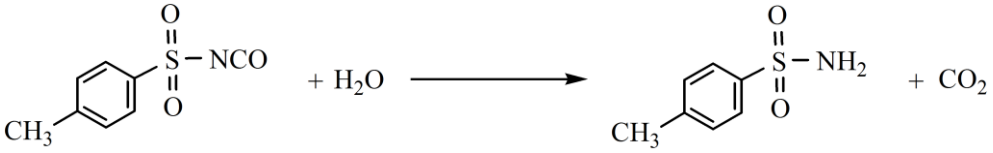

Eq. 2-7

This same reaction is used to destroy residual TSI by quenching it with an excess of H_2O and then titrating the acidic carbamate with TAB.

Compared to the methods based on the reaction with acetic anhydride, the TSI-based procedure has a number of advantages. It does not require refluxing at elevated temperature, and is applicable to lower OHV samples, it is relatively rapid, it uses smaller amounts of sample and it is pyridine-free. This method is not affected by sample moisture per se, although sample moisture contents of >1% may limit the assumed excess TSI available. The method may also be affected by

acids having a pK_a near that of the acidic carbamate [4]. Thus, ASTM E1899-08 is generally considered accurate when applied to dry, neutral, refined products; in other cases, it is suggested that its results be compared with those obtained using ASTM E222-10 to make an appropriate correction.

Both the acetic anhydride and the TSI methods have been adapted to auto-titrators to reduce analytical time and labour, but they are still problematic for routine polyol quality control (QC) analyses where a simpler instrumental approach would be desirable. Fourier transform infrared (FTIR) spectroscopy has been used for this purpose in the form of ASTM D6342-12 [6]. This near-infrared method requires the use of a range of chemometric tools including multiple linear regression (MLR), principal component regression (PCR), and/or partial least squares (PLS) regression, to develop calibration models. Other methods based on mid-FTIR spectroscopy have been developed [7] and [8] using attenuated total reflectance (ATR) accessories. These methods also rely heavily on chemometrics and tend to be relatively insensitive due to the inherently short path length of ATR measurements. Although advanced chemometrics are powerful tools for developing quantitative IR methods [9], establishing a robust calibration remains a relatively complex exercise that requires a reproducible and accurate reference method [10]. It also depends heavily on the availability of representative samples [6] and requires extensive validation. Thus, the FTIR-based OHV methods currently available require a substantive effort to be made for calibration development and are ultimately limited to a subset of all potential polyol types rather than providing a universal calibration. Furthermore, although turnkey, pre-calibrated near-IR instrumentation does exist for polyol analysis [11], it still usually requires tuning of the calibration to suit the sample type being analyzed, with bio-polyols not generally being represented. Just prior to submission of this manuscript a new ATR method for determination of OHV based on polyol

OH silylation was published [12] which uses a stoichiometric reaction to replace the problematic OH signal with a methyl silyl ether. The latter has a far stronger IR signal which is both more readily measured and less prone to hydrogen bonding effects, but requires a one hour reaction at 60°C. A simple Beer's law calibration is devised by making measurements at 1251 cm^{-1} and relating them to the OHVs of samples analyzed by ASTM E 1899-08.

Recently, we have developed bio-based polyols (Liprol™) from renewable lipid feedstocks such as canola oil and demonstrate how they can be used in polyurethane products [13]. Central to this work is the accurate analysis of OHV, which is required for polyol development, manufacture and QC testing. A reliance on the lengthy standard methods to obtain OHVs is problematic in our work and in general for polyol manufacture or testing for polyurethane applications. Thus, we sought after a generalized FTIR method to replace AOCS Cd 13-60 and other titrimetric procedures currently in use. This was achieved through the use of the stoichiometric reaction on which ASTM 1899-08 is based. In this way, a simple split-sample FTIR transmission method is proposed that is capable of providing accurate OHVs for alcohols and polyols in <10 min.

2.2 Experimental

2.2.1 Materials

All solvents toluene, tetrahydrofuran, and alcohols (1-butanol, 1-hexanol, 1-propanol, 1-heptanol, 1,2-propanediol, 2-octanol, and 1-nonanol) were of analytical grade or better and were obtained from Fisher Scientific Ltd. (Nepean, ON, Canada). *p*-toluenesulfonyl isocyanate (96%) was purchased from Sigma-Aldrich (St. Louis, MO), and Canola oil was obtained locally. Three commercial polyols having OHVs of 55, 66, and 280 mg KOH/g were purchased from Bayer

Corporation (Pittsburgh, PA). Canola oil based polyols were prepared using a two-step process, entailing epoxidation [14] followed by hydroxylation using the method of Curtis and Liu [15].

2.2.2 Instrumentation

The FTIR spectrometer used in this work was an ABB-Bomem WorkIR (ABB-Bomem, Quebec, QC, Canada), equipped with an MCT-A detector. Spectra were collected over the range of 4000–400 cm^{-1} at a resolution of 4 cm^{-1} and a gain of 1.0 by co-adding 16 scans (~30 s). To minimize moisture vapor variations, the spectrometer was purged with dry air using a Balston dryer (Balston, Lexington, MA). Samples and standards were aspirated into a 25-μm CaF_2 transmission cell using vacuum, with cell loading being controlled by a manually operated valve. A Bruker Alpha FTIR spectrometer equipped with a single-bounce diamond attenuated total (ATR) reflectance accessory was used to collect survey spectra.

2.2.3 FTIR Calibration

The calibration of the FTIR spectrometer for the determination of OHV was performed by preparing, in toluene, solutions of a structurally defined pure alcohol that has a molecular weight of M g/mol and *nOH* hydroxyl groups per molecule. These solutions were reacted with a solution of TSI in toluene. Then, the spectral changes in the "ester" region that are due to carbamate formation and thus related to the alcohol concentration, were measured. The OHV of any structurally defined, pure alcohol can be determined using Eq. 2-8

$$\text{OHV (mg KOH/g)} = (\text{nOH}/\text{M}) \times 56100 \qquad \text{Eq. 2-8}$$

In the present study, the alcohol used was 1-nonanol, a 1^o alcohol having an OHV of 388.9 mg KOH/g. This was selected since it is a stable, relatively non-volatile and readily available alcohol, although any other defined alcohol could serve as a standard.

2.2.4 1-Nonanol Calibration

Amounts of 1-nonanol ranging from 50–400 mg in ~50-mg increments were weighed into 20-ml vials. This was followed by the addition of 5 ml of toluene by re-pipette and vortexing to ensure dissolution. The concentration of 1-nonanol (mg/l) was then calculated from the total of alcohol plus toluene volume (V_1 in Eq. 2-9). Then, using a calibrated re-pipette, two 2.0-ml aliquots (V_2 in Eq. 2-9) of each solution were transferred into separate vials. To one, 5 ml of TSI solution (6% w/v in toluene) was added while to the other, 5 ml of toluene was added. In this way, a reagent-treated sample and its corresponding sample blank were prepared. These were needed in order to obtain a differential spectrum, by subtracting the spectrum of the sample blank from that of the reagent-treated sample. A calibration equation was obtained from a plot of concentration of the 1-nonanol standards against the integrated intensity measured between 1780 and 1690 cm^{-1} in the differential FTIR spectra (i. e., standard minus blank). A best-fit linear regression relationship was derived from this calibration plot.

2.2.5 OHV Determination Using the 1-Nonanol Calibration

The protocol that was employed for the determination of OHV of samples using the 1-nonanol calibration, is summarized in Figure 2-1. It utilizes the same split-sample procedure that was employed in devising the 1-nonanol calibration (described above), from which a differential spectrum is generated. The integrated intensity between 1780 and 1690 cm^{-1} in the differential spectrum is then measured, so that the OHV of the sample can be determined from the calibration curve, using Eq. 2-9:

$$OHV = (S \times A - B) \times (V_2 + V_3) \times (V_1 / V_2) \times (1 / W) \times (388.9 / 1000) \qquad \text{Eq. 2-9}$$

Where: OHV= Hydroxyl value (mg KOH/g), S= Slope of calibration curve, B= Intercept of calibration curve, A = Integrated intensity between 1780 and 1690 cm^{-1}, W = Sample weight (g), V_1 = Sample volume (W/ρ) + initial volume of toluene added to sample (ml), ρ= Sample density (usually ~0.82 g/ml), V_2 = Aliquot taken from V_1 (ml), V_3 = Volume of TSI/toluene added to V_2 (ml).

For samples to be analyzed using a 25-µm cell, weights of ~100 to 1000 mg were typically used for the anticipated OHV which were ranging from 55 to 1477 mg KOH/g.

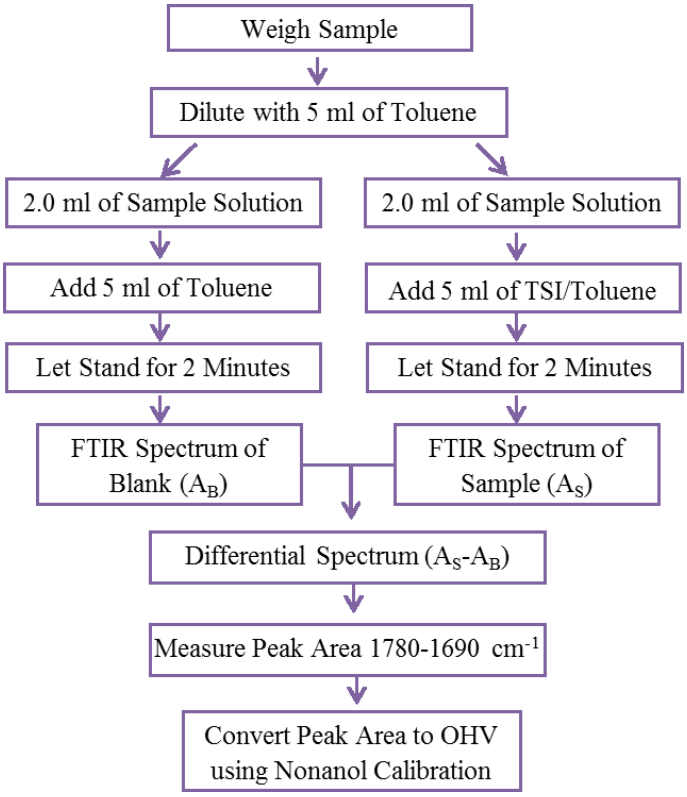

Figure 2-1 General split-sample FTIR protocol used for the assessment of OHV.

2.2.6 Validation

In the validation, pure alcohols were used which have OHVs that are defined by their molecular formulas. In addition, both commercial petrochemical polyols and laboratory produced

bio-polyols (Liprol®) were used with OHVs measured using AOCS Cd 13-60. In all cases, the samples were analyzed using the TSI-FTIR split-sample analytical procedure. The alcohols included a series of 1º and 2º alcohols (1-propanol, 1-butanol, 1-hexanol, 1-heptanol, 2-octanol, and 1-nonanol, for which OHV = 933.5, 756.9, 549.1, 482.8, 430.8 and 388.9 mg KOH/g, respectively), a di-alcohol, 1,2-propanediol (OHV = 1474.6 mg KOH/g), and as well as their mixtures. The polyols included commercial polyols having OHVs of 263, 66 and 55 mg KOH/g and Liprol polyols, with OHVs in the range of 50-300 mg KOH/g. Mixtures of the commercial polyol (OHV= 55 mgKOH/g) and a Liprol (OHV= 290mgKOH/g) were also prepared, so that the overall OHV of these mixtures varied depending on the ratio of each polyol used. Then, various amounts of water (up to 3.9% w/w) were added to these mixtures in order to determine if the presence of moisture produced deviations of the measured FTIR OHV from the expected theoretical OHV.

2.3 Results and Discussion

2.3.1 General Concepts

The FTIR methodology developed is based on ASTM E1899-08, but rather than titrating with Bu_4NOH, the carbamate formation resulting from the TSI-OH reaction is quantified from the change in the integrated intensity between 1780 and 1690 cm^{-1} which is due to carbamate absorption. Note that this change in intensity is measured in the differential spectrum obtained by the split-sample procedure shown in Figure 2-1. For illustration, Figure 2-2 shows a series of spectra of TSI-reacted with a range of 1-nonanol concentrations, without using the split-sample procedure.

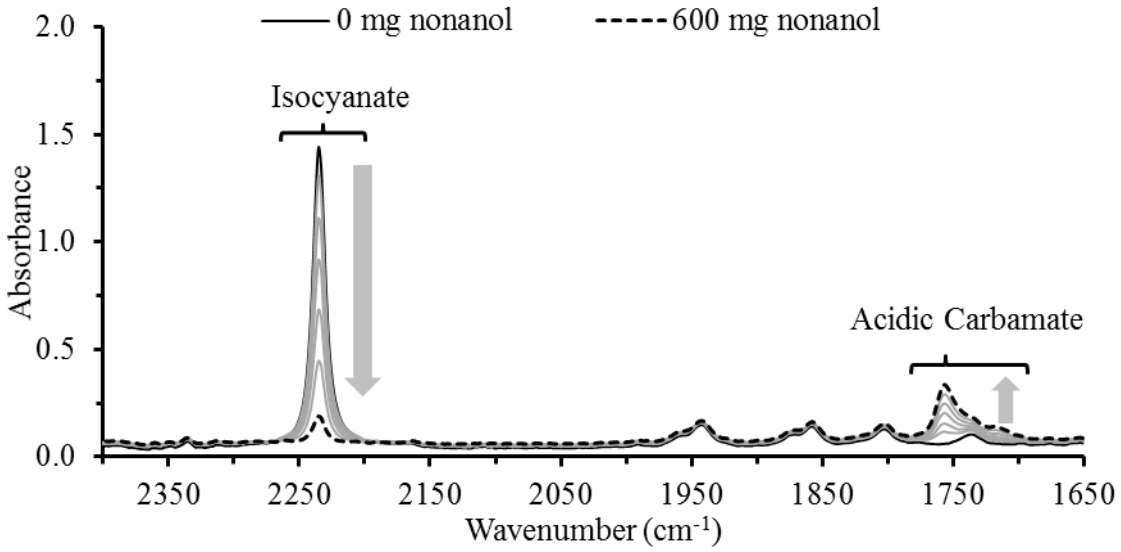

Figure 2-2 FTIR spectra showing changes in the isocyanate band of TSI and the carbamate-ester region as a result of reacting TSI with 0-600 mg of nonanol, with the lowest isocyanate band representing 600 mg nonanol. Arrows show direction of absorbance changes.

As can be seen, the strong absorption band of the TSI isocyanate functional group, N=C=O, at 2235 cm^{-1} drops proportionately as the nonanol concentration rises, with a corresponding increase in the carbamate band in the 1780-1690 cm^{-1} region. Either the isocyanate loss and/or carbamate formation can potentially be used for the quantitative measurement of OHV of polyols. The isocyanate band, however, is problematic, as TSI reacts not only with OH groups, but also with moisture (H-OH) Eq. 2-7, and hence, the OHV would be biased upward to the extent that moisture is present in the sample. Since the "apparent" OHV of water is very high (3114.3 mg KOH/g), the OHV of samples with moisture contents ranging from 0.1% up to 1% would be over-predicted by 3.1 to 31.1 mg KOH/g, respectively. In contrast, carbamate-ester band formation is solely due to the TSI-OH reaction and should not be affected by moisture unless the amount of TSI consumed by the reaction with moisture leaves insufficient TSI for the reaction.

Bio-polyols derived from triacylglycerols or other lipids that contain ester functional groups have significant C=O absorption bands in the 1780-1690 cm^{-1} region that can confound quantitation based on the carbamate-ester band. This is illustrated in Figure 2-3 abc, where the spectrum of a polyol in toluene (Figure 2-3a) and its TSI-reacted counterpart (Figure 2-3b) are presented along with their resulting differential spectrum (Figure 2-3c) obtained using the split-sample procedure.

Spectrum 3c has the common spectral features of the solvent and the sample subtracted out, leaving only the spectral change associated with the TSI-OH reaction; i.e. the absorption band of the carbamate functional group. Thus, since the variable contributions of the sample over the spectral range can affect quantitation, it is imperative that the split-sample procedure be followed to ensure accuracy. The only limitation is that the path length of the cell has to be such that the carbamate band of the sample does not exceed an absorbance of ~1.0 so as to leave enough energy available to obtain a good signal-to-noise ratio.

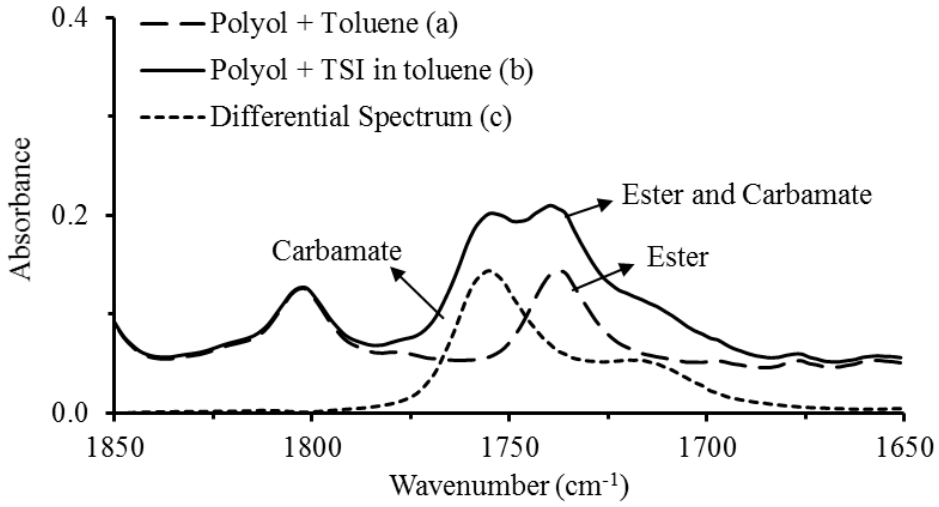

Figure 2-3 abc FTIR spectra of a polyol having an OHV of 88 mg KOH/g in toluene, split into two equal portions with (a) 5 ml of toluene added, (b) reacted with 5 ml of TSI toluene and (c) their differential spectrum (spectrum b minus a).

In principle, an alternative approach would be to measure the OHV of polyols directly by mid-FTIR spectroscopy. Figure 2-4 presents the neat ATR-FTIR spectra of toluene, 1-nonanol, and two lipid-based polyols having OHVs of 280 and 115 mg KOH/g, respectively, and indicates the regions where key functional groups absorb. From the standpoint of polyols, the most relevant absorptions are the OH stretching and C-OH bending vibrations, which could be used to measure OHV by mid-FTIR spectroscopy. The OH stretching band at between 3700 and 3400 cm^{-1} [7] is measurable, albeit broad, but is affected by hydroxyl type (1^o vs. 2^o) [8]. This band also overlaps with the OH absorption bands of hydroperoxides and water, if either are present, and quantitation may be further confounded by complex hydrogen bonding effects [16]. Similar issues pertain to the measurement of the C-OH bending vibration. Despite this, the limitations associated with measuring OHV in a neat sample could be overcome by using sophisticated chemometric approaches such as PLS. Using these methods, calibration models can be developed that relate the

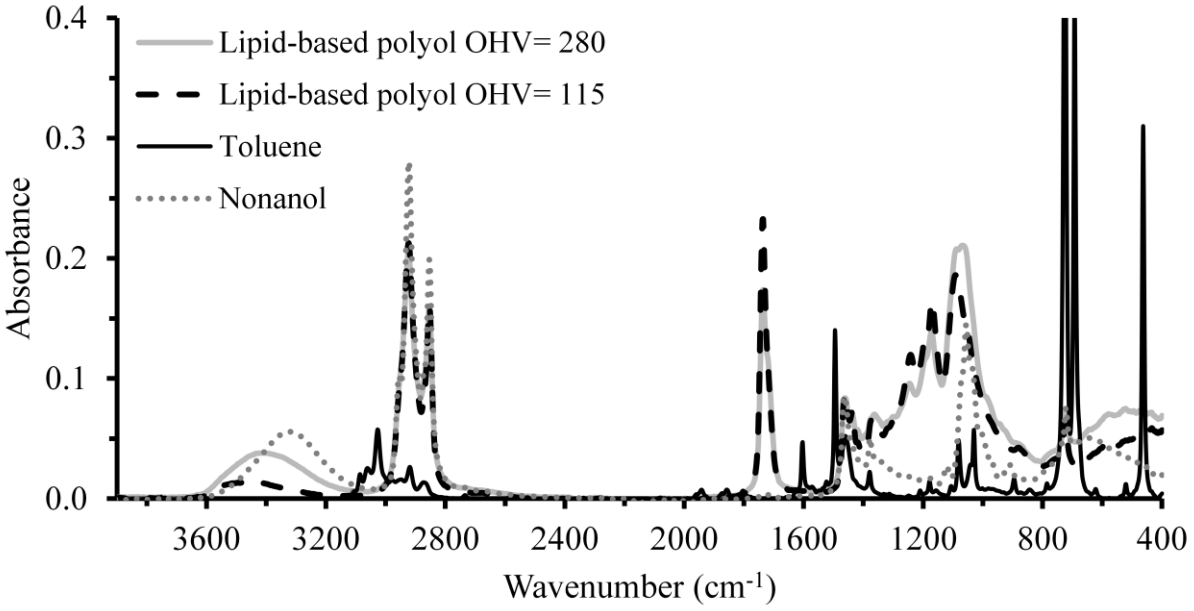

Figure 2-4 ATR Spectra of neat toluene, 1-nonanol, and lipid-based polyols having OHV of 280 and 115 mg KOH/g illustrating the key absorptions of interest.

spectral data for a set of representative samples to their OHVs obtained using a primary reference method, such as AOCS Cd 13-60. By using multiple regions, e.g., the OH, the ester carbonyl, C=O and CH regions, and optimizing the region selection so as to minimize the prediction error, a workable calibration can usually be devised. However, although viable calibrations *can* be developed with sufficiently large and representative sample sets, such calibration development tends to be complex, time consuming and expensive. These calibrations also tend to be restricted in scope to specific polyol types rather than being universal. In contrast, the TSI-FTIR method proposed in this work is a primary method in its own right. The TSI-FTIR method parallels ASTM E1899-08 by relying on a straightforward stoichiometric reaction that is specific to OH groups and is simple to develop a calibration for.

Using the split-sample technique a typical standard curve obtained for a 25-μm cell is illustrated in Figure 2-5. As depicted in Figure 2-2, the carbamate band area increases proportionately as the 1-nonanol concentration rises. Similar standard curves have also been obtained in tetrahydrofuran and acetonitrile, alternate solvents which may be useful should solubility issues arise; however, only data for toluene is presented in this paper. The linear regression equation relating the carbamate band area to the concentration of 1-nonanol is:

$$C = 3.39 \times A - 0.345 \qquad SD = 0.10 \qquad R^2 = 0.9998 \qquad \text{Eq. 2-10}$$

Where: C =1-Nonanol concentration (mg/ml), A = Integrated intensity of carbamate absorption band at 1780-1690 cm^{-1} in the differential spectrum.

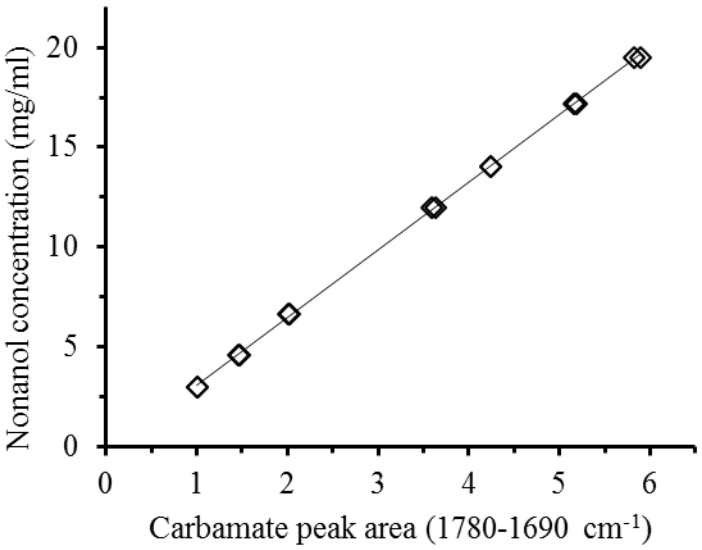

Figure 2-5 Typical calibration curve obtained using the split-sample procedure after reacting TSI with 1-nonanol in toluene and relating the carbamate band area (1780-1690 cm^{-1}) change to the 1-nonanol concentration.

When this calibration equation is applied to the differential spectrum of an unknown sample, the value of C represents the calculated nonanol concentration (mg/ml) in the final solutions prepared in the split-sample procedure. To calculate the OHV of the unknown, the initial sample weight (W) is converted to volume using the polyol density ($\rho \approx 0.82$ g/ml), and this volume is tracked as toluene is added (V_1), adjusted for the amount of V_2 taken from V_1 and its subsequent dilution with toluene-TSI (V_3). Thus, Eq. 2-10 consists of two parts: first, calculation of the apparent nonanol concentration, C_9OH, (mg/ml) from the standard curve ($C_9OH = S \times A_{1780\text{-}1690} - B$) of the carbamate band area; and second, calculation of the mg-equivalent of nonanol in the initial sample:

$$\text{mg - equivalent nonanol} = (C_9OH) \times (V_2 + V_3) \times (V_1 / V_2) \qquad \text{Eq. 2-11}$$

This value is then converted to OHV using the structurally determined OHV of 1-nonanol (388.9 mg KOH/g) and the initial sample weight:

$$OHV = \text{mg - equivalent nonanol} \times (0.3889 / W) \quad \text{Eq.2-12}$$

By substituting the calibration regression Eq. 2-10 into Eq. 2-9 to give Eq. 2-13, the OHV of an unknown sample can be calculated:

$$OHV = (3.39 \times A - 0.345) \times (V2 + V3) \times (V1 / V2) \times (1 / W) \times (388.9 / 1000) \quad \text{Eq. 2-13}$$

2.3.2 Analysis of Pure Alcohols

By analyzing structurally defined pure alcohols using the split-sample technique and applying Eq. 2-13, one can compare the predicted OHVs to the theoretically expected values as determined by Eq. 2-8. Figure 2-6 presents a plot of experimentally determined OHVs against the calculated theoretical OHVs for a series of pure alcohols and gravimetrically prepared mixtures of those alcohols. In each case, the alcohol solutions were analyzed in duplicate by both the TSI-FTIR split-sample method and by AOCS Cd 13-60; the results being compared to the calculated theoretical OHVs of the pure compounds and their mixtures.

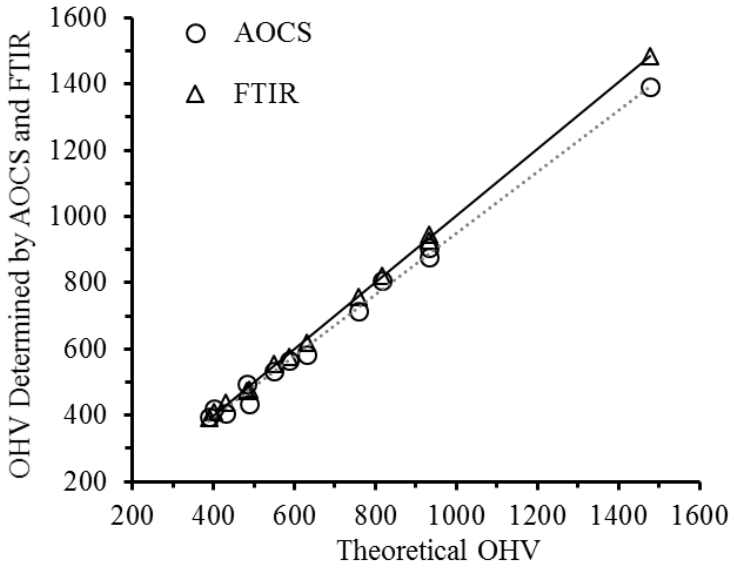

Figure 2-6 Plot of means of duplicate AOCS Cd 13-60 and TSI-FTIR OHV analytical results for pure alcohols and their mixtures plotted against their calculated, theoretical OHVs and compared to the ideal values (line).

The linear regression equations and statistics obtained for the TSI-FTIR and AOCS results relative to the calculated theoretical (OHV_T) values are presented in Eq. 2-15 and Eq. 2-14:

$OHV_{FTIR} = 1.010 \times OHV_T - 6.54$ SD = 7.4 mg KOH/g $R^2 = 0.9994$ Eq. 2-15

$OHV_{AOCS} = 0.935 \times OHV_T + 13.61$ SD = 24.1 mg KOH/g $R^2 = 0.9920$ Eq. 2-14

It is clear from these results that both methods track the theoretical OHV of the pure alcohols and their mixtures well. However, the FTIR predictions are closer to theoretical values as seen by the slope of the regression line with the FTIR results being within 1% of the ideal value of 1.0, while for the AOCS Cd 13-60 method, the slope deviates from this ideal value by about 7%. From the standpoint of reproducibility and accuracy, expressed in terms of the mean differences and standard deviations of the differences for reproducibility (MD_r and SDD_r) and accuracy (MD_a and SDD_a), a comparative summary is presented in Table 2-2.

Table 2-2 MD and SDD for reproducibility and accuracy of the TSI-FTIR and AOCS Cd 13-60 OHV results obtained for pure alcohols and their mixtures relative to their calculated theoretical values.

Method	MD_r[a]	SDD_r[b]	MD_a[a]	SDD_a[b]	CV[c]
AOCS Cd 13-60	11.3	8.5	32.3	22.5	4.6
TSI-FTIR	7.2	5.3	7.1	5.1	1.2

[a] MDr and MDa represent Mean of differences between duplicate analyses for reproducibility and accuracy, respectively.
[b] SDDr and SDDa represent Standard Deviation of differences between duplicate analyses for reproducibility and accuracy, respectively.
[c] Coefficient of Variation

The reproducibility data indicates that the FTIR procedure has less variability in its duplicates, consistent with lower R^2 value in the regression equation. In terms of accuracy, the overall mean differences from the expected theoretical mean difference of 0.0 is smaller for FTIR method compared to AOCS method, but reproducibility (mean difference between duplicate measurements) of both methods is similar.. The coefficient of variation (CV), which reflects overall variation relative to the analytical mean, is about 4x higher for the AOCS method. Thus, based on these defined model systems, the FTIR procedure is both more accurate than the AOCS procedure.

2.3.3 Analysis of Polyols

Three well-defined commercially available polyols with known OHVs and five polyols prepared in our laboratory covering a range of OHV from 50 to 300 mg KOH/g were selected for further duplicate FTIR and AOCS OHV analysis. These samples were also tested for moisture by a previously reported FTIR method [17] to ensure that their moisture contents were < 0.05%. The results obtained are presented in Figure 2-7.

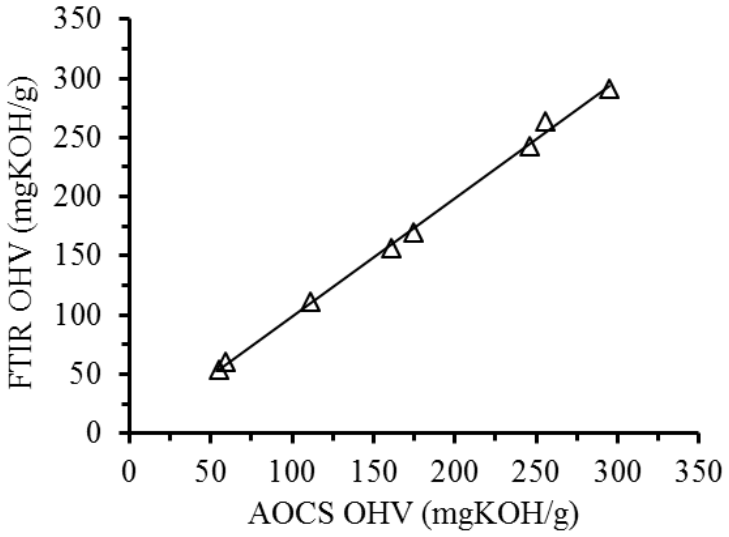

Figure 2-7 Plot of AOCS Cd 13-60 OHV analytical results vs. those obtained using the TSI-FTIR OHV method for selected polyols.

The regression equation for the plot is:

$$OHV_{FTIR} = 1.006 \times OHV_{AOCS} + 2.06 \quad SD = 2.42 \text{ mg KOH/g} \quad R^2 = 0.9980 \qquad \text{Eq. 2-16}$$

The regression equation indicates excellent correspondence between the results obtained by the FTIR and the AOCS Cd 13-60 procedure. As noted above, such perfect correspondence between the results from the AOCS procedure and the theoretical value was not obtained for pure alcohols and their mixtures, which may be attributable to the fact that under reflux conditions, a small proportion of the shorter chain alcohols may be lost, thus reducing the OHV determined by the AOCS Cd 13-60 method.

2.3.4 Variables Affecting Quantitation

A number of issues that can potentially affect quantitation include polyol structure and the presence of moisture in the sample. Moisture can affect the ASTM E1899-08 method by limiting the amount of TSI available for reaction with the polyols; however, in the FTIR method, the TSI

excess is very substantive so it is highly unlikely that this would be the case. To confirm this, validation samples were prepared by blending a lipid-based polyol (OHV= 280 mg KOH/g) with a commercial polyol (OHV= 55 mg KOH/g and water was added in randomly varying amounts (≤0.05 to 3.9% w/w). These mixtures were analyzed by the FTIR method to determine their OHVs, and the values obtained were compared to the expected values based on the gravimetric proportions of each polyol in the mixtures. The mean results of duplicate analyses are presented in Table 2-3.

Table 2-3 Results obtained for polyol mixtures made up of a commercial polyol and a lipid-based polyol, with random amount of water added to the mixtures.

Mixture	Moisture (%w/w)	Theoretical OHV[a]	FTIR OHV[a]	DD_r[b]	DD_a[b]	RE (%)[c]
1	0.86	90.10	88.42	0.28	1.68	1.86
2	0.54	141.3	139.7	0.00	1.62	1.15
3	0.05	162.5	163.1	3.08	1.54	0.34
4	0.05	234.7	239.7	0.10	5.00	2.11
5	2.01	55.00	55.63	0.02	0.63	1.13
6	1.40	88.42	91.99	0.98	3.57	4.04
7	1.65	96.49	98.85	0.70	2.36	2.44
8	1.04	167.1	167.0	1.63	0.81	0.07
9	2.37	118.7	124.0	0.01	5.28	4.44
10	3.20	106.1	104.1	0.01	2.01	1.89
11	3.90	57.00	57.35	0.88	0.44	0.61
12	0.21	256.6	258.4	1.36	1.84	0.72
MD	-	-	-	1.71	2.23	-
SDD	-	-	-	1.64	1.56	-
Mean	0.90	155.1	156.9	-	-	1.73

[a] mg KOH/g
[b] DD_r and DD_a represent differences between duplicate analyses for reproducibility and accuracy, respectively.
[c] Relative Error

The best-fit relationship obtained by linear regression of the expected OHV against the FTIR OHV from the data presented in Table 2-3 is:

$$OHV = 1.010 \times OHV_{FTIR} - 0.21 \qquad SD = 2.50\ mgKOH/g \qquad R^2 = 0.9986 \qquad \text{Eq. 2-17}$$

These regression results are in agreement with those obtained without the addition of water (see Eq. 2-16). In terms of the ancillary statistics, the AOCS and FTIR overall mean OHVs were very similar (155.1 vs. 156.9) and the relative error is acceptable at <2%. In summary, the presence of moderate amounts of moisture (at least up to 4%) in the polyol samples does not affect the measurement of OHV by the proposed FTIR method.

Additional factors also examined in this study include the relative reactivity of alcohol type (1^o vs. 2^o) as well as the response of the TSI-FTIR method to carboxylic acids and amines. In terms of pure alcohols, even tertiary alcohols reacted fully with TSI within 2 min. The relative error (RE) values obtained for 1^o and 2^o alcohols, ranged from 0.13 to 1.17% vs. 0.54 to 1.85%, respectively, indicating that there were no substantive differences between 1^o and 2^o alcohols reacting with TSI, whereas 2^o alcohols are known to be about ~3x less reactive with phenyl isocyanate [18]. Carboxylic acids, as represented by nonanoic acid, were determined to be non-reactive while benzylamine did react with TSI resulting in a decrease in the intensity of the isocyanate absorption; however, the spectral changes produced did not affect the carbamate region where measurements are being made.

2.4 Conclusion

The TSI-FTIR method performs as well as or better than the commonly used standard acetic anhydride based methods, being both simpler and more rapid that any of the titration-based methods listed in Table 2-1. The method uses <1 g of sample, very little solvent and does not

involve refluxing or titration and their attendant problems. The FTIR method is not affected by moisture and avoids the requirement to correct for carboxylic acid acidity or amine basicity. Although other FTIR-based methods for the determination of OHV exist [6-8,12] these all depend on calibration against a primary reference method and all use sophisticated chemometrics to obtain a calibration, other than the new silylation method [12]. As a result, with the exception of the silylation method, these methods tend to be limited to a restricted universe of samples and are problematic for the general analysis of polyols. In contrast, the TSI-FTIR method is a primary method in its own right, relying simply on Beer's law and the use of a pure, defined alcohol to develop a calibration.

As currently structured, the TSI-FTIR method does have one drawback, and that is the requirement to prepare and analyze two samples (sample and blank) to obtain one result. However, for low-volume QC and process control analyses, the TSI-FTIR procedure is still a significant step forward in terms of simplicity and analytical speed, requiring about 10 min to prepare and analyze a sample. From the standpoint of commercial laboratories interested in processing hundreds of samples/day and for automation of this analysis, the split-sample approach could be problematic. It may be possible to develop a single-sample method as has been shown for other FTIR methods developed by the McGill IR Group [19] that also started out as split-sample procedures.

2.5 References:

[1] Official Methods and Recommended Practices of the American Oil Chemists' Society (1997), 4th edn. American Oil Chemists' Society, Champaign, 1993, revised (1997).

[2] American Society for Testing and Materials ASTM D4274-11 (2011).

[3] American Society for Testing and Materials ASTM E222-10 (2010).

[4] American Society for Testing and Materials ASTM E1899-08 (2008).

[5] German National Standard DIN 53240-2 (2007).

[6] American Society for Testing and Materials ASTM D6342-12 (2012).

[7] Ferrao, M. F., Godoy, S. C., Gerbase, A. E., Mello, C., Furtado, J. C., Petzhold, C. L., Poppi, R. J., Non-destructive method for determination of hydroxyl value of soybean polyol by LS-SVM using HATR/FT-IR, *Analytica Chimica Acta*. 2007, *595*, 114-119.

[8] Godoy, S. C., Ferrao, M. F., Gerbase, A. E., Determination of the hydroxyl value of soybean polyol by attenuated total reflectance/fourier transform infrared spectroscopy, *Journal of the American Oil Chemists Society*. 2007, *84*, 503-508.

[9] Fuller, M. P., Ritter, G. L., Draper, C. S., Partial Least-Squares quantitative analysis of infrared spectroscopic data. Part I: Algorithm implementation, *Applied Spectroscopy*. 1988, *42*, 217-227.

[10] van de Voort, F. R., Sedman, J., Russin, T., Lipid analysis by vibrational spectroscopy, *European Journal of Lipid Science and Technology*. 2001, *103*, 815-826.

[11] Chemical Online (2011) MB3600-CH20 chemicals analyzer. http://www.chemicalonline.com/doc/mb3600-ch20-chemicals-analyzer-0001. Accessed May 2013.

[12] Chalasani, S. R. K., Dewasthale, S., Hablot, E., Shi, X., Graiver, D., Narayan, R., A spectroscopic method for hydroxyl value determination of polyols, *Journal of the American Oil Chemists Society*. 2013, *90*, 1787-1793.

[13] Kong, X., Liu, G., Curtis, J. M., Novel polyurethane produced from canola oil based poly(ether ester) polyols: Synthesis, characterization and properties, *European Polymer Journal*. 2012, *48*, 2097-2106.

[14] Anuar, S. T., Zhao, Y. Y., Mugo, S. M., Curtis, J. M., Monitoring the epoxidation of canola oil by non-aqueous reversed phase liquid chromatography/mass spectrometry for process optimization and control, *Journal of the American Oil Chemists Society*. 2012, *89*, 1951-1960.

[15] Curtis, J. M., Liu, G. G., Polyol synthesis from fatty acids and oils. 2012, *WO 2012-009801*.

[16] Ma, K., van de Voort, F. R., Ismail, A. A., Sedman, J., Quantitative determination of hydroperoxides by Fourier transform infrared spectroscopy with a disposable infrared card, *Journal of the American Oil Chemists Society*. 1998, *75*, 1095-1101.

[17] van de Wort, F. R., Sedman, J., Cocciardi, R., Juneau, S., An automated FTIR method for the routine quantitative determination of moisture in lubricants: An alternative to Karl Fischer titration, *Talanta*. 2007, *72*, 289-295.

[18] Ionescu, M., Petrovic, Z. S., Wan, X., Primary hydroxyl content of soybean polyols, *Journal of the American Oil Chemists Society*. 2008, *85*, 465-473.

[19] van de Voort, F. R., Sedman, J., Yaylayan, V., Laurent, C. S., Determination of acid number and base number in lubricants by Fourier transform infrared spectroscopy, *Applied Spectroscopy*. 2003, *57*, 1425-1431.

CHAPTER 3

A Single-sample Method to Determine the Hydroxyl Values of Polyols Using Mid-FTIR Spectroscopy[2]

3.1 Introduction

Overall, the split-sample FTIR OHV method described in Chapter 2 is simple, accurate and rapid; using only a small amount of sample, solvent and reagent compared to more conventional OHV methods. In addition, the method is not sensitive to moisture, amines or acidic constituents, the latter being a possible source of error in the original ASTM procedure from which it is derived. However, despite being rapid (<10 min/sample from preparation to analysis), the split-sample method requires the analysis of two samples to obtain one result, which is both time-consuming in terms of sample preparation as well as problematic from the standpoint of automation [1]. A number of quantitative FTIR methods that have started out as split-sample procedures [1-7] were ultimately modified to single-sample methods so that the analysis could be automated using an autosampler-equipped FTIR. This Chapter describes the conversion of the split-sample FTIR OHV method to a simplified single-sample procedure which is amenable to automated FTIR analysis.

[2] A version of this chapter has been published: Tavassoli-Kafrani, M. H., Curtis, M. J., and Van de Voort, F. R., *European Journal of Lipid Science and Technology*, 2015, *117*, 65-72.

3.2 Experimental

3.2.1 Materials

See Chapter 2 section 2.2.1.

3.2.2 Instrumentation

The instrument used was the same as the instrument described in the previous Chapter (see Chapter 2 section 2.2.2). Reagent solutions, samples and standards were aspirated into a 100 μm CaF_2 transmission cell using vacuum from 20 ml screw capped glass reaction vials.

3.2.3 TSI Standards

Ten reagent standards ranging from 0-1.5% TSI (w/v) were prepared in anhydrous toluene and shaken on a vortex mixer to ensure dissolution. A single beam air background was taken and stored, followed by taking the single beam spectrum of each standard; these were ratioed against the air background to produce the absorbance (Abs) spectrum of the standards. The corresponding differential Abs spectrum of each TSI standard was obtained by subtracting solvent spectrum from each standard. The FTIR response (area) to TSI concentration (mmol/L) *vs.* the -N=C=O functional group absorption of TSI lying between 2298.9 and 2094.5 cm^{-1} was measured relative to a two point baseline located at 2414.7 and 1973.0 cm^{-1}. A calibration curve was derived by linear regression of the TSI concentration *vs.* the peak area changes in these differential spectra and the relation was used to calculate the relative change in TSI concentration which would result if TSI were reacting solely with the polyols being analyzed.

3.2.4 Moisture Compensation

To a dry polyol of defined OHV, moisture was added gravimetrically to cover a moisture range of 0-3%. Approximately 100 mg of each sample was weighed out and subjected to the single-

sample FTIR OHV analytical procedure described in 3.2.5. Differential Abs spectra were again obtained by subtracting the spectrum of TSI-reagent used to prepare the standards from the spectrum of each standard after the reaction. The –N=C=O band was measured as described previously in addition to the CO_2 band (max ~2335 cm^{-1}) arising from the reaction of TSI and H_2O; with the CO_2 area measured between 2331 and 2347 cm^{-1} relative to baseline points taken at 2302 and 2356 cm^{-1}. A moisture compensation calibration was derived by linear regression of the peak area of the CO_2 band in relation to the quantity of H_2O added to react with TSI. In addition, the area increase in the CO_2 band was related to the area loss of isocyanate band resulting from the same reaction. The CO_2 calibration was used to correct the OHV determined for the sample to compensate for the reaction of TSI with moisture.

3.2.5 OHV Determination by FTIR

Depending on the anticipated OHV of a polyol sample over a range of 55-300 mg KOH/g, between 150-25 mg of the sample was weighed into a 20 ml glass vial. To this 10 ml of 1.0% (w/v) TSI-toluene was added and the vial was capped to prevent the loss of any CO_2 formed. Samples were shaken for 1 min on a vortex mixer and left to stand for a further 5 min at room temperature to ensure that the reaction was complete. After taking an air background, the TSI-toluene reagent was aspirated into the transmission flow cell and its absorbance spectrum determined. Subsequently, the reacted samples were aspirated into the cell and their absorbance spectra determined using the same air background. The sample differential spectra were obtained by subtracting the reagent spectrum (common to all the samples prepared with that reagent lot) from sample spectra. The peak area of the –N=C=O and CO_2 bands in these differential spectra were then used to calculate the OHV of the sample, using the isocyanate (3.2.3) and moisture compensation calibrations (3.2.4).

3.2.6 Validation

In order to evaluate the general performance of the single-sample FTIR method, a series defined alcohols and mixtures thereof were analyzed for their OHV using both the single-sample and split-sample FTIR (Chapter 2) methods and the results were compared to the theoretical OHVs determined using Eq. 3-1 for pure alcohols of known structure:

$$OHV\ (mg\ KOH/g) = (nOH/Mw) \times 56100 \qquad \text{Eq. 3-1}$$

Where: nOH= number of hydroxyl groups in the molecule, Mw= molecular weight (g)

The alcohols analyzed included 1° and 2° alcohols ranging in OHV from 388.9 to 1474.6 mg KOH/g, as well as mixtures thereof. In addition, commercial polyols, our own canola-based polyols (Liprol®) and mixtures of polyol types to which up to 2.91% water had been gravimetrically added, were analyzed.

3.3 Results and Discussion

3.3.1 General Concepts

The original split-sample FTIR method uses the basic chemistry of ASTM 1899-08 (Eq. 3-2), but rather than titrating the acidic carbamate formed, the FTIR method measures the carbamate band spectrally, converting its area into OHV using a calibration based on pure nonanol (Chapter 2).

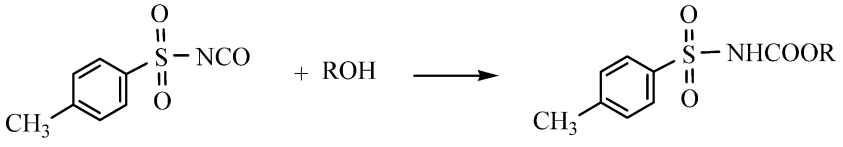

TSI Carbamate

Eq. 3-2

The dominant spectral changes associated with Eq. 3-2 are illustrated in Figure 3-1 where nonanol provides the OH functional group for the reaction with TSI.

Figure 3-1 illustrates that there is a proportionate increase in the carbamate band along with a concomitant loss of the isocyanate reagent band as it reacts with nonanol. Although theoretically either band could be used to measure OHV, the carbamate band was selected for the original method because TSI reacts with moisture as per Eq. 3-3, making the isocyanate measurement moisture sensitive.

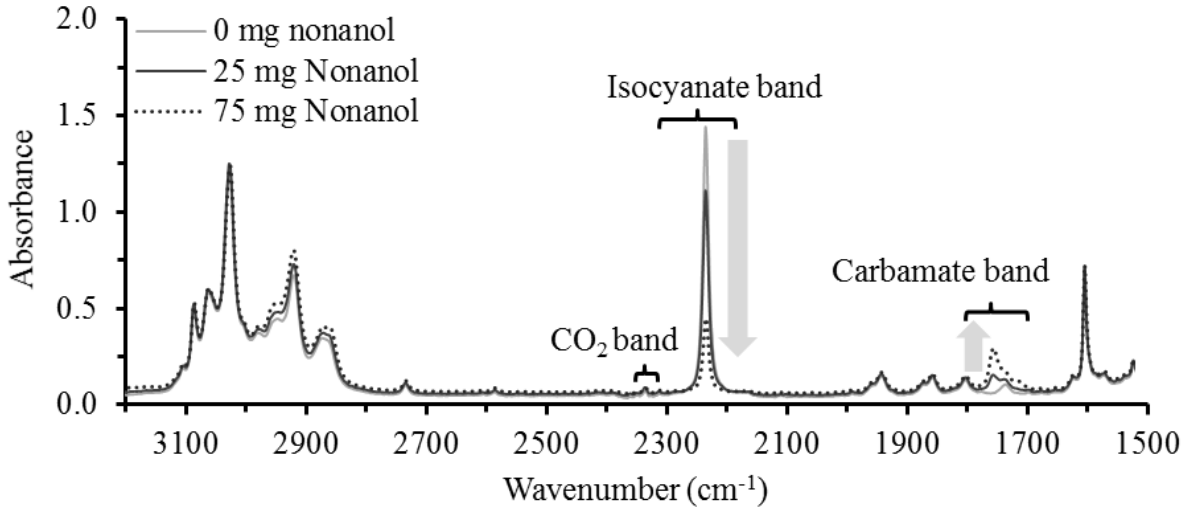

Figure 3-1 Relative spectral changes occurring as nonanol (0-75 mg) is added to a 1% solution of TSI in toluene, illustrating the loss of the isocyanate band at ~2235 cm^{-1} and the concomitant formation of the carbamate band absorbance in the 1750 cm^{-1} region. The region where CO_2 absorbs is presented for reference and the dashed line represents the spectrum of the highest concentration of nonanol.

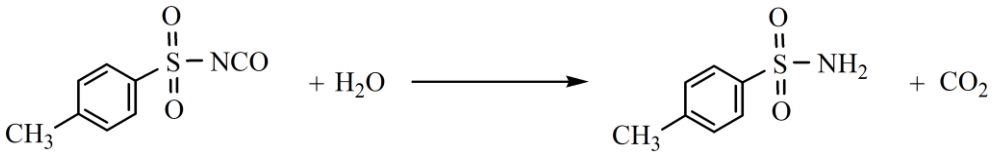

Eq. 3-3

TSI *p*-toluenesulfonamide

Having gained substantial in-house experience with the split-sample FTIR method, we noted that the generally imperceptible and usually constant CO_2 band (Figure 3-1) did occasionally change substantially. Although moisture is compensated for in the carbamate-based FTIR split-sample method (Chapter 2), any obvious spike in the CO_2 band implied that there was measurable moisture present in the sample. Since the "apparent" OHV of water as calculated by Eq. 3-1 is very high (3114.3 mg KOH/g), a sample with a moisture content ranging from 0.1% to 1% would over-predict its OHV by 3.11 to 31.1 mg KOH/g, respectively. Thus, the potential errors associated with using the isocyanate band for OHV determination can be very significant and so was not originally pursued for measurement of OHV. It is clear from Figure 3-1, that the TSI isocyanate functional group (-N=C=O) with its very strong absorption at ~ 2235 cm^{-1} drops proportionately as nonanol concentration rises and would serve as an excellent measure of OHV were it not for its strong moisture sensitivity. Figure 3-2 shows how the isocyanate peak area changes for a serial dilution of TSI-toluene, using in a 100 μm CaF_2 cell, and is representative of the OHV changes that would occur if the moisture contribution were fully compensated for. The linear regression equation relating TSI isocyanate band area loss to TSI concentration in a 100 μm cell is:

$$[TSI] = 2.103 \times A + 0.196 \qquad SD = 0.33 \qquad R^2 = 0.9990 \qquad \text{Eq. 3-4}$$

ate band between 2298.9 and 2094.5 cm^{-1} measured relative to baseline points at 2414.7 and 1973.0 cm^{-1}.

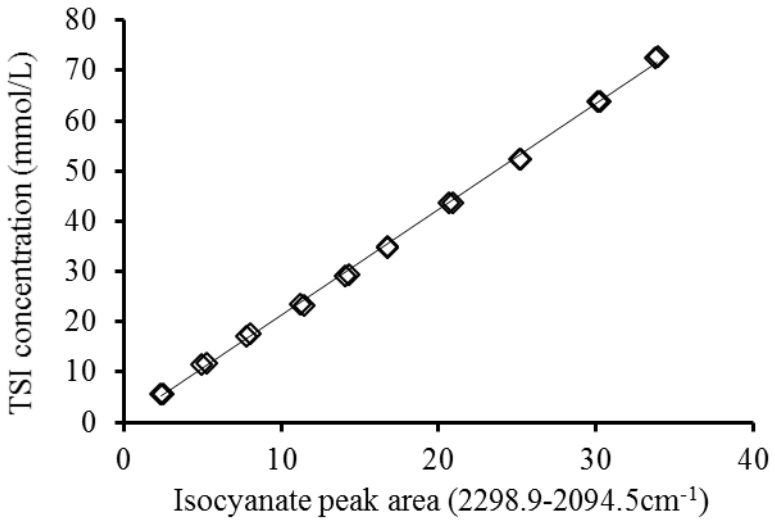

Figure 3-2 Regression relationship derived from a serial dilution of TSI in anhydrous toluene which can be used to calculate the OHV of a defined weight of an undefined polyol mixture if moisture compensation were available.

In the original split-sample FTIR method, the TSI reaction is carried out in an open vial and spectral measurements are made in a short path length cell (25μm). Since neither of these practices is conducive to measuring small amounts of a volatile gas such as CO_2 in the sample, the path length was increased to 100 μm and the reaction carried out in a sealed vial. Then, the spectra of the TSI-toluene reagent before and after gravimetric water addition were collected, and from these differential spectra were generated. Figure 3-2 illustrates the spectral changes occurring as moisture levels added to TSI increase, resulting in a diminution of the isocyanate band with a concomitant increase in the CO_2 band. Figure 3-3 illustrates that the relationship between the isocyanate peak area loss and CO_2 production band is linear relative to moisture addition as predicted by Eq. 3-3.

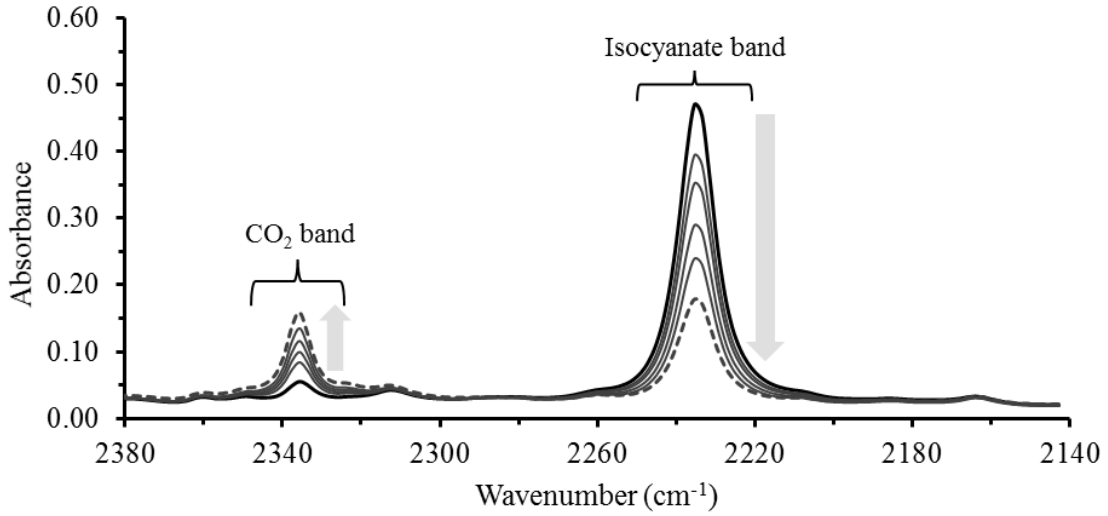

Figure 3-3 Spectra illustrating the reaction between water and TSI-toluene resulting in a loss of the TSI isocyanate band (~2235 cm^{-1}) and the concomitant production of CO_2 (~2335 cm^{-1}).

The linear regression equation obtained by plotting the isocyanate peak area loss against the corresponding CO_2 peak area gain is presented below:

$$Y = 5.768\ x - 0.005 \qquad SD = 0.017 \qquad R^2 = 0.9992 \qquad \text{Eq. 3-5}$$

Where: Y= loss in isocyanate peak area measured between 2298.9 and 2094.5 cm^{-1} relative to baseline points at 2414.7 and 1973.0 cm^{-1}, x = gain in CO_2 peak area measured between 2331 and 2347 cm^{-1} relative to baseline points at 2302 and 2356 cm^{-1}.

This relationship was subsequently used to correct the isocyanate band for the presence of moisture, with the concentration of TSI reacting with "non-aqueous" based OH groups being calculated by applying Eq. 3-6.

$$[TSI_{OH}] = 2.103 \times (A - Y) + 0.196 \qquad \text{Eq. 3-6}$$

Where: $[TSI_{OH}]$ = [TSI] consumed by hydroxyl groups (mmol/l), A = TSI area loss, Y = TSI area loss due to H_2O (Eq. 3-5).

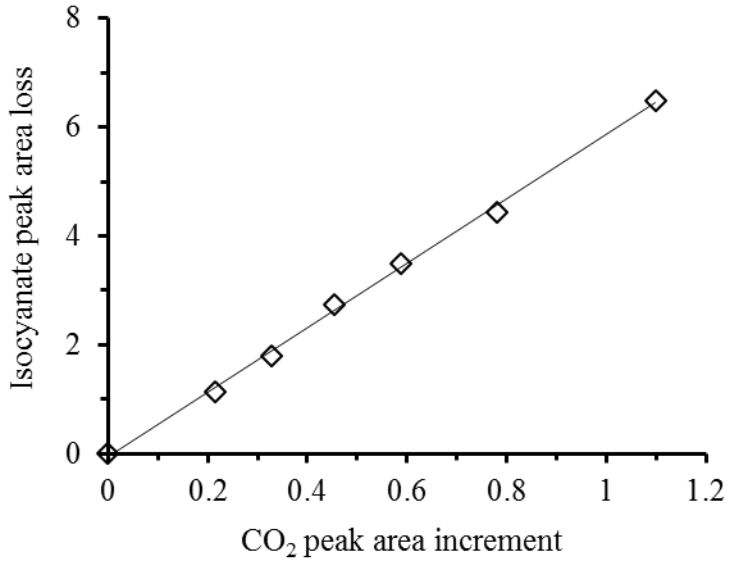

Figure 3-4 Isocyanate peak area loss plotted against CO_2 area gain as moisture is added.

According to the Eq. 3-2, each mole of isocyanate reacts with 1 mole of OH; therefore, the number of moles of isocyanate consumed is equal to the number of moles of OH groups present in the sample. This allows for the determination of OHV (mg KOH/g) using Eq. 3-7:

$$OHV = ([TSI_{OH}]/S) \times \{(V_1 + V_2) / 1000\} \times 56.1 \qquad \text{Eq. 3-7}$$

Where: OHV= hydroxyl value (mg KOH/g sample), $[TSI_{OH}]$ = TSI consumed by hydroxyl groups (mmol/l) (Eq. 3-6), S= weight of sample (g), V_1= ml TSI solution added, V_2= ml sample (ρ/S), ρ is the density of sample (usually ~ 0.82 g/ml).

3.3.2 Analysis of Pure Alcohols

The OHV of series of dry (<0.05%), structurally defined alcohols and gravimetrically prepared mixtures thereof were analyzed in duplicate by both the single-sample FTIR method based on isocyanate band loss and by the split-sample FTIR method based on carbamate formation.

The OHV results obtained experimentally were then compared to the theoretical OHV values which can readily be calculated for pure compounds of known structure using Eq. 3-1.

The linear regression equations obtained for the plots depicted in Figure 3-4 are presented in Eq. 3-8 and Eq. 3-9. In addition, the zero-regression equations obtained when the same data is forced through the origin are given in Eq. 3-10 and Eq. 3-11.

$$FTIR_{OHV\text{-}Split\ Sample} = 1.007 \times OHV_{Calc} - 4.65 \qquad SD = 7.90 \qquad R^2 = 0.9997 \qquad \text{Eq. 3-8}$$

$$FTIR_{OHV\text{-}Single\ Sample} = 0.981 \times OHV_{Calc} + 10.53 \qquad SD = 10.53 \qquad R^2 = 0.9994 \qquad \text{Eq. 3-9}$$

$$FTIR_{OHV\text{-}Split\ Sample} = 1.003 \times OHV_{Calc} \qquad SD = 7.81 \qquad R^2 = 0.9997 \qquad \text{Eq. 3-10}$$

$$FTIR_{OHV\text{-}Single\ Sample} = 0.992 \times OHV_{Calc} \qquad SD = 10.75 \qquad R^2 = 0.9994 \qquad \text{Eq. 3-11}$$

The zero-regression equations facilitate a direct comparison of slopes and each is well within 1% of the ideal slope of 1.0. Since the regression statistics are not altered significantly by the removal of the intercepts, this confirms that the two FTIR methods, which are in close agreement with each other, also agree well with the theoretical values. Thus for pure alcohols and mixtures thereof, the single-sample FTIR method has similar reproducibility and accuracy as the split-sample FTIR method, which was previously demonstrated to be more accurate and reproducible than AOCS Cd 13-60 (Chapter 2).

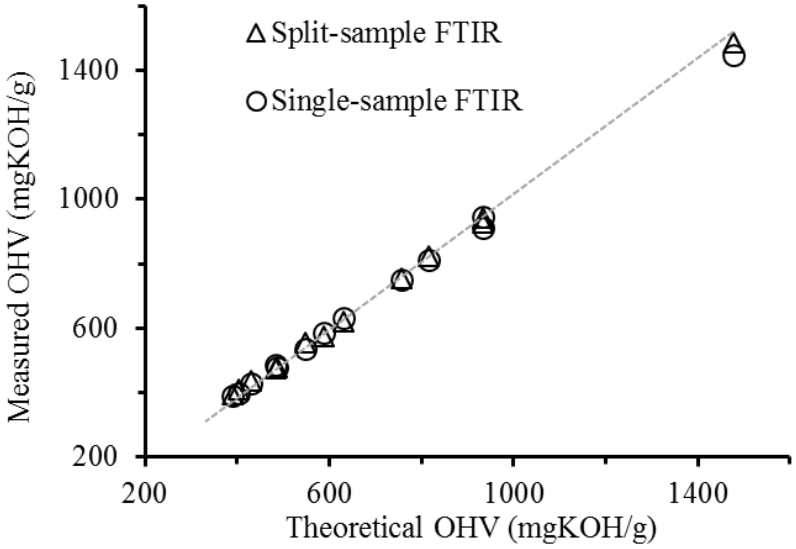

Figure 3-5 Comparison of split-sample and single-sample FTIR results for pure alcohols and their mixtures relative to their calculated OHV.

3.3.3 Analysis of Polyols

The OHV of three well defined, commercially available petrochemical polyols as well as eight lipid-based polyols prepared in our laboratory were analyzed by FTIR method to determine if the performance achieved for the model alcohols also applied to more complex polyols. These polyols are varied both in terms of their molecular weights and their structures. Pre-analysis of all of these samples for moisture [7] indicated that they all contained <0.05% H_2O and could thus be considered dry for practical purposes. Under these conditions, analysis of these 11 samples by the two FTIR methods again produced very similar results as can be inferred by a linear regression of the results obtained relating the methods to each other:

$$\text{FTIR}_{\text{OHV-Single Sample}} = 0.9973 \times (\text{FTIR}_{\text{OHV-Split Sample}}) + 0.40 \quad SD = 1.69 \quad R = 0.996 \qquad \text{Eq. 3-12}$$

Thus, the single-sample FTIR method performs very much like the split-sample method for either simple alcohols or polyols whenever moisture is not a significant factor (e.g., <0.05%).

3.3.4 Variables Affecting Single-sample FTIR Quantitation

3.3.4.1 Moisture

It is apparent from Eq. 3-3 and Figure 3-3 that the single-sample method is very moisture sensitive, with substantive isocyanate signal loss occurring when significant moisture is present in the sample. Eq. 3-3 also indicates that CO_2 should be produced in amounts proportionate to the moisture content. These amounts should be measurable by FTIR, given an adequate cell path length to provide sufficient sensitivity to monitor its formation and if it is assured that CO_2 is not lost during sample handling and measurement. To evaluate whether CO_2 moisture compensation is potentially viable, polyols mixtures were gravimetrically prepared by blending various amounts of a higher OHV Canola-based polyol (290 mg KOH/g) with a lower OHV commercial polyol (55 mg KOH/g) so as to vary OHV quantitatively. Moisture was gravimetrically added to these mixtures in varying amounts, up to ~3%, and the mixtures analyzed for OHV using the single-sample FTIR method both with and without moisture compensation (Eq. 3-7). The results of these experiments are presented in Table 3-1.

The effect of moisture on the OHV results is evident when examining the moisture-compensated and uncompensated predictions in Table 3-1. The OHV values are clearly biased high when higher moisture levels are present, while the OHV of samples with <0.05% moisture are a close match to the calculated values. Moisture compensation achieved *via* the CO_2 band brings those erroneous results in-line with the expected values using the technique described in Section 3.2.4. The linear regression relationship obtained for the moisture corrected data *vs.* the gravimetrically calculated values is:

$$OHV = 1.0001 \times (OHV_{FTIR}) + 1.81 \qquad SD = 3.91 \quad R^2 = 0.9978 \qquad \text{Eq. 3-13}$$

Eq. 3-13 indicates excellent concurrence between the single-sample moisture-compensated OHV data and the OHV results expected from the gravimetric mixtures. It is important to reiterate that each 0.1% moisture in a polyol results in an OHV overestimation of ~3 mg KOH/g using the single-sample FTIR method. Although this is not an issue when polyols are dry it is clearly problematic when this is not the case. Thus, incorporation of the CO_2 moisture-compensation procedure is required for the single-sample method to become a generalized method on par with the split-sample FTIR and conventional AOCS methods, both of which are moisture insensitive.

Table 3-1 Single-sample FTIR OHV (mg KOH/g) results obtained for polyol mixtures to which various amounts of moisture were gravimetrically added and determined with and without moisture compensation.

Mixture	% H_2O Added	Calculated OHV	OHV - No H_2O Comp[a]	DD_r[b]	DD_a[b]	CV_a[c]	OHV - H_2O Comp[a]	DD_r[b]	DD_a[b]	CV_a[c]
1	0.91	84.8	111.8	10.9	27.0	31.8	85.4	14.5	0.6	0.8
2	0.54	146.2	156.0	6.3	9.8	6.7	142.0	4.7	4.2	2.9
3	0.68	213.2	232.6	3.5	19.4	9.1	213.4	3.6	0.3	0.1
4	<0.05	251.6	259.2	4.3	7.6	3.0	257.9	7.3	6.3	2.5
5	<0.05	289.8	291.1	2.4	1.3	0.4	290.0	3.3	0.2	0.1
6	2.01	265.0	322.9	8.8	57.9	21.8	260.6	5.4	5.1	1.7
7	1.45	89.2	137.5	11.0	48.3	54.1	93.6	6.8	4.4	4.9
8	1.68	94.9	146.3	5.4	51.4	54.2	98.3	1.1	3.4	3.6
9	1.15	280.8	317.2	5.6	36.4	13.0	284.4	6.4	3.6	1.3
10	1.04	170.2	200.6	2.9	30.4	17.9	167.9	2.6	2.3	1.3
11	2.91	265.0	360.9	10.8	95.9	36.2	267.8	3.7	2.8	1.0
12	0.17	217.3	227.8	3.0	10.5	4.8	223.0	2.6	5.7	2.6
13	<0.05	58.3	60.7	0.9	2.4	4.1	59.5	1.2	1.2	2.1
14	2.32	175.8	257.0	6.0	81.2	46.2	183.7	0.1	7.9	4.5
MD	-	-	-	5.8	34.3	-	-	4.1	3.4	-
SDD	-	-	-	3.2	28.4	-	-	3.6	2.3	-
Mean	-	187.7	220.1	-	-	21.7	185.9	-	-	2.1

[a] Compensation
[b] DDr and DDa represent differences between duplicate analyses (reproducibility) and difference from theoretical OHVs (accuracy), respectively.
[c] Coefficient of Variation

3.3.4.2 Carboxylic Acids and Amines

To investigate whether carboxylic acids and amines react with TSI under FTIR reaction conditions, various amounts of nonanoic acid (50-200 mg) as well as benzyl amine (16-90 mg) were analyzed directly by the single-sample FTIR method. Studies of the differential spectra indicated that no significant change occurs in the isocyanate absorption in the case of nonanoic acid. Nonanoic acid can be considered a representative carboxylic acid, most of which have pK_as in the range of 3-4. Given enough time (>1h), nonanoic acid will begin to slowly react with TSI to produce CO_2 as per Eq. 3-14.

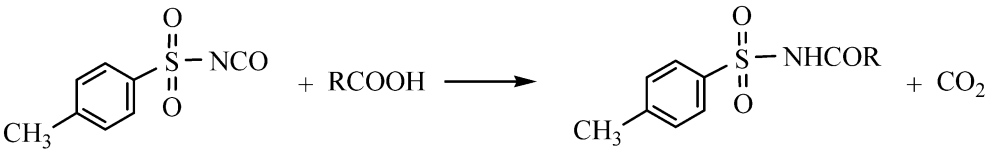

Eq. 3-14

Based on its reactivity, there is little, if any significant change expected under routine analytical conditions, albeit there is a possibility of isocyanate loss if samples were to stand overnight prior to analysis. Even in such a circumstance, however, the CO_2 produced, much like moisture, could be used to compensate for any the isocyanate loss. Thus, carboxylic acids are not considered a potential source of analytical error. In contrast, amines do react faster with TSI and will result in a loss of isocyanate as per Eq. 3-15.

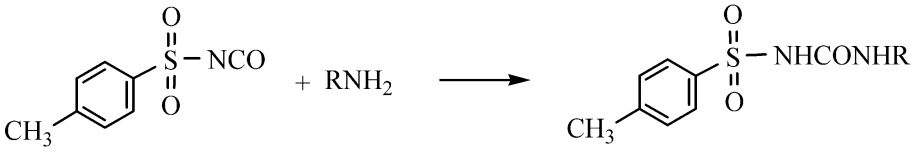

Eq. 3-15

A future study may find a means of compensating for this reaction, but since pure polyols typically do not contain amines this is not considered a major limitation of the single-sample FTIR

method. However, care should be exercised when using any method that involves the use of reactions with isocyanates for measuring the OHV of polyol formulations which may contain amine catalysts.

3.4 Conclusion

Based on our experience with the split-sample FTIR OHV method, the observation that the CO_2 band in sample spectra varied significantly from time to time, led to its examination as a possible means of developing an isocyanate-based single-sample FTIR method. This approach had originally been discounted due to its high sensitivity to sample moisture. It was demonstrated that when moisture was not a significant factor, the isocyanate single-sample FTIR method performed much like the split-sample FTIR procedure described in Chapter 2, but not when moisture levels exceeded 0.10%. By adjusting the path length from the original 25 μm to 100 μm, the CO_2 band becomes readily measurable and its area change was shown to be directly related to added moisture. Thus, the CO_2 band can be used to compensate for the additional consumption of isocyanate by moisture, making the single-sample FTIR method a viable and accurate procedure. The single-sample method is not affected by carboxylic acids, but as is expected for other methods involving the isocyanate reaction, the presence of amines, such as added catalysts, could bias the results to higher values. The single-sample approach is of practical interest as it overcomes the necessity of preparing two separate samples to obtain one analytical result. This is not a major issue if the number of samples to be analyzed is low, but for higher sample throughput, both sample preparation time and the time taken to obtain an analytical result become important. With the single-sample FTIR OHV procedure, it is now possible to automate the method with the use of an autosampler-equipped FTIR, as has been done previously for the analysis of edible oils and for lubricants [1,8].

3.5 References:

[1] Van De Voort, F. R., Sedman, J., Pinchuk, D., An overview of progress and new developments in FTIR lubricant condition monitoring methodology, *Journal of ASTM International*. 2011, *8*, 1-14.

[2] Xiuzhu, Y., Voort, F. R., Sedman, J., Jin-Ming, G., A new direct Fourier transform infrared analysis of free fatty acids in edible oils using spectral reconstitution, *Analytical and bioanalytical chemistry*. 2011, *401*, 315-324.

[3] Li, H., van deVoort, F. R., Sedman, J., Ismail, A. A., Rapid determination of cis and trans content, iodine value, and saponification number of edible oils by Fourier transform near-infrared spectroscopy, *Journal of the American Oil Chemists Society*. 1999, *76*, 491-497.

[4] van de Voort, F. R., Sedman, J., Yaylayan, V., Laurent, C. S., Determination of acid number and base number in lubricants by Fourier transform infrared spectroscopy, *Applied Spectroscopy*. 2003, *57*, 1425-1431.

[5] Hui, L., Voort, F. R. v. d., Ismail, A. A., Cox, R., Determination of peroxide value by Fourier transform near-infrared spectroscopy, *Journal of the American Oil Chemists' Society*. 2000, *77*, 137-142.

[6] Ma, K., van de Voort, F. R., Ismail, A. A., Sedman, J., Quantitative determination of hydroperoxides by Fourier transform infrared spectroscopy with a disposable infrared card, *Journal of the American Oil Chemists Society*. 1998, *75*, 1095-1101.

[7] van de Wort, F. R., Sedman, J., Cocciardi, R., Juneau, S., An automated FTIR method for the routine quantitative determination of moisture in lubricants: An alternative to Karl Fischer titration, *Talanta*. 2007, *72*, 289-295.

[8] Al-Alawi, A., van de Voort, F. R., Sedman, J., Ghetler, A., Automated FTIR analysis of free fatty acids or moisture in edible oils, *Journal of Laboratory Automation*. 2006, *11*, 23-29.

CHAPTER 4

Stoichiometric Determination of Moisture in Edible Oils by Mid-FTIR Spectroscopy[3]

4.1 Introduction

Moisture is ubiquitous in biological materials, including in isolated fats and oils where it can serve as both a reactant and reaction medium. Although lipids are predominantly hydrophobic, they can readily absorb and retain small amounts of moisture. This is problematic in that it can facilitate the hydrolysis of the ester linkage of triacylglycerols, which can occur enzymatically or when subjected to thermal stress, producing free fatty acids. As these are less resistant to autoxidation, their presence can lead to the development of rancidity, off-flavours, as well as reducing the smoke point of oils. To ensure stability, fats and oils should contain <0.3% (3,000 ppm) moisture, preferably ~0.05% [1]. Given this influence on quality, moisture determinations are routine at all stages of oil processing and use. Traditional physical methods based on distillation or evaporation all have inherent limitations in terms of either analytical time or accuracy. Karl Fischer (KF) type procedures [2-4] are considered the gold standard for moisture determination and are sanctioned by most officiating bodies. They are based on the reaction of moisture with a mixture of sulphur dioxide and iodine in the presence of a base and solvating alcohol with quantification achieved by potentiometric [5,6], titrimetric or

[3] A version of this chapter has been published: van de Voort, F. R., Tavassoli-Kafrani, M. H., and Curtis, M. J., *Analytica Chimica Acta*, 2016, *918*, 1-7.

coulometric [7,8] means. Although KF analysis implies a single procedure, there are actually several competing versions encompassing many variables, including proprietary reagent formulations, various titrator designs and different methods of end-point determination. There is also the optional inclusion of an ancillary distillation accessory, which in particular is used to minimize errors or biases caused by interfering constituents such as aldehydes, ketones, and hydroperoxides [9] that are commonly associated with hydrophobic matrices like edible oils or lubricants. The intra-laboratory accuracy for any particular KF procedure tends to be quite good, however, inter-method and inter-laboratory performance, is less so [10]. The moisture changes measured by a KF procedure are usually considered to reflect reliable, real, and accurate differences in moisture for that system. However, since different KF procedures are subject to many factors that influence the accuracy of the moisture values that are obtained, the results from each procedure should ideally be confirmed against certified water standards if they are to be considered as absolute values.

Nevertheless, in general KF analyses are known to provide a high degree of specificity and reproducibility along with reasonable levels of accuracy. However, they can be relatively expensive to implement, operate and maintain and hence there is an interest in alternative instrumental approaches. Fourier transform infrared spectroscopy has developed into a widely used tool for analysis of a wide range of key quality parameters of fats and oils as well as lubricants [11], through its ability to spectrally monitor functional group absorptions. Moisture determination is no exception, with a variety of such approaches having been taken, including direct spectral measurement [12-14], the use of stoichiometric reactions [15] as well as extraction-based procedures [16-21]. Direct

moisture measurement is possible given the high absorptivity of water, however, the effects of hydrogen bonding and spectral interferences from other undefined hydroxyl compounds and underlying matrix absorptions generally makes direct quantitation problematic. These issues can be overcome to some extent through the use of chemometrics such that attenuated total reflectance (ATR) FTIR has been used for the direct measurement of moisture in edible oils by applying partial least squares (PLS) analysis. Although useful in fairly specific circumstances, the short path length inherent to ATR accessories severely limits the sensitivity of this approach. Even using transmission spectroscopy in order to gain added sensitivity, PLS calibrations can be problematic to develop. This is partly because they rely on the results from a primary method, which has its own inherent error and this is compounded by the need to ensure that the standards used for calibration are representative in relation to the variety and types of samples to be analysed [11].

One means of overcoming such complications is through the use of stoichiometric reactions, dimethoxypropane (DMP) having been used to measure moisture in this manner in mineral-based lubricants [15]. In that work, the acetone produced by the reaction of DMP with H_2O is used to determine the moisture content of the oil. This approach, however, is not amenable to lipids *per se* as the υC=O absorption of ester linkage of the triacylglycerols (1680-1800 cm^{-1}) strongly interferes with the υC=O absorption of the acetone produced. A more general FTIR approach used for both edible oils and mineral-based lubricants is the extraction of moisture from the hydrophobic matrix using a dry oil-immiscible aprotic polar solvent such as acetonitrile [18,19], or dimethyl sulfoxide [20]. After separation, the spectrum of the solvent extract is compared to that of the dry solvent and the moisture is quantified using a calibration devised from the differential spectra of gravimetrically

moisture-spiked solvent standards. This method has recently been applied to moisture measurement in transformer oils [22].

However, although the FTIR methods described above can be workable, they still generally do not match the performance characteristics of established KF methods in terms of sensitivity, accuracy or reliability. This Chapter describes a new stoichiometric, reaction-based FTIR method that uses a reaction producing CO_2 from the moisture present in the oil matrix. The CO_2 can be quantified spectroscopically and its concentration is directly related to the moisture present in the oil sample. This new method has analytical performance characteristics that are comparable to those of established KF procedures.

4.2 Experimental

4.2.1 Materials

Refined vegetable oils including canola, sunflower, flax and coconut were obtained locally. Reagent grade toluenesulfonyl isocyanate (96%), toluene and dioxane were all obtained from Sigma Aldrich.

4.2.2 Instrumentation

FTIR spectroscopy was carried out using an ABB-Bomem WorkIR (ABB-Bomem, Quebec, Canada), a component of the COAT system used by commercial lubricant analysis laboratories for the automated determination of acid number (AN) and base number (BN) of in-use lubricants as well as for general condition monitoring [22].

4.2.3 Spectroscopy and Sample Handling

Spectra were collected over range of 400–6000 cm^{-1} at a resolution of 4 cm^{-1} at a gain of 1.0 using 16 scans (~30 sec scanning). The spectrometer was purged with dry air

using a Balston Dryer (Balston, Lexington, MA) so as to minimize moisture vapour and atmospheric CO_2 variations. To avoid CO_2 loss from TSI-reacted samples, the reaction was carried out in 15 ml screw capped test tubes which were opened only at the time of analysis. Samples were aspirated directly into a 115 μm CaF_2 transmission flow cell using a long stainless steel needle connected by Luer-Lock and tubing to the IR cell inlet and outlet to a 3-way control valve, onto a trap to collect the liquid and to the vacuum source. Toluene was used as a rinse solvent to wash out the lines and IR cell between samples, followed by air aspiration to remove any residual solvent from the system.

4.2.4 Calibration Standards and Oil Samples

Dioxane dried over molecular sieves (D_o) is gravimetrically spiked with distilled water to produce a bulk standard solution having ~15,000 ppm of added moisture, its exact value determined by the respective weights of the two components. This bulk standard is gravimetrically diluted with the same dry dioxane to produce individual standards (D_{H2O-x}), where x represents ppm of added moisture, ranging from 0-1000 ppm. For oils, bulk oil-specific samples (e.g., canola) were prepared in two basic forms; as a "dry oil" (O_D), kept over molecular sieves and a corresponding "wet oil" (O_W) stored over excess moisture, both kept in sealed bottles for a minimum of 1 week to equilibrate prior use. These O_D-O_W oil pairs are blended gravimetrically in various proportions as required so make a series of $O_{DW(y)}$ mixtures, with y ranging from 0 →1.0 O_W. As such, the moisture content of each sample in the blend series is undefined per se, however, the change in moisture is proportionate to the amount of Ow in the blend. One set of blend samples was split into three portions, with one portion analysed by FTIR and the others sent to two independent commercial laboratories for KF analysis (ASTM 6304-07c and D1533-12).

4.2.5 Sample Preparation

A standardized sample preparation protocol was devised consisting of dispensing ~15 ml of sample (dioxane standard or an oil) by re-pipette into a tared 15 ml plastic centrifuge tube having ~ 2 ml additional head space, recording the weight of sample (±1 mg) and adding ~0.4 ml of neat TSI by micro-pipette, recording the total weight and the immediately capping the tube. These weights are used to calculate the ppm (w/w) moisture predicted for the sample from the calibration relationship devised. For dioxane, the tube is inverted several times to mix the reagent with the solvent and left to stand for a minimum of 10 min to ensure completion of the reaction. In the case of oils, the tube is thoroughly mixed on a vortex mixer for 30 sec to react and also left to stand for 10 min. If turbidity forms in any oil samples as a result of the reaction, the sample is centrifuged for 5 min at 2000x *g* to clarify them prior to FTIR spectroscopy. Prepared samples are kept hermetically sealed, are stable and must be analysed immediately upon opening.

4.2.6 Basic Spectroscopy

A single-beam air background spectrum is initially recorded and stored, followed by a single beam spectrum of the sample (dioxane standard or oil), depending on whether one is calibrating or analysing, respectively. Immediately after opening, the sample is loaded into the IR cell by controlled aspiration via the loading valve and the container re-capped. The single beam spectrum of the sample collected is ratioed against the stored single beam air background to produce an Absorbance (Abs) spectrum of the sample in the cell; the air background being refreshed every 30 minutes or so. The Abs spectra collected for the moisture-spiked dioxane reacted with TSI ($D_{H2O\text{-}x+TSI}$) serve as calibration standards, while TSI-reacted O_{DWy} oil blends serve as oil unknowns for which the moisture content is to be

predicted. Calibration and quantification are both based on differential spectroscopy, which requires the subtraction of a reference spectrum; dry dioxane (D_{o+TSI}) initially serving as a reference spectrum for calibration standards, while for oils, the reference spectrum is a molecular sieve dried oil (O_{Do}). Differential spectra (ΔAbs) are produced by a 1:1 subtraction of the reference spectrum from each of the samples analysed; e.g., $\Delta Abs = Abs_{Sample} - Abs_{Reference}$. For calibration, the peak area under the CO_2 absorption band at ~2335 cm^{-1} is measured in the ΔAbs spectra using a two point baseline located at 2300 and 2380 cm^{-1} and is subsequently related to the ppm of "added" water by linear regression. This relationship is then used to calculate moisture in ppm from the CO_2 produced in TSI-treated oil samples.

4.3 Results and Discussion

4.3.1 Analytical Concepts

The methodology presented in this Chapter was developed from the single-sample, automatable FTIR method (described in Chapter 3) to determine the hydroxyl value (OHV) of polyols. In single-sample method (Chapter 3), the measured hydroxyl value was corrected for the moisture by spectrally measuring the CO_2 produced from the reaction of water and TSI (Eq. 4-1). The ability to compensate adequately for moisture variations by measuring CO_2 led to further exploration of the TSI-H_2O reaction as a direct and specific means of quantifying moisture in hydrophobic matrices.

4.3.2 Dioxane Model System and Calibration

4.3.2.1 Moisture in Dioxane

Dioxane is an aprotic solvent of intermediate polarity which when dried (D_{H2O-0}) readily solubilizes moisture, TSI and its reaction products; including CO_2 plus the TSI-amide formed when it reacts with water (Eq. 4-1). Thus, dioxane was considered a useful solvent to study the TSI-H_2O reaction and determine if moisture can be accurately quantified by FTIR spectroscopy through the CO_2 produced. Figure 4-1 illustrates a series of absorbance spectra obtained for dioxane moisture-spiked standards reacted with TSI, covering a range of 0-1000 ppm of added H_2O ($AbsD_{H2O-0+TSI} \rightarrow AbsD_{H2O-1000+TSI}$) to which ~0.4 ml of neat TSI has been added as outlined earlier.

In these spectra, the dominant and constant spectral features are those of dioxane (e.g., off-scale CH absorptions in the 3000-2800 cm^{-1} region) which comprise the bulk of the sample spectral contributions along with its many other distinctive bands upon which are superimposed the variable spectral contributions of the CO_2 formed (~2335 cm^{-1}), the loss of TSI (~2232 cm^{-1}) and the formation of the TSI-amide (~3230 cm^{-1}); all expected outcomes of the TSI-H_2O reaction (Eq. 4-1).

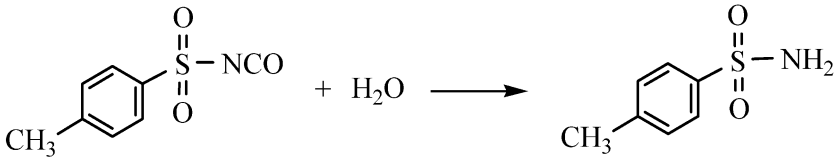

TSI *p*-toluenesulfonamide (TSA) Eq. 4-1

4.3.2.2 Differential Spectroscopy

The spectral changes in Figure 4-1 can be made more apparent (Figure 4-2) by using the sieve-dried dioxane-TSI to which no moisture has been added ($AbsD_{H2O\text{-}0+TSI}$) as the reference spectrum and subtracting it 1:1 from each of the subsequent water-spiked dioxane-TSI spectra ($AbsD_{H2O\text{-}x+TSI}$) to produce a series of differential spectra ($\Delta Abs = AbsD_{H2O\text{-}x+TSI} - AbsD_{H2O\text{-}0+TSI}$).

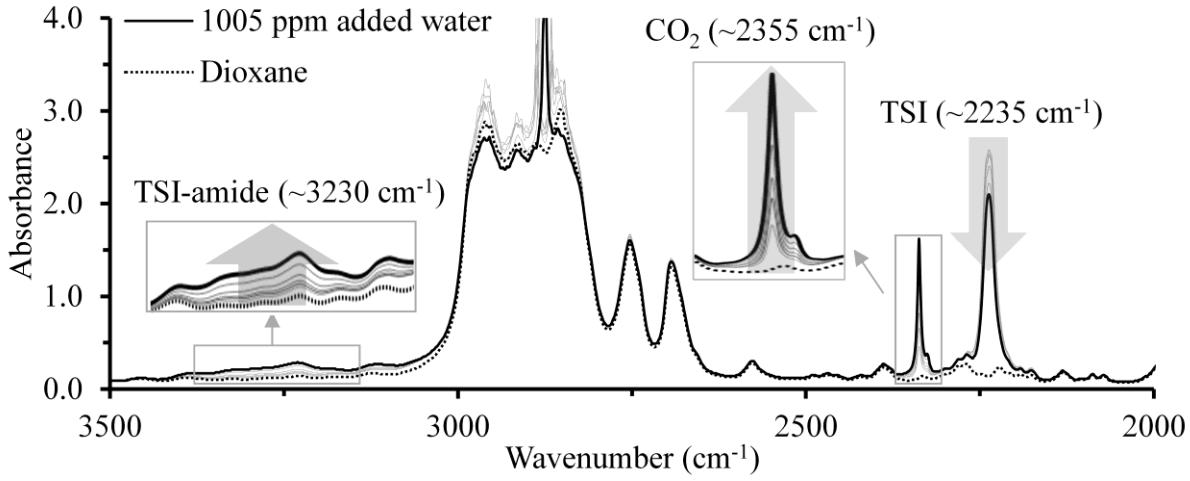

Figure 4-1 Spectra of H_2O-spiked dioxane containing 0-1000 ppm of added moisture reacted with TSI illustrating the formation of CO_2, the loss of TSI and the formation of the TSI-amide. Only the spectrum of dioxane is devoid of any CO_2 absorption (**……**) as per inset.

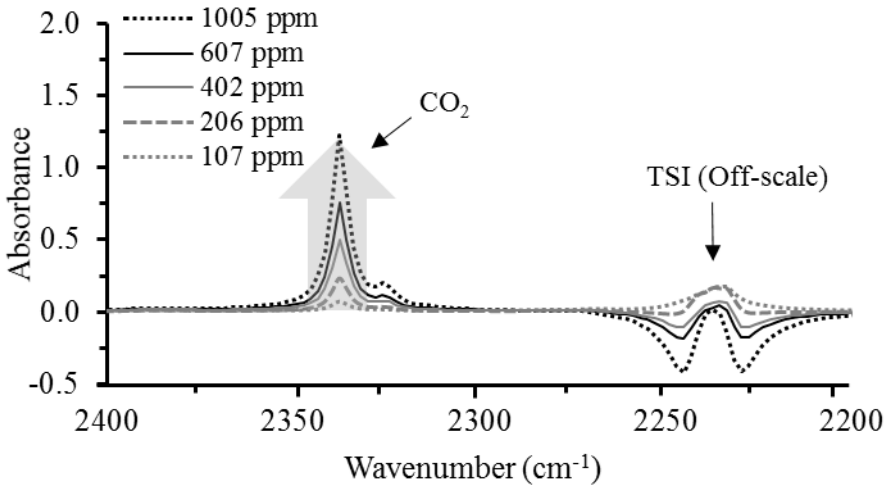

Figure 4-2 Differential spectra illustrating CO_2 being produced as a function of moisture added to dry dioxane after the spectrum of dry dioxane-TSI is subtracted from each water added standard.

The differential spectra in Figure 4-2 can be used to relate the CO_2 response directly to the amount of gravimetrically added moisture as all the common spectral features are subtracted out, leaving only the spectral changes associated with the TSI-H_2O reaction.

A negative, but rising TSI band results, however, because it is effectively off-scale at this path length (Abs >2.5 in Figure 4-1), the spectral subtraction results are meaningless. On the other hand, CO_2, the product of interest, is on-scale and increases with added moisture. Relating the CO_2 band area from 2383 to 2295 cm^{-1} using baselines set at 2100 and 2500 cm^{-1} to the added moisture (ppm) by linear regression produces the following relationship:

$$\text{Added } H_2O \text{ ppm} = 81.66 \times \text{Area } (2383 - 2295\ cm^{-1}) - 0.0454 \quad SD = 18 \quad R^2 = 0.9985 \quad \text{Eq. 4-2}$$

Eq. 4-2 is representative of absolute moisture changes in dioxane, as all other spectral contributions have been subtracted, including any moisture inherent to the dry dioxane. The relationship indicates that the moisture added to produce the dioxane-H_2O standards

can be measured to within ~20 ppm over a range of 0-1000 ppm, representing a CV of ~4%. The slope and intercept obtained when the predictions calculated are compared to the actual added moisture are very close to 1.0 (0.9996) and zero (-0.38), indicating their excellent correspondence.

4.3.2.3 Inherent Moisture and CO_2 Contributions

Although the approach used above provides an absolute measure of the changes in added moisture, it does not account for any of the inherent moisture that may be present in D_{H2O-0}, as these contributions have all been subtracted. To determine the inherent dioxane H_2O and TSI CO_2 contributions, one can derive an alternate set of differential spectra by using $AbsD_{H2O-0}$ as the reference spectrum rather than $AbsD_{H2O-0+TSI}$. By using dioxane without TSI as the reference spectrum, one is in effect subtracting a "spectrally dry" solvent from each of the TSI-reacted spectra, as no measurable CO_2 is present or produced. Thus, even if the sieve-dried dioxane used is not physically dry (generally the case), without TSI present, the solvent is by definition "spectrally" anhydrous because no CO_2 is present in solution. Even so, it is important to ensure that the moisture content of dioxane is minimal (e.g., sieve dried) so as to prevent unnecessary reagent consumption and the possibility of off-scale CO_2 responses. Using $AbsD_{H2O-0}$ as the reference spectrum, the resulting differential spectra will have a positive, but decreasing TSI band as it reacts with moisture (as per Figure 4-5) because the TSI contributions will not be ratioed out in the differential spectra. Predicting the moisture content from the CO_2 responses of these ΔAbs spectra using Eq. 4-2 produces Eq. 4-3, having a similar slope and intercept as the predictions derived from Eq. 4-2, but differs in having a significant moisture intercept rather than one close to zero.

$$\text{Predicted } H_2O \text{ ppm} = 0.9988 \times \text{Actual } H_2O \text{ ppm} + 324.66 \quad SD = 18 \quad R^2 = 0.9985 \quad \text{Eq. 4-3}$$

This intercept represents a best-fit estimate of the amount of "moisture" present in the sieve–dried dioxane used to develop the calibration. With this information in hand, one can replace the original "added" moisture calibration (Eq. 4-2), with Eq. 4-4 to predict the true moisture content of any dioxane sample analysed for moisture.

$$\text{True } H_2O \text{ ppm} = 81.66 \times \text{Area } (2383 - 2295 \text{ cm}^{-1}) + 324.66 \quad \text{Eq. 4-4}$$

$$SD = 18.3 \qquad R^2 = 0.9985$$

Although somewhat circuitous, this discussion provides the rationale as to how one can derive a valid calibration to determine absolute moisture. Ultimately, this can be achieved simply by analysing ΔAbs spectra comprised of [$AbsD_{H2O\text{-}x+TSI}$ - $AbsD_{H2O\text{-}0}$] for their CO_2 peak area responses and regressing those area values against the gravimetrically added moisture expressed as ppm. Thus, Eq. 4-2 is the basic relationship used to predict the absolute moisture content of a sample based on the standardized FTIR analytical procedure developed.

4.3.2.4 CO_2 Volatility

One of the issues to be considered is the fact that a spectral measurement is being made is of a gas in a liquid, which is not a conventional procedure in itself, with the obvious concern about potential CO_2 losses during analysis. Figure 4-3 presents comparative, duplicate predictive results obtained for a set of H_2O-spiked dioxane standards analysed consecutively within 5 min of each other, re-capped between analyses.

There is minimal divergence observable between the two plots in terms of slope differences between the consecutive analytical runs, with linear regression of one against the other producing the following relationship:

$$H_2O \text{ ppm Run2} = 0.958 \times H_2O \text{ ppm Run1} + 16.51 \qquad \text{Eq. 4-5}$$

$$SD = 21 \qquad R^2 = 0.9950$$

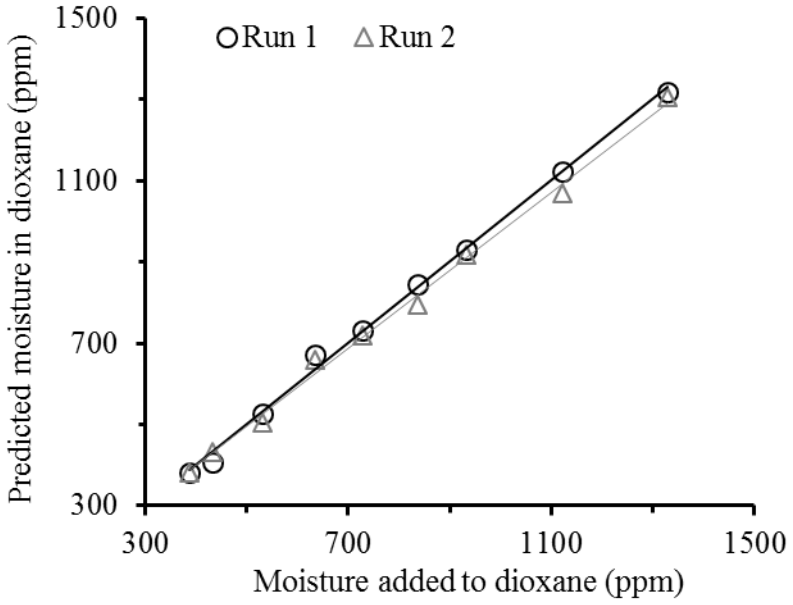

Figure 4-3 Moisture predictions obtained relative to actual amount of H_2O added to dioxane for consecutive individual samples analysed twice, each ~5 minutes apart, capping between analyses.

The slope of slightly <1.0 indicates that the relative CO_2 differences between the runs progressively increases somewhat with increasing moisture content, with the overall SD of Run2 increasing by ~3 ppm relative to Run1. Comparing mean differences between the predictions of the two runs indicates an average loss of ~1.9 % moisture as CO_2 between

runs. If a sample is left open and re-analysed consecutively over time, the regression relationship continues to deteriorate progressively. Thus, CO_2 quantification can be problematic if a sample container is left open for more than 5 min, but reliable results can be obtained for at least 2 consecutive analyses without quantification being compromised significantly. Thus for the dioxane-H_2O model, the TSI reaction is clearly stoichiometric, the CO_2 produced is retained adequately with appropriate sample handling and is readily measured spectroscopically.

4.3.3 Analysis of Dry-Wet Oil Blends

Oil represents a more hydrophobic and viscous matrix for the TSI-H_2O reaction to take place in and one of the consequences is that the TSI-amine formed may not be fully soluble in oil at higher moisture concentrations, resulting in sample turbidity and centrifugation may be necessary to clarify such samples. However, the analytical protocol and spectral processing of O_{DW} blends parallels that of dioxane in all respects so the reference spectrum used is O_{D0}, molecular sieve-dried oil without TSI present. For these gravimetrically blended oil samples, the moisture contents of O_{D0} or O_{W1} are not known, however, by definition the CO_2 spectral response predicted by Eq. 4-2 must be linearly related to the proportion of O_W in the oil blend if the reaction proceeds stoichiometrically. Figure 4-4 illustrates the differential spectra ($\Delta Abs = O_{DWy+TSI} - O_{DW0}$) obtained for a pair of spectra representing lower and higher moisture samples of O_{DW} blend spectra (where y = 0→1.0 Ow), using 15 g of canola oil reacted with ~0.4 ml of neat TSI, with the neat base oil (O_{DW0}) spectrum, without TSI present subtracted from each sample.

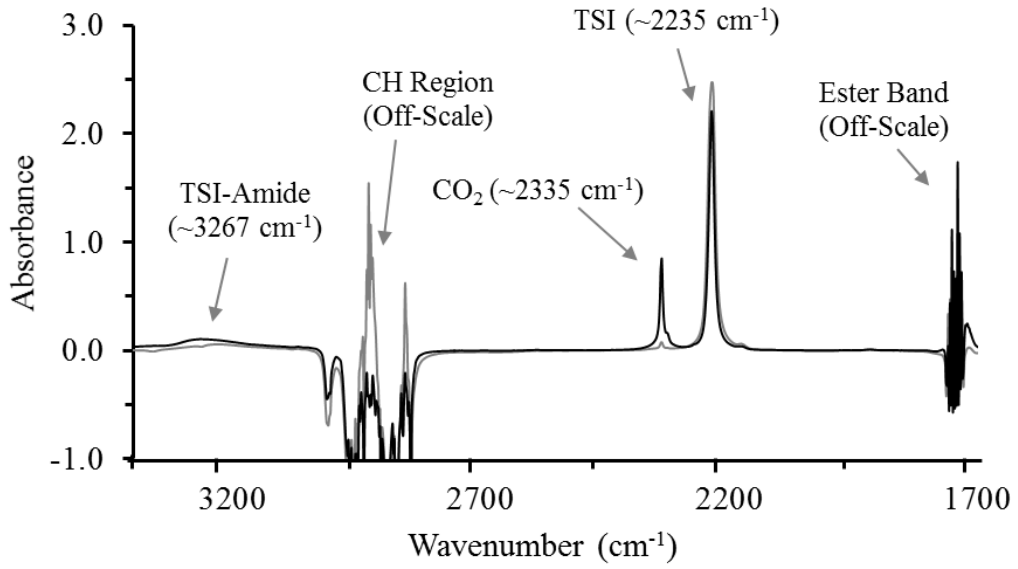

Figure 4-4 Differential spectra obtained by spectral subtraction of TSI-free canola oil (O_{D0}) from moisture variable TSI-reacted canola oil dry-wet oil blends (__ $O_{DW0.1+TSI}$ and ___ $O_{DW0.8+TSI}$).

These differential spectra parallel those of the dioxane model with a loss of TSI along with the formation of CO_2 and the TSI-amide. Here strong, noisy off-scale CH (~3000-2800 cm^{-1}) and O-C=O (1745 cm^{-1}) triacylglycerol ester linkage absorptions of the oil dominate rather than those of dioxane, but otherwise, the CO_2 band behaves very much as it did in the dioxane system, responding to increasing amounts of moisture as the amount of O_w in the blend rises. Other than for the moisture saturated standard (O_{WD1}), no turbidity was observed in any of the blends as a result of TSI-amide formation, the latter centrifuged to avoid spectral artefacts that might affect quantification. A plot of the moisture predictions obtained for duplicate consecutive analyses using Eq. 4-4 for the $O_{WD0\rightarrow1}$ blends were somewhat better in terms of SD than for dioxane, having SD's of <12 ppm. This is attributed to a combination of higher oil viscosity as well as greater matrix hydrophobicity which better retains the CO_2. As in the case of dioxane, even though O_{D0} was kept over

molecular sieves, it contained between 152-148 ppm residual moisture. This same experiment was repeated for a variety of other oils, producing essentially similar results in terms of linearity and SD's, all in the order of 10-15 ppm, the key difference being the amount of base moisture each "dry" oil contained, which ranged from 150 to 250 ppm. Thus, CO_2 linearity in the differential spectra relative to the proportion of O_W in the blend indicates that the TSI reaction proceeds in a manner very much like in dioxane, but with somewhat improved CO_2 retention characteristics.

4.3.4 Reference Oil

In the $O_{DW0\rightarrow1}$ canola oil blends as well as the other oil blends analysed, each oil-blend set consisted of a single oil-type, with the identical oil being used to prepare both the blends as well as the TSI-free reference oil. Thus, the oils used to produce their corresponding ΔAbs spectra effectively guarantee that the oil spectral contributions are accurately ratioed out. However, if applying this method for the general analysis of oils, the provenance and oil type could well be unknown. Theoretically, this is not an issue if a split-sample analysis is used, one half reacted with TSI and the other half used as the reference oil and the corresponding differential spectrum analysed; the reference oil being "spectrally" dry. Although such a split-sample approach works well, it requires the analysis of two samples to obtain a single result. For any method, whether manual or particularly if it is to be automated, minimizing sample preparation and analysis time is important and a single-sample analysis is clearly a preferred embodiment. For a generalized method a reference oil is required and would have to be selected or designated arbitrarily. Thus, there is the distinct possibility that the reference oil used could differ spectrally from the oil sample(s) being analysed which could potentially lead to residual underlying absorptions

that may affect CO_2 quantification. Here the TSI-H_2O method has a distinct advantage over previously developed stoichiometrically-based FTIR methods (e.g., AN, BN and H_2O) in that the reaction product, CO_2, absorbs in a region of the mid-infrared spectrum where no strong oil absorptions exist (see Figure 4-5). Figure 4-5 illustrates the spectrum of low moisture TSI-reacted canola oil along with three unreacted, TSI-free neat oils for comparison period. These oils selected for their divergence in their iodine value (IV) and saponification number (SN) characteristics, common determinants of spectral variability. In broad sweep spectrum in Figure 4-5, the CO_2 absorption produced by TSI-reacted canola (~200 ppm H_2O) appears substantive relative to the neat unreacted oils, which have negligible absorption in the CO_2 region. The inset illustrates however that there some minor differences, particularly for coconut oil, likely due to overtone contributions arising from the fingerprint portion of the spectrum.

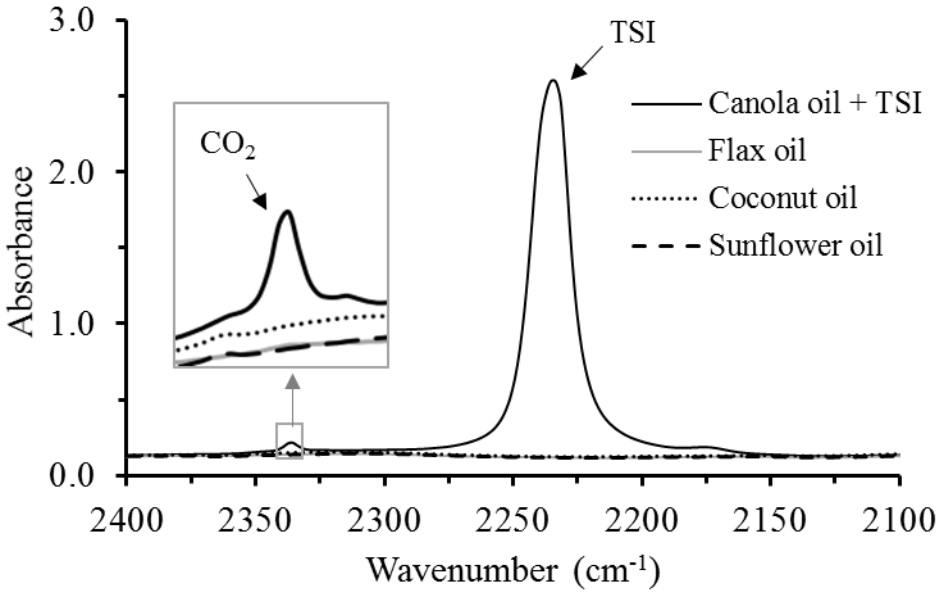

Figure 4-5 Superimposed spectra over the spectral range of 2400-2100 cm^{-1} of a low-moisture TSI-reacted canola oil compared to unreacted sunflower (- - -), coconut (. . .) and flax oil (____).

Calculating the effect of these variations by exchanging other oils to act as reference oils in the stead of the canola oil reference results in a worst-case bias of ~2 ppm, which can be further minimized and stabilized if the reference oil restricted consistently to one oil type. The lack of significant spectral compositional variability of oils in this region of the spectrum is one of the key advantages of the $FTIR_{TSI\text{-}H2O}$ CO_2 method, effectively making the results oil-type independent. Because of this, the $FTIR_{TSI\text{-}H2O}$ method can be run in the single-sample mode without requiring additional compensatory procedures. Typically a 5-5 gap-segment 2nd derivative transform has been used to further isolate the spectral response of interest and dampen oil-dependent spectral variations [19]. This approach has been used for the analysis of in-use lubricants which can be significantly affected by a wide range of undefined contaminants, with partial least squares (PLS) often utilized to further model non-correlating spectral variations to ensure correspondence to the primary reference method it is calibrated against [22]. The $FTIR_{TSI\text{-}H2O}$ method avoids these complications and serves as a primary method by virtue of gravimetric addition, thus theoretically providing a direct measure of the absolute moisture content of a sample. However, as structured, these oil blend results only serve to indicate that moisture is being tracked proportionately, with no direct numerical comparison to the results that might be obtained by well recognized KF methods.

4.3.5 FTIR vs. KF Results

To obtain a sense of where the $FTIR_{TSI\text{-}H2O}$ method stands in terms of quantitative capability relative to conventional KF procedures, a bulk set of O_{DW} sunflower oil blend samples was split into three portions. One portion was analysed by the $FTIR_{TSI\text{-}H2O}$ method developed, with the other portions sent to two certified commercial laboratories for KF

analysis; all samples were analysed in duplicate by each method. One laboratory used a direct coulometric procedure (ASTM 6304-07c) while the other used a heater-distillation unit in conjunction with coulometric detection (ASTM D1533-12). Figure 4-6 presents plots of duplicate moisture predictions obtained for each method relative to the proportion of OW in the blend along with their respective linear regression SD's.

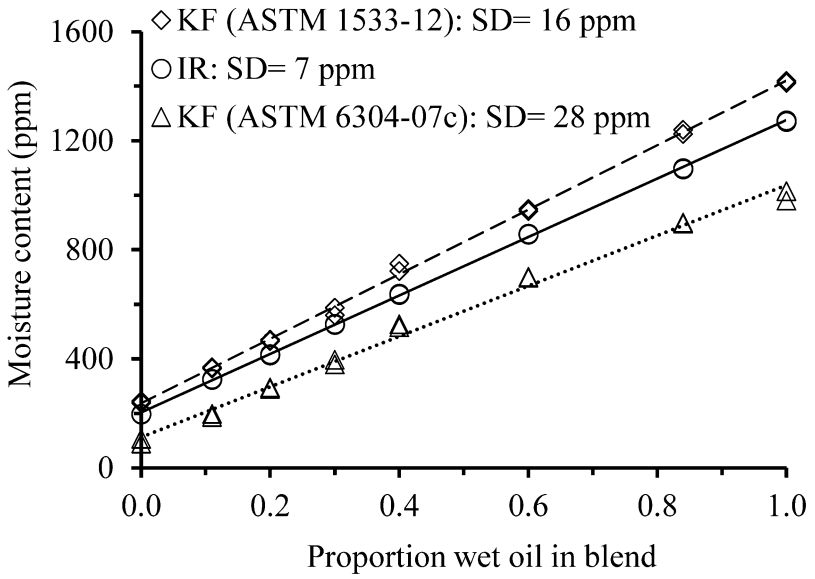

Figure 4-6 Plot of analytical results obtained for a series of dry-wet sunflower oil blends ($O_{DW0\rightarrow1}$) as determined by three methods relative to the proportion of O_W present in the blend.

All plots are linear with each method responding to the expected changes in blend moisture in a similar manner; albeit the absolute moisture values are method dependent. The FTIR results lie between those of the KF methods and it has the lowest regression SD. As to which of these results is "correct" is moot, as even in the realm of KF analysis this issue has yet to be resolved [10]. The accepted wisdom is that the KF procedures are the closest one can come to obtaining "absolute" moisture values given its well understood stoichiometry. However, the reality is that KF results obtained are in fact method, reagent and laboratory dependent and thus ultimately still relative. This has been clearly demonstrated for transformer oils where accurate analysis of very low moisture contents is critical [23]. Given these limitations, the $FTIR_{TSI\text{-}H2O}$ method clearly performs in a manner comparable to these well-established KF procedures, however, more detailed and independent confirmatory work will be required to further validate its comparative performance.

4.4 Conclusions

The key advantage of the $FTIR_{TSI\text{-}H2O}$ method is that it is based on a simple stoichiometric reaction producing CO_2. This is a strongly IR absorbing end product with an absorbance maximum located in a spectral region where most organic compounds do not absorb, thus minimizing interferences that can affect quantification. The calibration and the sample preparation are simple procedures using the TSI reagent which is readily available and inexpensive. The method has most of the positive characteristics associated with KF procedures including specificity, reproducibility, accuracy and good sensitivity. However, it lacks some key complications of KF, such as the use of proprietary reagent formulations and the use of multiple modes of end-point determination, whilst being more

amenable to automation. Any FTIR spectrometer equipped with a flow cell can be used to manually load and analyse pre-reacted samples. In addition, with relatively minor changes this methodology should be adaptable to an FTIR equipped with a programmable autosampler for the automated analysis of edible oils and other hydrophobic systems, such as in-use lubricants or transformer oils [21,22]. It may also be possible to extend and further generalize the methodology to apply to more complex systems such as food products or pharmaceuticals. To do this, it should be used in conjunction with an aprotic polar moisture extraction solvent such as acetonitrile or DMSO, which can be subsequently analysed for extracted moisture. In its current form, the $FTIR_{TSI\text{-}H2O}$ procedure is capable of quantifying moisture in edible oils in a manner comparable to standard KF procedures, providing a unique, alternative instrumental method for moisture determination.

4.5 References:

[1] Sonntag, N. O. V.: Analytical methods, in: *Bailey's industrial oil and fat products* Ed. D. Swern, John Wiley & Sons, New York 1982, pp. 484–487.

[2] Official and Tentative Methods of the American Oil Chemists' Society, Ed. D. Firestone, American Oil Chemists' Society, Champaign 1989.

[3] Chemical Online (2011) MB3600-CH20 chemicals analyzer. http://www.chemicalonline.com/doc/mb3600-ch20-chemicals-analyzer-0001. Accessed May 2013.

[4] American Association of Cereal Chemists AACC 14-15A (1995).

[5] Cedergren, A., Luan, L. W., Potentiometric determination of water using spent imidazole-buffered Karl Fischer reagents, *Analytical Chemistry*. 1998, *70*, 2174-2180.

[6] Rosvall, M., Lundmark, L., Cedergren, A., Computer-controlled, coulometric Karl Fischer system for continuous titration of water based on zero current potentiometry, *Analytical Chemistry*. 1998, *70*, 5332-5338.

[7] Cedergren, A., Jonsson, S., Diaphragm-free cell for trace determination of water based on the Karl Fischer reaction using continuous coulometric titration, *Analytical Chemistry*. 1997, *69*, 3100-3108.

[8] Cedergren, A., Jonsson, S., Progress in Karl Fischer coulometry using diaphragm-free cells, *Analytical Chemistry*. 2001, *73*, 5611-5615.

[9] Cedergre.A, Reaction rates between water and Karl-Fischer reagent, *Talanta*. 1974, *21*, 265-271.

[10] Margolis, S. A., Effect of hydrocarbon composition on the measurement of water in oils by coulometric and volumetric Karl Fischer methods, *Analytical Chemistry*. 1998, *70*, 4264-4270.

[11] van de Voort, F. R., Ghetler, A., Garcia-Gonzalez, D. L., Li, Y. D., Perspectives on quantitative mid-FTIR spectroscopy in relation to edible oil and lubricant analysis: evolution and integration of analytical methodologies, *Food Analytical Methods*. 2008, *1*, 153-163.

[12] Man, Y. B. C., Mirghani, M. E. S., Rapid method for determining moisture content in crude palm oil by Fourier transform infrared spectroscopy, *Journal of the American Oil Chemists' Society*. 2000, *77*, 631-637.

[13] A. Rohman, Y. B. C. M., Analysis of water content in soap formulation using Fourier transform infrared (FTIR) spectroscopy, *Journal of Applied Sciences Research*. 2009, *5*, 717-721.

[14] Cerretani, L., Giuliani, A., Maggio, R. M., Bendini, A., Toschi, T. G., Cichelli, A., Rapid FTIR determination of water, phenolics and antioxidant activity of olive oil, *European Journal of Lipid Science and Technology*. 2010, *112*, 1150-1157.

[15] van de Voort, F. R., Sedman, J., Yaylayan, V., Saint Laurent, C., Mucciardi, C.,, Quantitative determination of moisture in lubricants by Fourier transform, *Applied Spectroscopy*. 2004, *58*, 193-198.

[16] Al-Alawi, A., Van De Voort, F. R., Sedman, J., A new Fourier transform infrared method for the determination of moisture in edible oils, *Applied Spectroscopy*. 2005, *59*, 1295-1299.

[17] Al-Alawi, A., van de Voort, F. R., Sedman, J., Ghetler, A., Automated FTIR analysis of free fatty acids or moisture in edible oils, *Journal of Laboratory Automation*. 2006, *11*, 23-29.

[18] van de Wort, F. R., Sedman, J., Cocciardi, R., Juneau, S., An automated FTIR method for the routine quantitative determination of moisture in lubricants: An alternative to Karl Fischer titration, *Talanta*. 2007, *72*, 289-295.

[19] Xianghe, M., Sedman, J., Voort, F. R. v. d., Improving the determination of moisture in edible oils by FTIR spectroscopy using acetonitrile extraction, *Food Chemistry*. 2012, *135*, 722-729.

[20] Ng, E.-P., Mintova, S., Quantitative moisture measurements in lubricating oils by FTIR spectroscopy combined with solvent extraction approach, *Microchemical Journal*. 2011, *98*, 177-185.

[21] Hadjadj, Y., Fofana, I., van de Voort, F. R., Bussieres, D., Potential of determining moisture content in mineral insulating oil by Fourier transform infrared spectroscopy, *Ieee Electrical Insulation Magazine*. 2016, *32*, 34-39.

[22] Winterfield, C., van de Voort, F. R., Automated Acid and Base Number Determination of Mineral-Based Lubricants by Fourier Transform Infrared Spectroscopy: Commercial Laboratory Evaluation, *JALA*. 2014, *19*, 577-586.

[23] Margolis, S. A., Amperometric measurement of moisture in transformer oil using Karl-Fischer reagents, *Analytical Chemistry*. 1995, *67*, 4239-4246.

CHAPTER 5

Measurement of Oxirane and Iodine Value Changes during the Epoxidation of Vegetable Oils by ATR-FTIR Spectroscopy[4]

5.1 Introduction

In the epoxidation of unsaturated vegetable oils, double bonds present on the fatty acid chains are converted into oxirane groups. These oxirane functional groups can be used as intermediate in order to produce a range of useful products such as polyols, epoxy resins, alkylamines, and polyesters, including alkyds and polyurethane [1].

Epoxidation of double bonds can be achieved in a variety of ways [2] with the use of percarboxylic acids being the most commonly used technique [3]. This is usually accomplished by forming a percarboxylic acid *in situ* by the reaction of short chain carboxylic acids, typically formic acid or acetic acid, with H_2O_2. The peracid produced in this manner acts as an oxygen carrier, facilitating the conversion of double bonds into oxirane groups with the release of the parent carboxylic acid, from which the peracid can be regenerated.

[4] A version of this chapter has been submitted as: Tavassoli-Kafrani, M. H., Curtis, M. J., and Van de Voort, F. R., *European Journal of Lipid Science and Technology,* 2016.

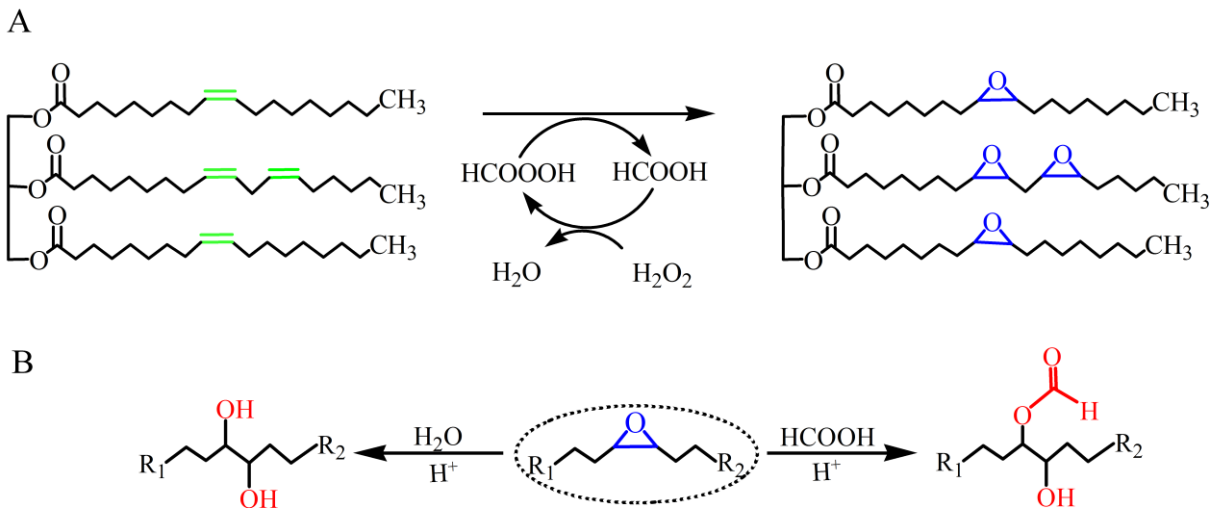

Figure 5-1 Schematic illustration of (A) the ideal epoxidation reaction of vegetable oil double bonds in the presence of formic acid and hydrogen peroxide and (B) the side reactions of oxirane group which can result in less than 100% conversion.

The overall oxirane formation reaction is illustrated in Figure 5-1A. However, side reactions facilitated by acid catalysis (Figure 5-1B) can result in oxirane ring opening. Thus, the OOC of epoxidized oils can vary and tend to be lower than the theoretical OOC calculated based on the overall degree of unsaturation of the oil. In both commercial production and in product development work, the ability to maximize OOC in relation to the reaction conditions is of high importance and to achieve this the ability to monitor OOC is critical.

The two common approaches used to track the progress of an epoxidation reaction are monitoring the loss of double bonds or monitoring the formation of OOC. Ideally, both parameters are monitored and the difference between the molar consumption of double bonds and formation of oxirane groups is a measure of the extent of any side reactions, and so reflects the overall selectivity of the reaction. The degree of unsaturation of oils and their derivatives is commonly expressed as iodine value (IV), defined as the weight of iodine absorbed by one hundred grams of

oil (gI_2/100 g). IV is usually determined directly by titration using standard methods such as those of the American Society for Testing Materials (ASTM) and other standards organizations [4-8]. These all involve the reaction of an excess amount of iodine with the oil in acetic acid and then titration of unreacted iodine with standard sodium thiosulfate solution to determine the amount of iodine that reacted with the oil. An alternate, albeit indirect approach, is by GC to determine the overall fatty acid composition of the oil [9,10], from which the IV can be calculated. Fourier transform infrared (FTIR) spectroscopy has also been used for the determination IV of fats and oils [11-14], generally based on measuring characteristic olefinic functional group absorbances. Mid-FTIR spectroscopy has found a variety of applications in the analysis of oils, its key advantage being a simple and rapid instrumental methodology, not requiring the use of solvents and reagents associated with wet chemical methods.

Like IV, the OOC of epoxidized oils is conventionally determined by standard wet chemical methods (ASTM D1652-11[15] or AOCS Cd 9-57 [16]), in this case by titration of the oil with hydrogen bromide in glacial acetic acid (Eq. 5-1).

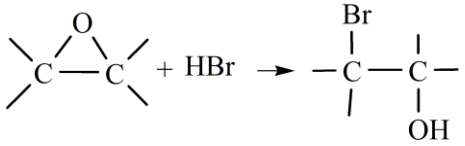

Eq. 5-1

A generalized near-FTIR (FT-NIR) procedure has been reported which measures oxirane, IV and moisture content of epoxidized soybean oil [17]. Unlike in mid-FTIR spectroscopy, where measurements are made using well-defined fundamental functional group absorptions, in FT-NIR methods overtone absorptions are examined for spectral changes. This process is dependent on chemometrics, such as partial least squares (PLS) procedures, to develop quantitative relationships between NIR data and data obtained using primary methods. Developing such calibrations can be difficult, time-consuming and is often limited to a single oil-type, as a universal calibration can be

overwhelming to develop given the spectral variability of between oil types. Hence, although this approach has the benefit of analytical simplicity once developed, it tends to be oil specific rather than a general procedure applicable for all oils. Based on our knowledge, no generalized mid-FTIR methods have been developed to date to track both IV and OOC changes over the course of epoxidation process. This Chapter describes the development of an ATR-FTIR method for the rapid determination of IV changes (ΔIV) and OOC during epoxidation. This method allows for monitoring the progress of oil epoxidation reactions and so optimizing the end-point of the reaction.

5.2 Experimental

5.2.1 Materials

Food-grade, refined canola oil was obtained from a local retailer, with commercial flax oil (NuLin 50) and camelina oil purchased from Viterra Inc. (SK, Canada) and Linnaeus Plant Science Inc. (BC, Canada), respectively. Hydrogen peroxide (technical grade ≥35%), formic acid (technical grade ≥85%) and sodium sulfate were purchased from Univar (AB, Canada) with analytical grade ethyl acetate obtained from Fluka Analytical Sigma-Aldrich (ON, Canada).

5.2.2 Instrumentation

The spectrometer used in this study was a Bruker Alpha FTIR spectrophotometer (Bruker Optics, Esslingen, Germany) equipped with an ATR single-bounce diamond crystal. Spectra were collected at a resolution of 4 cm^{-1} over the range of 410-4000 cm^{-1}. A total of 24 scans (~30 sec) were acquired and averaged using OPUS software version 6.5 provided by Bruker. A background spectrum of the clean ATR crystal was collected before applying and collecting the sample spectrum. The ATR crystal wiped with a 1-propanol wetted tissue between analyses and allowed

to dry before anlysing the subsequent sample. Spectral examination, measurements, and processing were carried out using Nicolet Omnic software.

5.2.3 Fatty Acid Composition by GC

Methyl ester derivatives of the oils were prepared by reacting of oil in a hexane solution with methanolic potassium hydroxide at 50 ºC for about 10 min. The methyl esters were separated and analyzed using a Perkin Elmer Clarus 500 gas chromatograph (Perkin Elmer Instruments LLC, CT, USA) equipped with a flame ionization detector (FID). Separation was achieved using a 100 m × 0.25 mm Supelco SP-2560 capillary column having a stationary phase film thickness of 0.2 µm. Two µl of the methyl ester solution was injected onto the column at 240 ºC using a split ratio of 20:1 and Helium as the carrier gas at a flow rate of 1.3 ml/min. The system was temperature programmed stepwise, starting at an initial oven temperature of 45 ºC, with an initial 4 min hold, followed by an increase to 175 ºC at 13ºC/min; a second 27 min hold at 175ºC, ramped up to 215ºC at 4 ºC/min and concluding with a 35 min hold for a total run time of 86 min with the detector maintained at 280ºC throughout the run.

5.2.4 Epoxidation of Oils

The epoxidation of the oils was performed using performic acid produced *in situ* by the reaction of formic acid with hydrogen peroxide. About 500 g of oil and ~300g of 35% hydrogen peroxide were transferred into a 2 L glass reactor equipped with a water heating/cooling system and an overhead mechanical stirrer. The mixture was stirred vigorously (~350 rpm) at room temperature while 30.8g of 85% formic acid was added to the reactor dropwise (~15 min) with constant stirring. Once all the formic acid had been added, the temperature was increased at a rate of ~10 °C per each 10 min from ~ 25°C to the final temperature of ~50 ± 5°C for canola and flax oils and ~60 ± 5°C for camelina oil. Because of the exothermic nature of the reaction, the

temperature was carefully controlled by cooling. The reaction was continued for 30-52 hours to complete the epoxidation reaction to produce a crude oil epoxide, the end product. Determination as to whether the reaction has gone to completion being a function of the plateauing of the IV and OOC analytical values. The crude epoxidized oil produced is then transferred to a large separatory funnel, and ~ 250 ml of ethyl acetate was added and after mixing, it was washed with four 500 ml aliquots of saturated NaCl solution. In each time the salt solution was discarded and the organic phase retained. The pH of the last salt water wash is assessed to verify that all residual acid had been removed (pH> ~5).Then sodium sulfate (~250g) was added to the organic phase (epoxidized oil in ethyl acetate) to remove residual water and then, the mixture was filtered through Whatman No. 1 filter paper to remove residual particulates. The ethyl acetate was then removed using a rotary evaporator under vacuum, to produce a purified epoxidized oil product.

5.2.5 Sampling and Analysis

Figure 5-2 presents a comparative schematic diagram illustrating the main steps associated with sample preparation for the ASTM titration and ATR-FTIR procedures. At various times of the epoxidation reaction, two 15 ml portions of the reaction mixture were collected; one portion for OOC and IV analysis by ATR-FTIR and the second portion for parallel titrimetric analyses. Sample preparation for the two approaches were similar, both using washing the sample multiple times with brine in a 45 ml centrifuge tube, the key difference was the requirement for ethyl acetate addition for the titrimetric samples and the need for its removal using rotary evaporation at the end of the procedure. Washing was accomplished using ~5 ml of saturated brine, the mixture was vigorously shaken and then centrifuged at ~2500 g for ~2 min. The washing step was performed for two further times. The final product from either process was stored in 10 ml capped glass vials and used for their respective analyses.

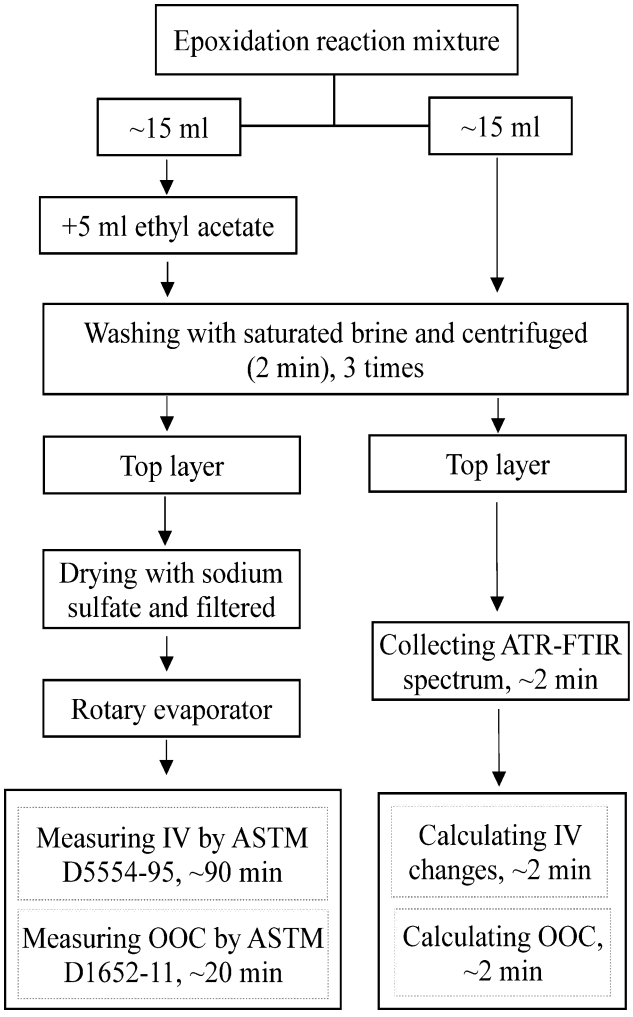

Figure 5-2 Comparison of sample preparation procedures for measuring IV and OOC using the ASTM and ATR-FTIR methods to measure and the time involved in each process.

5.2.6 Oxirane and Iodine Value by Titration

Titrimetric IV and OCC determinations of in-process reaction samples were made using ASTM D5554-95 [4] and ASTM D1652-11 [15], respectively.

5.2.7 Calibration

In developing FTIR calibrations for IV and OOC, bulk samples of epoxidized canola oil (ECO) and canola oil (CO) were analyzed for the IV and OOC using the standard titrimetric methods (Section 5.2.6). Subsequently, a series of 10 g samples were prepared by gravimetrically blending ECO and CO in various ratios of 0.0→1.0 ECO relative to the sum of the two components (ECO/(ECO + CO)) using ECO intervals of ~0.1. The ATR-FTIR spectra of these blended samples were collected. The spectrum of the canola oil sample was subtracted from the spectrum of each blended sample to obtain its differential spectrum (Δ_{Abs} =A_{Blend}-A_{CO}). The area of the bands associated with double bond absorptions as well as that of the oxirane absorptions were determined in the resulting differential spectra as per 5.2.8 and plotted against the titrimetric IV and OOC values determined for the same samples, respectively. Calibrations were derived by linear regression of the IV and OOC areas *vs*. the titrimetric results. These calibrations were used to measure the changes in IV and OOC of samples collected over the course of the epoxidation reaction using the FTIR absorptions associate with double bonds and oxirane groups.

5.2.8 OOC and IV Determination by ATR-FTIR

The ATR-FTIR spectra of samples taken during the epoxidation process were collected over time (t) after being prepared for analysis as per Figure 5-2. For each sample taken, the differential spectrum relative to that of the starting oil (ΔAbs = A_t - A_0) was determined and the area related to double bond absorptions was calculated over the region of 3017.5-3004.2 cm^{-1} relative to baseline points located at 3035.2-2500.4 cm^{-1}. The oxirane band area was calculated for the same spectra using two regions; 1497.3-1432.0 cm^{-1} and 862.3-762.2 cm^{-1}, with the baselines points located at the start and end of each region. The measured peak was converted to their respective IV and OOC contents using calibration curves derived in Section 5.2.7.

5.2.9 Validation

Canola, camelina, and flax oils were epoxidized according to the procedure described in Section 5.2.4, with samples collected over the course of the epoxidation reaction. The IV and OOC of these samples were also determined by standard titrimetric methods after the purification process outlined in Figure 5-2, and results were compared to the values determined by ATR-FTIR. These particular oils were chosen as systems for study because each has a substantially different fatty acid profile and cover a wide range of IV values (~119→211 $gI_2/100g$).

5.3 Results and Discussion

5.3.1 Fatty Acid Profile of Vegetable Oils

Table 5-1 presents the dominant unsaturated fatty acids present in canola, camelina and flax oils, as determined by GC analyses, along with their calculated IV.

Table 5-1 Gross unsaturated fatty acid composition of selected oils as determined by GC.

Oil	saturated	Fatty acid (%)				IV ($gI_2/100g$)
		C18:1	C18:2	C18:3	C20:1	
Canola	6.6	62.8	19.3	8.9	1.2	119
Camelina	12.1	21.7	24.5	27.7	13.1	152
Flax	8.3	13.3	15.8	61.3	0.2	211

Oleic acid is the major fatty acid in canola oil, representing ~ 63% of the total fatty acids while in flax oil, linolenic (C18:3) is the most abundant fatty acid present in a similar amount. Camelina oil contains similar amounts of all three common unsaturated fatty acids, oleic, linoleic and linolenic fatty acids, all in the range of 21.7-27.7% in addition to the significant amount of

eicosanoic acid (~13%). As such, these oils cover a wide range of IV, their range being representative of many other vegetable oils commonly considered for epoxidation.

5.3.2 Epoxidation

As noted, along with the desired epoxidation reaction, side reactions such as ring opening of the epoxide groups by water or formic acid can occur which can lower the final OOC of the end product. Ring opening by water results in formation of secondary hydroxyl groups, and ring opening by formic acid leads to formation of a secondary hydroxyl group and ester linkage (Figure 5-1B). In order to minimize ring-opening reactions and achieve maximum OOC, the optimum time for epoxidation under any specified reaction conditions must be determined.

Figure 5-3 illustrates the spectra of canola oil samples taken over time while undergoing epoxidation; each first washed with brine and then subjected ATR-FTIR analysis, with the insets providing more detail. As can be seen, variations are apparent in the double bond absorption regions as well as in the fingerprint region. There is a relatively strong signal due to the double bond CH stretch absorption at ~3010 cm^{-1} as well as a weaker double bond C-C stretch around ~1654 cm^{-1}. Both of these start at a maximum value and drop as epoxidation proceeds as double bonds are lost to the reaction. The oxirane groups have a relatively distinct absorption at ~826 cm^{-1}, representing the stretching of C-O-C of oxirane group as well as a weaker but sharper absorption at ~ 1470 cm^{-1} due to oxirane C-C stretching, these increasing as the reaction proceeds. The changes in absorption of these bands were used to develop an ATR-FTIR method for the simultaneous measurement of ΔIV and OOC.

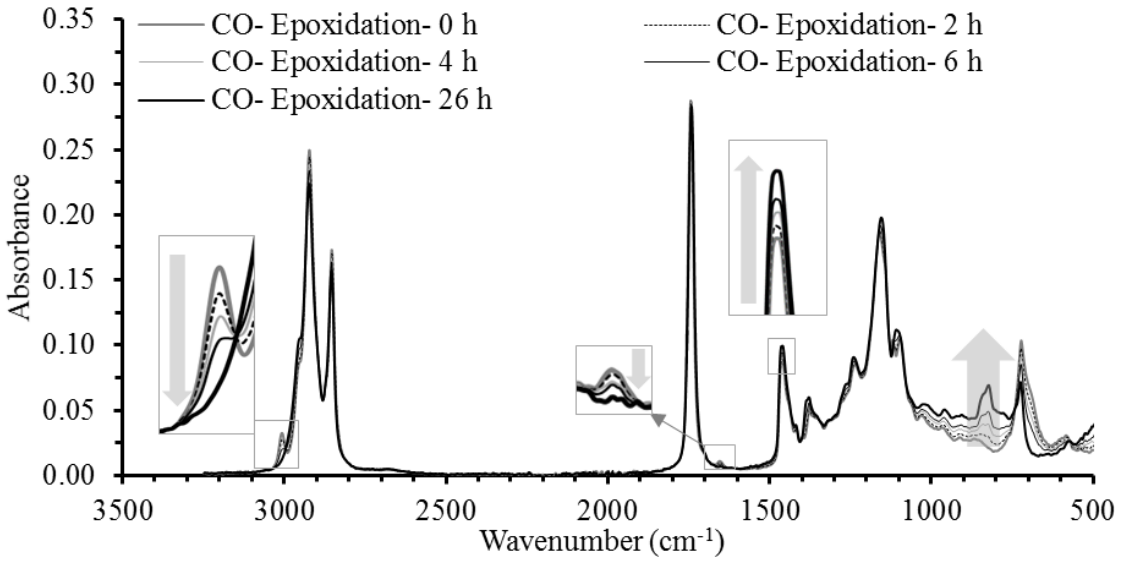

Figure 5-3 The ATR-FTIR spectra of canola oil (CO) undergoing epoxidation, the inset providing more detail and the arrows indicating the direction of absorbance changes as a function of epoxidation time.

5.3.3 Calibration

Calibration standards were prepared as per Section 5.2.7 by gravimetrically blending an epoxidized canola oil (ECO) with an unreacted canola oil (CO) to vary the OOC and IV. Figure 5-4 presents the ATR-FTIR differential spectra (ΔAbs) of these gravimetric blends obtained by subtracting the CO spectrum from each of the blended samples.

Calibrations were derived by measuring the band area of the double bond CH stretch region ~ 3010 cm^{-1} to determine IV and both oxirane absorptions (~1470 cm^{-1} and ~ 826 cm^{-1}) regions to determine OOC in these differential spectra. The IV and OOC values assigned to the spectra of the blends were simply based on the values calculated from the titrimetric analysis of the unreacted canola oil and the fully epoxidized canola oil, taking into account the proportion of each in the blend. Figure 5-5 illustrates the calibration plots obtained along with their respective linear regression relationships.

These calibrations theoretically represent the ideal relationship one would expect if the epoxidation reaction proceeds stoichiometrically, without any side reactions. Although ideal and not necessarily representative of the actual spectral changes taking actually place in the reaction process, such a calibration provides a simple means by which one can convert the absorption changes observed in the differential spectra of real samples undergoing epoxidation to their corresponding apparent IV and OOC titrimetric values. The key question is whether these simulated reaction blends and the calibrations derived therefrom are capable of adequately predicting IV and OOC, given that in the real reaction, additional spectral changes might occur which may confound the predictions relative to those obtained by the standard methods.

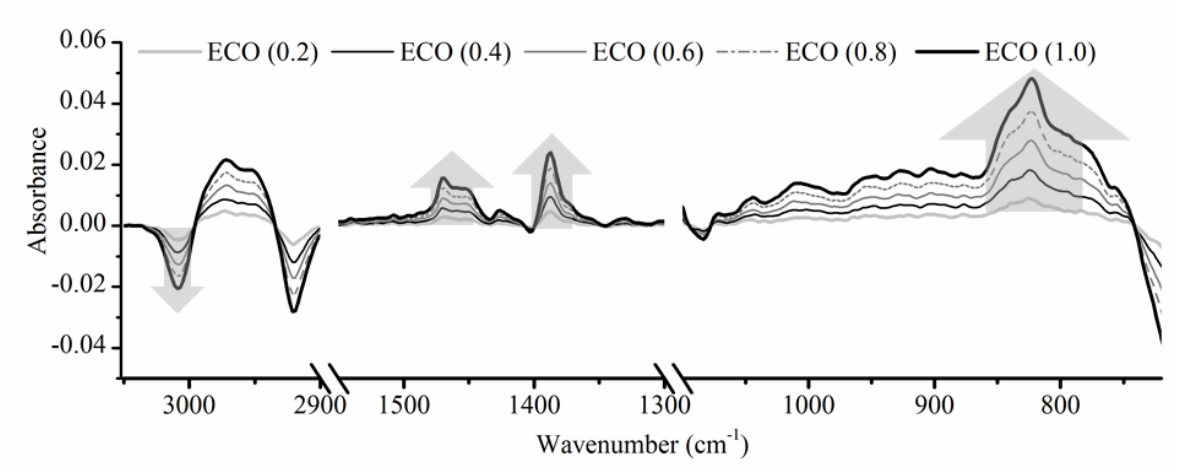

Figure 5-4 Spectral changes observed in the differential spectra of canola oil calibration standards produced by proportionately blending canola oil and fully epoxidized canola oil, the highlighting the areas used for deriving a calibration for IV (~ 3010 cm^{-1}) and OOC determination (~1470 cm^{-1} and at ~ 826 cm^{-1}).

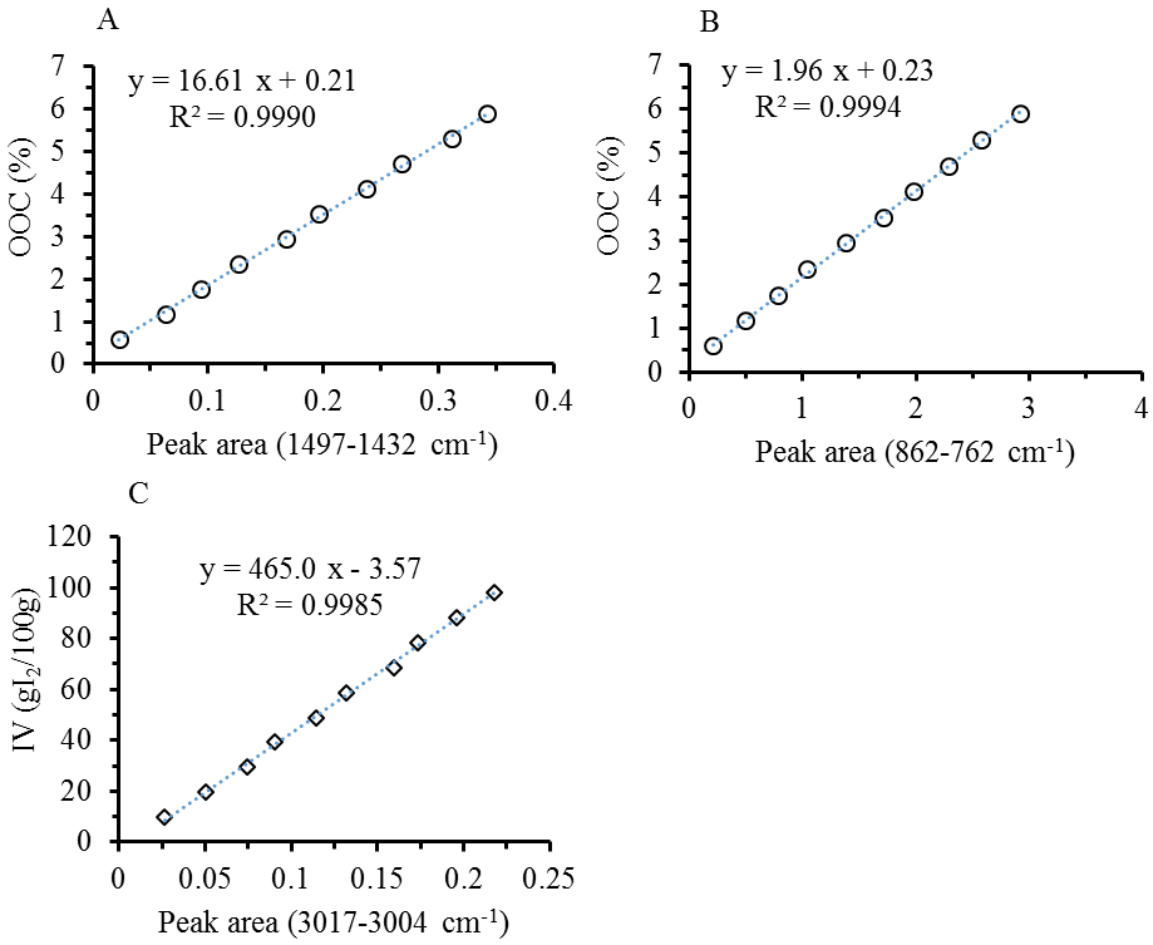

Figure 5-5 Plots of OOC and IV of a series of ECO-CO blends (0 →100% ECO) vs. band area measured in the differential spectra ($\Delta Abs = A_{blend}-A_{CO}$). (A) oxirane content against 1497-1432 cm^{-1} band area; (B) oxirane content against 862-762 cm^{-1} band area; and (C) IV against 3017-3004 cm^{-1} band area.

5.3.4 Validation

To validate the calibration model devised, camelina, flax, and another canola oil were subjected to epoxidation and samples were collected over time and brine-washed. These samples were analyzed by ATR-FTIR and the ASTM titrimetric methods to predict their IV and OOC and the results were compared.

5.3.4.1 Oxirane Oxygen Content

Figure 5-6 represents the changes in OOC (%) for camelina, flax and canola oils during the epoxidation as measured by ASTM D1652-11 (Δ) and by ATR- FTIR, using each of the two oxirane correlated regions; ~1497-1432 cm^{-1} (o) and 862-762 cm^{-1} (∗) as measured in the differential spectra. In all cases, the OOC increases, reaches a maximum and then decreases slightly as the ring opening reactions occur after plateauing. There is an excellent correspondence between the ASTM OOC predictions and those obtained by the $FTIR_{(1497-1432)}$ band. However, the predictions obtained using the $FTIR_{(862-762\ cm)}$ band deviate significantly for flax and less so for camelina oils, being biased to significantly higher values as the reaction begins to plateau. The response of this band appears to be dependent on the unsaturated fatty acid makeup, albeit the effect is seen predominantly in the latter phases of the reaction. It is likely that given the greater response to flax specifically and camelina oil to a lesser degree and the correct response to canola oil, that this effect may be due to the presence of additional unconjugated oxirane groups leading to absorption increases not accounted for in the canola oil calibration model. What is clear is that the $FTIR_{(1497-1432)}$ band does track the ASTM results well for all three oils and does not appear to be affected by any notable interferences.

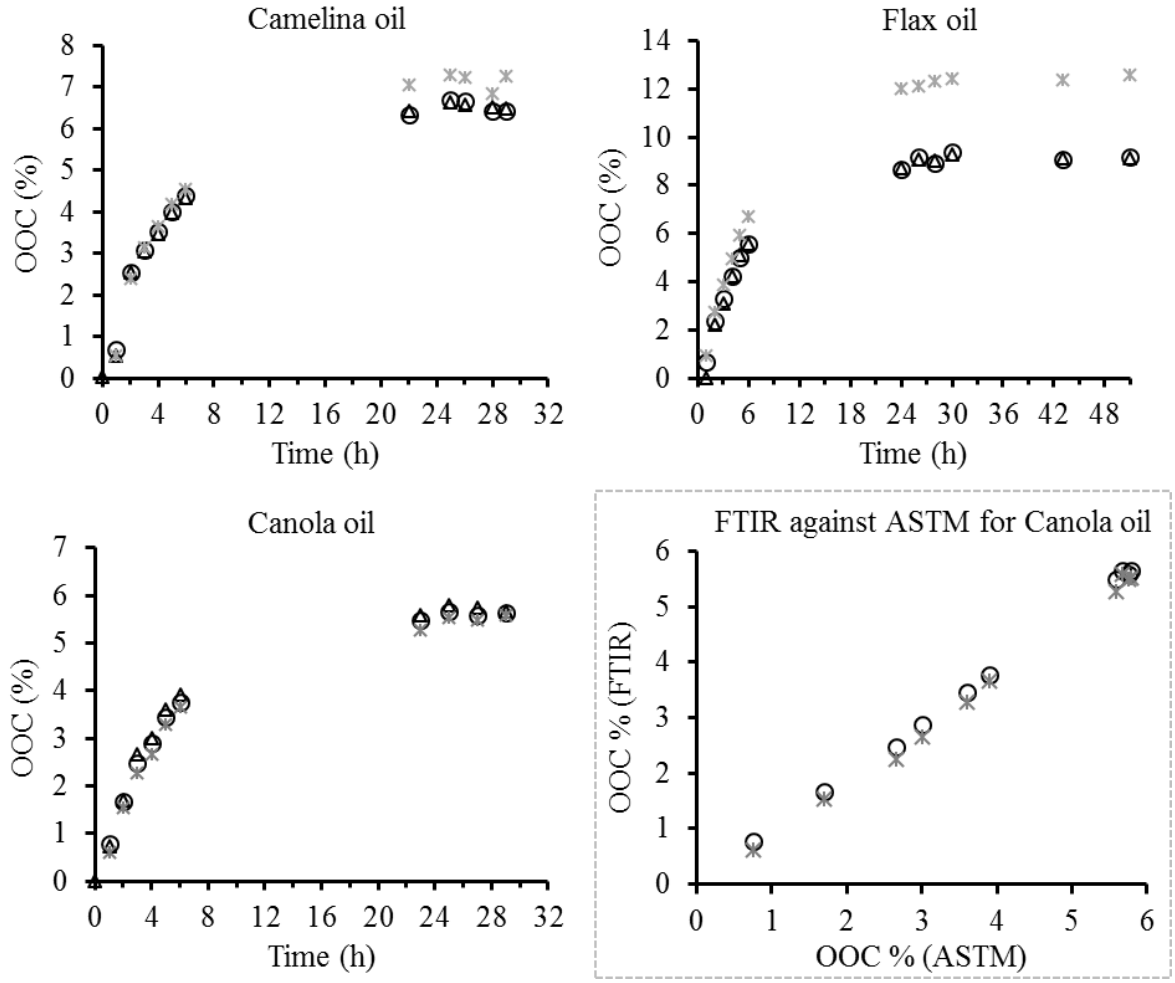

Figure 5-6 Monitoring the OOC (%) during the epoxidation of camelina oil, flax oil and canola oil using ASTM D1652-11 (Δ), $FTIR_{(1497\text{-}1432)}$ (o), and $FTIR_{(862\text{-}762)}$ (*) methods along with the linear regression plot for the OOC (%) measured by FTIR methods against that of ASTM D1652-11 method for canola oil epoxidation as an example.

It was found that overall both the $FTIR_{(862\text{-}762)}$ and $FTIR_{(1497\text{-}1432)}$ bands produced linear correlations to results from the ASTM method, but that only the regression equations obtained for $FTIR_{(1497\text{-}1432)}$ (Table 5-2) produced slopes consistently close to the desired value of ~1.0 along with relative error and CVs of an acceptable magnitude.

Table 5-2 Summary of the regression relationships obtained for plots of OOC predicted by FTIR *vs*. the results of ASTM D1652-11 titrimetric determinations.

	Slope	Intercept	R^2	Mean RE [a] (%)	Mean CV [b] (%)
Canola oil					
$FTIR_{(1497-1432)}$	0.984	-0.04	0.999	2.77	1.05
$FTIR_{(862-762)}$	0.997	-0.24	0.997	6.56	0.92
Camelina oil					
$FTIR_{(1497-1432)}$	0.982	0.08	0.999	1.14	0.93
$FTIR_{(862-762)}$	1.117	-0.24	0.996	7.10	0.98
Flax oil					
$FTIR_{(1497-1432)}$	0.987	0.11	0.999	1.16	0.72
$FTIR_{(862-762)}$	1.412	0.57	0.992	32.04	1.10

[a] RE: relative error of OOC measured by FTIR from OOC determined by ASTM
[c] CV: coefficient of variation of duplicate measurements of OOC by FTIR

The reaction time required to achieve a maximum OOC is an important parameter to determine for any oil undergoing epoxidation, which can be much more readily monitored and quantified using ATR-FTIR. Either band can be used to determine the endpoint spectrally, simply by monitoring the absorbance. However, unless those values are converted to OCC, one has no sense of what the actual values are, which can only be determined with any degree of confidence if the $FTIR_{(1497-1432)}$ band is used. Using this technique, the reaction end-points were determined to be at 25, 25, and 30 h by both the FTIR and ASTM methods for canola, camelina, and, flax oils respectively.

5.3.4.2 Loss of Double Bonds

In addition to OOC measurement, it is useful to be able to monitor the loss of double bonds as the epoxidation reaction proceeds since it provides an estimate of the selectivity of the reaction towards epoxide formation. Amongst the regions associated with double bond absorptions, the ~ 3017-3004 cm^{-1} region showed the best correlation to the IV changes determined by the ASTM D5554-95.

In order to demonstrate this, a series of samples were prepared by blending canola oil and epoxidized canola oil so as to provide samples with a range of both OOC and IV. Figure 5-5C presents a plot of IV, as determined by the ASTM method, *vs.* the peak area in the differential spectra of these samples (i.e. $\Delta_{Abs} = A_{Blend} - A_{CO,}$ see Section 5.2.7). A linear relationship is obtained which allows for the direct conversion of the spectral peak area into IV. However, all unconjugated double bonds absorb in the region of the IR spectrum used, albeit at slightly different maxima. Thus, it would not be completely accurate to use this relationship directly for all oil types, as it is specific to canola oil. A proposed alternative is to use the changes in the peak areas measured for this region of the IR spectrum, as a generalized measure of the change in IV (ΔIV), rather than measuring an absolute IV.

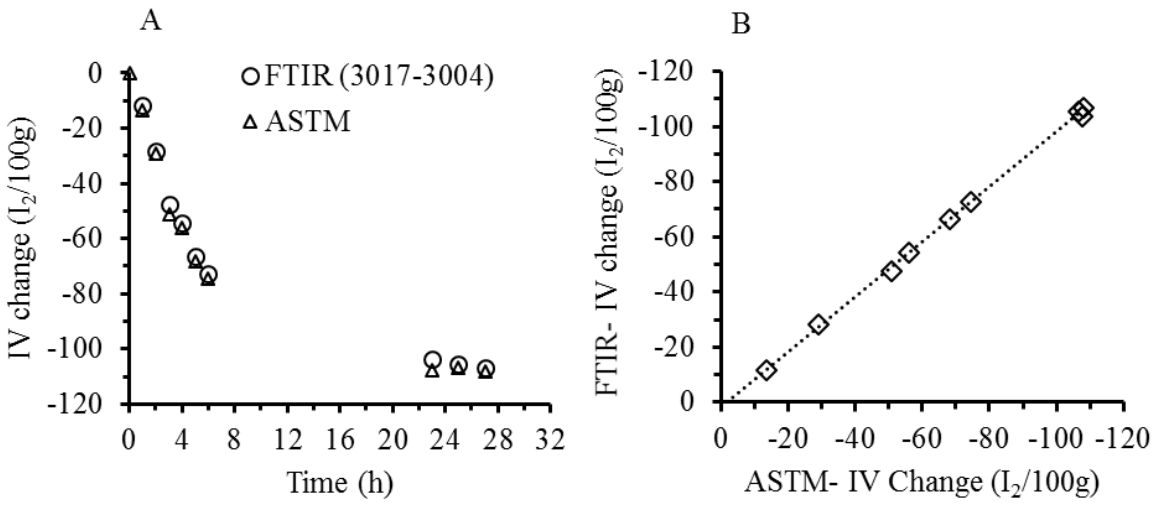

Figure 5-7(A) Plot of ΔIV (gI_2/100 g) *vs.* the epoxidation reaction time for canola oil determined by ASTM D5554-95 and by predictions obtained using the $FTIR_{(3017\text{-}3004\ cm\text{-}1)}$ area measurements, and (B) linear regression plot ΔIV determined by FTIR against that determined by ASTM D5554-95.

In this way, using the same differential spectra obtained earlier for the epoxidation reaction, the ΔIV values were determined from the areas under the 3010 cm^{-1} band for each of the oils. Figure 5-7A illustrates ΔIV for canola oil as a function of time as determined by both the IR and titrimetric methods, both of which give very similar results. The loss of IV was high initially followed by an exponential decay to an asymptote. Similar trends were observed for camelina and flax oils (data not shown). The equivalence between ΔIV ASTM vs ΔIV IR methods is illustrated in Figure 5-7A which shows a linear relationship with a slope of 1. The regression equations obtained from these plots are summarized in Table 5-3.

There is an excellent agreement between ΔIV values measured by the $FTIR_{(3017\text{-}3004)}$ method and the ASTM D5554-95 method, as illustrated by the regression equations presented in Table 5-3. This is valid for oils having an IV range of 119 to 211 I_2/100g, which encompasses most oils containing one to three double bonds. As such, FTIR can also be used to monitor the loss of double bonds in the form of ΔIV as well as OOC during the epoxidation of vegetable oils.

Table 5-3 Linear regression comparison ΔIV measured by the ATR-FTIR$_{(3017\text{-}3004)}$ method *vs.* the ASTM D5554-95 method.

Oil	Slope	Intercept	R^2	Mean RE [a] (%)	Mean CV [b] (%)
Canola oil	0.997	-1.70	0.999	2.84	1.80
Camelina oil	0.986	1.94	0.997	2.81	1.62
Flax oil	1.002	2.44	0.998	2.48	2.22

[a] RE: relative error of ΔIV measured by FTIR from ΔIV determined by ASTM
[c] CV: coefficient of variation of duplicate measurements of OOC by FTIR

5.3.4.3 Conversion, Yield, and Selectivity of the Epoxidation

In addition to monitor OOC and ΔIV, it is useful to calculate conversion of double bonds, yield of the oxirane groups, and selectivity of the reaction since these calculated values can give an estimation of the efficiency of the epoxidation reaction. Although, the OOC and ΔIV can be directly measured by the FTIR method, but the initial IV (IV_i) of each oil is needed in order to determine conversion (relative loss of IV) and yield of the reaction at any time during the epoxidation. The initial IV of each oil, which is available in Table 5-1, was used to calculate OOC $_{\text{Calculated Max}}$% for each oil and the yield of the epoxidation at the end point of the reaction.

The conversion % of double bonds which is defined by the percentage of the double bonds reacted in the epoxidation was calculate by the Eq. 5-2.

$$\text{Relative loss of IV (Conversion \%)} = (\text{FTIR } \Delta IV / IVi) \times 100 \qquad \text{Eq. 5-2}$$

Assuming all double bonds in oil are converted to oxirane groups, the maximum calculated OOC% can be obtained using Eq. 5-3 [18].

$$\%\ OOC_{\text{Calculated Max}} = [(IV / 2Ai) / (100 + ((IV/ 2Ai) \times Ao))] \times Ao \times 100 \qquad \text{Eq. 5-3}$$

Where Ao and Ai are the atomic weight of oxygen (16.0) and iodine (126.9) and ΔIV is the consumed iodine value.

And the yield of the epoxidation at the end point of the reaction (i.e. at maximum OOC measured by the $FTIR_{(1497-1432)}$) was calculated by the Eq. 5-4.

$$\% \text{ Yield} = ((FTIR_{(1497-1432)} \text{ OOC\% }) / \% \text{ OOC }_{\text{Calculated Max}}) \times 100 \quad \text{Eq. 5-4}$$

The selectivity of the reaction which can be defined as the % of consumed double bonds which are converted into oxirane groups was calculated from the following Equation:

$$\% \text{ Selectivity} = ((FTIR_{(1497-1432)} \text{ OOC\% }) / \% \text{ OOC }_{\text{Calculated Max for } \Delta IV}) \times 100 \quad \text{Eq. 5-5}$$

During epoxidation, the weight of the oil increases due to the incorporation of oxygen as epoxy groups formed, thus a small part of the ΔIV is due to this increase in total mass. The mass increase can be calculated from the OOC % measured by the FTIR method (Eq. 5-6) and used to correct the ΔIV for this mass increase (Eq. 5-7).

$$\% \text{ mass increase} = (100 / (100 - \text{FTIR OOC\%})) \times 100 - 100 \quad \text{Eq. 5-6}$$

$$\Delta IV_{Corrected} = IV_0 - [((IV_0 - \Delta IV) \times (100 + \% \text{ mass increase}) / 100] \quad \text{Eq. 5-7}$$

In order to investigate the effect of mass increase in ΔIV, the FTIR ΔIV obtained during the reaction was corrected for the mass increase and compared to ΔIV (data not shown). Unlike, the mass increase percentage which arises over the course of the reaction and reaches to around 6-10% (depends on OOC %) at the end of the reaction, the calculated difference between $\Delta IV_{Corrected}$ and ΔIV (i.e. $\Delta IV - \Delta IV_{Corrected}$) was small and almost constant during the reaction. The average $\Delta IV - \Delta IV_{Corrected}$ during the reaction was ~1.2 ± 0.5 $gI_2/100g$ for canola oil, 1.8 ± 0.8 $gI_2/100g$ for

camelina oil and 3.1 ± 1.5 $gI_2/100g$ for flax oil. This can be explained by the Eq. 5-7. At the early stage of the reaction, which the IV_0-ΔIV is high, the % mass increase is low, and in contrast, at the end of the reaction which % mass increase is higher, the IV_0-ΔIV is low. This results in a small and almost constant difference between $\Delta IV_{Corrected}$ and ΔIV during the reaction. Flax oil which had the highest initial IV showed a higher difference between $\Delta IV_{Corrected}$ and ΔIV, whereas, the difference was smaller in canola which had the lowest initial IV.

Unlike the ΔIV-$\Delta IV_{Corrected}$, the relative difference between ΔIV and $\Delta IV_{corrected}$ (i.e. 100 × (ΔIV-$\Delta IV_{corrected}$) / (ΔIV)) was higher at the early stage of the reaction (~ 6% for canola and camelina, and ~ 13% for flax after 1 h reaction) and diminished (to <1%) toward the end of the reaction. This is due to the smaller ΔIV at the early stage of the reaction which increases toward the end of the reaction. Consequently, the relative difference (%) between the selectivities calculated from ΔIV versus those from $\Delta IV_{corrected}$ were higher at the early stage of the reaction and decreased as reaction continued. Figure 5-8 shows the changes in the selectivities calculated from $\Delta IV_{Corrected}$ and ΔIV during the epoxidation of canola oil (as an example).

This results demonstrate that at the end of the reaction (i.e. the maximum yield), the selectivity of the epoxidation can be determined by the ΔIV and OOC measured by the FTIR method, with no need to know the initial IV. However, as discussed above the initial IV of oil might be needed to correct ΔIV for the mass increase, if the selectivity is calculated for the early stages of the reaction, such as in a study of reaction kinetics.

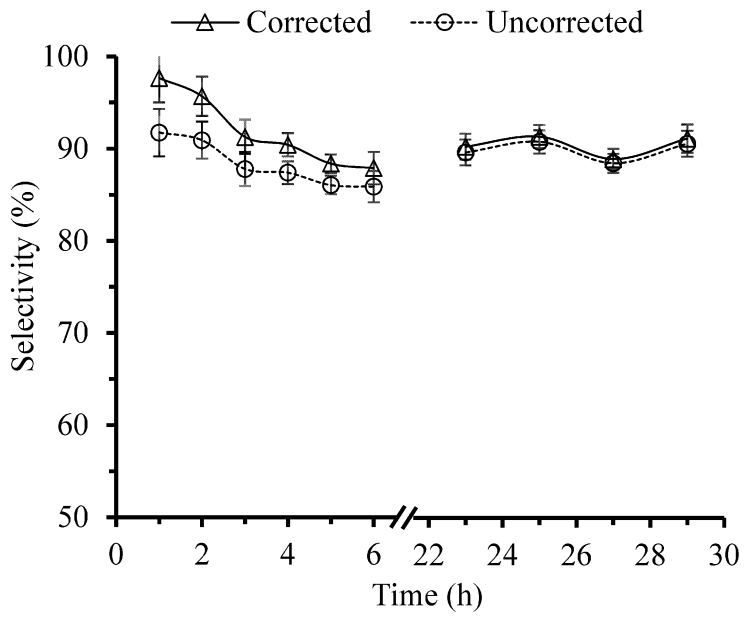

Figure 5-8 The selectivity (uncorrected) and corrected selectivity calculated from ΔIV and ΔIV corrected for mass increase (due to the formation of oxirane groups), respectively, during the epoxidation of canola oil.

The conversion and selectivity at the end of the epoxidation, which were calculated from both ΔIVCorrected and ΔIV, are given in Table 5-4.

At the end of the epoxidation reaction, the conversion and selectivity calculated from $\Delta IV_{Corrected}$ were very close to those of calculated from ΔIV.

It can be seen from Table 5-4 that when the maximum experimental OOC is reached, the degree of conversion of double bonds in canola and flax oils was similar (~ 90%). However, flax oil, which had the highest IV, showed lower selectivity (~ 83.9%) and yield (~76.6%) compared to canola oil.

Table 5-4 Calculated conversion, selectivity, and yield of the epoxidation of oils at the end of the reaction along with corrected conversion and selectivity calculated from the corrected ΔIV for mass increase ($\Delta IV_{Corrected}$), reaction temperature, and the maximum OOC measured by FTIR.

Oil	Temperature [a] (ºC)	OOC% [b]	Conversion (%) [c]		Selectivity (%) [d]		Yield (%) [f]
				Corrected [e]		Corrected [e]	
Canola	50	5.7	90.2	89.7	90.7	91.3	81.1
Camelina	60	6.7	88.3	87.5	88.5	89.2	78.9
Flax	50	9.2	91.2	90.3	83.2	83.9	76.6

[a] Temperature used in the epoxidation, [b] OOC measured by FTIR, [c] conversion of double bonds calculated from Eq. 5-2, [d] selectivity of conversion of double bonds into oxirane groups calculated from Eq. 5-5, [e] calculated from ΔIV corrected for mass increase due to the formation of oxirane groups, [f] yield of the OOC calculated from Eq. 5-4.

5.4 Conclusion

The solvent and reagent free ATR-FTIR methods described in this paper provide a simpler and more rapid means of monitoring OOC and IV changes during the epoxidation of triacylglycerols sourced from common vegetable oil sources. These methods are calibrated against standard titrimetric procedures and have been validated to produce similar results, but using a simpler and readily implemented, FTIR single bounce ATR method. Especially useful is that two key parameters, OOC and ΔIV, the two measures of critical importance for monitoring the progress of triacylglycerol oil epoxidation, can be obtained by a single analysis. This facilitates the studying, monitoring and optimizing epoxidation processes. Additionally, if the initial IV of an oil is known, this method is useful to calculate the yield, conversion, and selectivity of the reaction during the epoxidation and study the kinetic of the reaction.

5.5 References:

[1] Cai, C., Dai, H., Chen, R., Su, C., Xu, X., Zhang, S., Yang, L., Studies on the kinetics of in situ epoxidation of vegetable oils, *European Journal of Lipid Science and Technology*. 2008, *110*, 341-346.

[2] Abdullah, B. M., Salimon, J., Epoxidation of vegetable oils and fatty acids: Catalysts, methods and advantages, *Journal of Applied Sciences*. 2010, *10*, 1545-1553.

[3] Anuar, S. T., Zhao, Y. Y., Mugo, S. M., Curtis, J. M., Monitoring the epoxidation of canola oil by non-aqueous reversed phase liquid chromatography/mass spectrometry for process optimization and control, *Journal of the American Oil Chemists Society*. 2012, *89*, 1951-1960.

[4] American Society for Testing and Materials ASTM D5554-95 (2006).

[5] American Oil Chemists' Society AOCS Cd 1d-92 (2009).

[6] Association of Official Analytical Chemistry AOAC 993.20 (1998).

[7] International Organization for Standardization ISO 3961 (2009). .

[8] International Union of Pure and Applied Chemistry IUPAC 2.205 (1987). .

[9] Association of Official Analytical Chemistry AOAC 28.060 (1984).

[10] Association of Official Analytical Chemistry AOAC 963.22 (1995).

[11] Sedman, J., van de Voort, F. R., Ismail, A. A., Maes, P., Industrial validation of Fourier transform infrared trans and iodine value analyses of fats and oils, *Journal of the American Oil Chemists Society*. 1998, *75*, 33-39.

[12] Hendl, O., Howell, J. A., Lowery, J., Jones, W., A rapid and simple method for the determination of iodine values using derivative Fourier transform infrared measurements, *Analytica Chimica Acta*. 2001, *427*, 75-81.

[13] Talpur, M. Y., Kara, H., Sherazi, S. T. H., Ayyildiz, H. F., Topkafa, M., Arslan, F. N., Naz, S., Durmaz, F., Sirajuddin, Application of multivariate chemometric techniques for

simultaneous determination of five parameters of cottonseed oil by single bounce attenuated total reflectance Fourier transform infrared spectroscopy, *Talanta*. 2014, *129*, 473-480.

[14] Adewale, P., Mba, O., Dumont, M.-J., Ngadi, M., Cocciardi, R., Determination of the iodine value and the free fatty acid content of waste animal fat blends using FT-NIR, *Vibrational Spectroscopy*. 2014, *72*, 72-78.

[15] American Society for Testing and Materials ASTM D1652-11 (2011).

[16] American Oil Chemists' Society AOCS Cd 9-57 (2009).

[17] Parreira, T. F., Ferreira, M. M. C., Sales, H. J. S., de Almeida, W. B., Quantitative determination of epoxidized soybean oil using near-infrared spectroscopy and multivariate calibration, *Applied Spectroscopy*. 2002, *56*, 1607-1614.

[18] Goud, V. V., Patwardhan, A. V., Dinda, S., Pradhan, N. C., Kinetics of epoxidation of jatropha oil with peroxyacetic and peroxyformic acid catalysed by acidic ion exchange resin, *Chemical Engineering Science*. 2007, *62*, 4065-4076.

CHAPTER 6

Quantification of Nonanal and Oleic acid formed during the Ozonolysis of Vegetable Oil Free Fatty Acids or Fatty Acid Methyl Esters[5]

6.1 Introduction

Environmental concerns regarding the use of petrochemicals as feedstocks for polymer production and the rapid depletion of this resource have led researchers to look for alternatives [1,2]. Vegetable oils are one such potential alternative to petrochemical feedstocks for polymer production [1]. The presence of a significant degree of unsaturation in vegetable oil allows for various chemical modifications such as hydrogenation, epoxidation, and ozonolysis to be performed. Ozone has been used to cleave fatty acids at double bond positions resulting in the formation of different compounds; carboxylic acids, aldehydes, ketones and alcohols being the major ones [3].

The mechanism of ozonolysis of vegetable oils has been studied in detail [4]. Briefly, ozone reacts with double bonds and forms an unstable intermediate compound named 1, 2, 3-trioxolane (molozonide) which decomposes into an aldehyde and carbonyl oxide (Figure 6-1). These products can engage in further reactions and yield other products such as oligomeric peroxides [5] and secondary aldehydes [6]. Ozonolysis has been used to produce polyols from unsaturated vegetable

[5] A version of this chapter has been published: Tavassoli-Kafrani, M. H., Foley, P., Kharraz, E., Curtis, J. M., *Journal of the American Oil Chemists' Society,* 2016, *93*, 303-310.

oil triacylglycerols by oxidizing double bonds into aldehyde groups and then reducing them to hydroxyl groups [7-9]. In addition, aldehydes produced in ozonolysis can be used in the fragrance industries [10,11].

Oleic acid is one of the major fatty acid component of many vegetable oils which can be ozonised to produce nonanal due to the presence of a double bond at the Δ^9 position. Hence, a method for the measurement of oleic acid and nonanal concentration during the ozonolysis of oleic acid containing oils would provide an indication of the extent of the ozonolysis reaction. Gas chromatography (GC) provides a high resolution and potentially rapid separation for many lipid derivatives. However, the direct analysis of ozonides by high temperature GC may result in the decomposition of ozonides into aldehydes and/or acids and therefore lead to inaccurate aldehyde values. Additional challenges in quantitative ozonolysis reaction monitoring by GC include: a) fatty acids can be difficult to quantify under a number of ozonolysis conditions given that they may be ionized and therefore be under represented without acid treatment; b) certain high molecular weight esters (e.g., diglycerides) and oligomers (e.g., ozonide oligomers) may be undetectable without derivatization; and, c) performing direct GC analysis of aldehydes from ozonolysis without derivatization results in poor reproducibility, for example standard deviations of up to 19% have been reported for nonanal measurement by direct GC [11,12]. It should be noted that this last factor may not be entirely due to GC analysis itself but also to the difficulties associated with sampling from unstable emulsions.

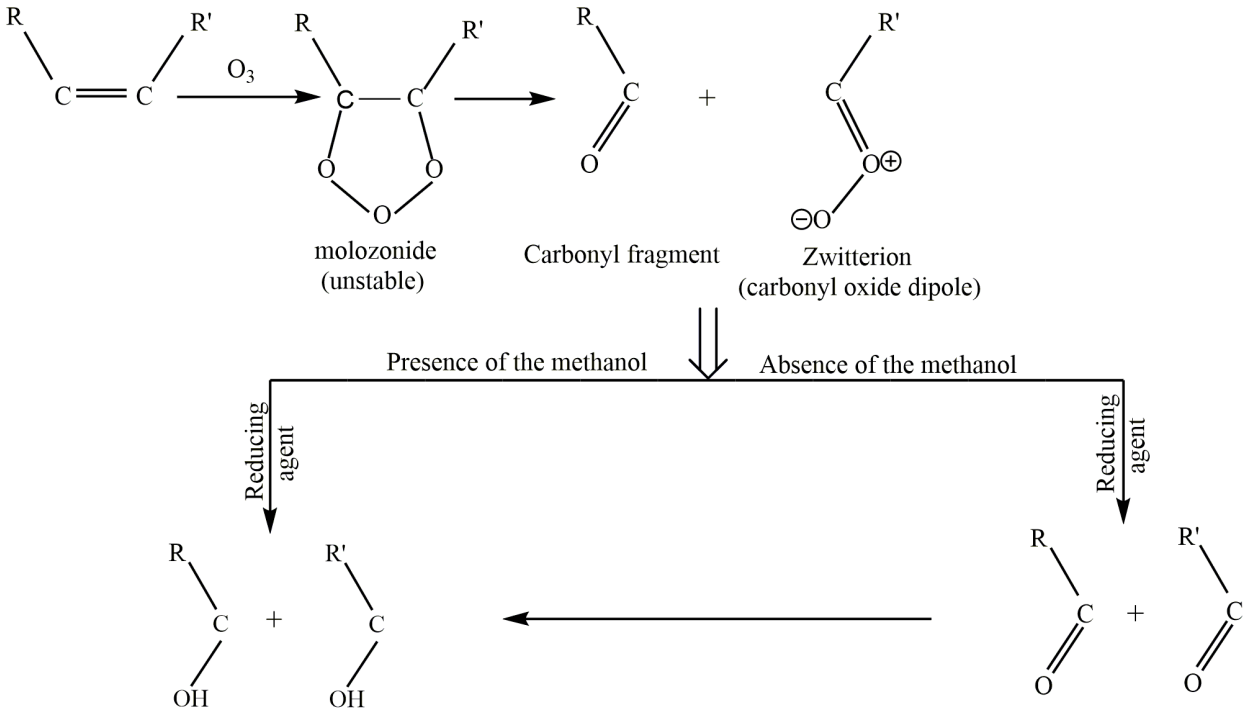

Figure 6-1 The mechanism of ozonolysis for unsaturated fatty acids.

In this Chapter we describe the conversion of aldehyde and carboxyl groups formed in the ozonolysis of unsaturated lipids into their dimethyl acetal and ester derivatives, respectively. These derivatives are more stable in the high temperatures used in GC analysis. A specific target for this work is the development of an accurate and reliable method for the measurement of nonanal and residual oleic acid from the ozonolysis of unsaturated fatty acids and FAME.

6.2 Experimental

6.2.1 Materials

Pure nonanal (97%), undecanal (97%), oleic acid (99%), 10-heptadecenoic acid (99%), boron trifluoride solution (12% w/w in methanol), and NaCl (99.5%) were purchased from Sigma Aldrich. Heptane and methanol were of HPLC grade and purchased from Caledon and Sigma Aldrich, respectively. Sodium bicarbonate and sodium sulfate was obtained from Sigma Aldrich.

Oleic acid (90%) used for the ozonolysis was in technical grade and obtained from Sigma Aldrich. All chemicals and solvents were used without additional purification.

6.2.2 Ozonolysis and Sampling

A mixture (600g) of canola oil FAME or oleic acid (90%) in water was prepared at the ratio of 1:1 w/w and transferred into a 2 L stainless steel ozonolysis reactor equipped with temperature controlling unit (Refrigerated/Heating Circulator, Julabo F25) and a speed controlled rotor unit. Ozone at a concentration of 50 g/m^3 (ozone/oxygen mixture) was generated by passing dry oxygen (99.6%, Praxair Canada Inc.) through an ATLAS100 ozone generator (model ATLAS100, ABSOLUTE OZONE, Canada). Ozone was introduced into the reactor as finely dispersed bubbles using a purpose-built coil with holes located at the bottom of the reactor. The ozonolysis of canola oil FAME or oleic acid (90%) was continued for 300 min using an ozone flow rate of 6.5 L/min at an oxygen pressure of 7 PSI. The temperature and agitation speed were kept at 0 °C and 800 ± 5 rpm during ozonolysis, respectively. Every 10 min, a 2 ml sample of the ozonolysis mixture was transferred into 10 ml glass vial with screw cap. Then 5 ml salty water (3%) was added to the sample and was shaken for 1 min in a vortex mixer. The sample was then centrifuged (2500 g) for 10 minutes. Around 0.5 ml of the top oily layer was transferred to a 2 ml vial with cap and stored at -18 °C before analysis with GC-FID.

6.2.3 Derivatization

Samples were removed from freezer and were allowed to melt at room temperature. Then about 40 mg of sample and 20 mg of undecanal and 10-heptadecenoic acid as internal standards, were accurately weighed into a 40 ml tube with a screw cap. Boron trifluoride solution (5 ml, 12% in methanol) and methanol (5 ml) were added into the tube and the solution was mixed for 1 min and then the tube was transferred into a 75 °C water bath for 5 min. After this period, the tube was

removed from the water bath and cooled to room temperature. Heptane (5 ml) was added and the tube was returned to the 75 °C water bath for a further minute. The solution was allowed to cool to ambient temperature then 5 ml of salty water (3% sodium chloride in water) was added into tube and after shaking for 1 min on a vortex mixer, the upper layer (organic) was transferred into another tube and washed with salty water a further two times. The organic layer was dried with sodium sulfate and then centrifuged for 2 min to remove sodium sulfate. The organic phase was stored in a 10 ml vial with a screw cap and was diluted with heptane to give a final concentration of close to 0.3 mg/ml of each internal standard for subsequent GC analysis.

6.2.4 GC Analysis

The GC instrument used in this study was an Agilent Technologies GC (model 6890N, USA) coupled with flame ionization detector (FID). Separation was performed on a HP 5 capillary column (30 m × 0.32 mm ID, film thickness 0.25 μm, SGE Analytical Science Pty Ltd, USA) using helium gas as the mobile phase at a flow rate of 1.8 ml/min. The oven temperature was programmed to start at 100 °C, then rise to 300 °C at a rate of 20 °C /min giving a total run time of 10 min. The injection was carried out at a split ratio of 20:1 with injection volume of 1μL. The temperatures of the injector and detector were both kept at 275 °C.

6.2.5 GC/MS Analysis and Mass Spectrometry

The GC/MS system used in this work was an Agilent GC/MS with electron ionization (EI) with triple-Axis Detector (Agilent technologies 5975C inert XL EI/CI MSD, Santa Clara CA, USA). The scan range was in the range of *m/z* 50 -1000 at a scan speed of 1.55 scans/sec with the electron multiple voltage of 1282 V. The separation was performed on the same column and using the same conditions as used for GC/FID analysis.

For mass spectrometry, a QSTAR Elite (Applied Biosystems/MDS Sciex, Concord, ON, Canada) mass spectrometer in positive electrospray ionization (ESI) with time of flight (TOF) mass analyzer was used. About 2 µl of derivatized product (in a heptane solution at concentration of ~ 0.1 mg/ml) was introduced into mass spectrometer by flow injection using methanol (containing 10 mmol ammonium formate) as mobile phase at flow rate of 200 µl/min for 2 min. The temperature of the ion source was set at 400 °C and the mass spectra were obtained over range of *m/z* 50-1000. The ion spray voltage, focus potential (FP), declustering potential (DP), and DP2 potential were 5000 V, 200 V, 50 V, and 10 V, respectively. Nitrogen was used for auxiliary gas 40, nebulizing gas 50, and curtain gas 30, all in arbitrary units.

6.2.6 Calibrations

A series of calibration solutions of nonanal and oleic acid ranging 0.1 to 1.0 mg/ml with 0.1 mg/ml intervals and containing 0.3 mg/ml of both internal standards (undecanal and 10-heptadecenoic acid) were prepared. In brief, amounts between 5 and 35 mg each of nonanal and oleic acid at 5 mg intervals were weighed into a 40 ml tube. Internal standards were added and the mixtures were derivatized and finally diluted in heptane. The solutions were injected into the GC-FID and the peak areas of derivatized nonanal, oleic acid, undecanal, and 10-heptadecenoic acid were measured. The calibration curve for nonanal was developed by plotting the area ratios of nonanal/undecanal against the concentration ratios of nonanal /undecanal for each standard solution. The calibration curve for oleic acid was developed in a similar way to the nonanal but using 10-heptadecenoic acid as internal standard. Linear regressions were performed in each plot and the equations obtained were used to quantify nonanal and oleic acid.

6.2.7 Validation

In order to validate the method, two procedures were performed. In the first procedure, oleic acid and a FAME of high oleic canola oil were ozonized and samples were collected over the course of the reaction. The amount of nonanal and oleic acid were measured by GC-FID after derivatization.

In the second procedure, either oleic acid or nonanal were added to the ozonolysis mixture of free fatty acid and FAME collected at 60 and 300 min of ozonolysis. Briefly, 10 samples were collected from the ozonolysis mixtures (10 samples for fatty acid and 10 samples for FAME mixtures for each time point). Then a series of solution containing 0-225 (mmol/100g) of added nonanal, with intervals of around 30 mmol/100g, were prepared by adding pure nonanal (98%) to the 10 samples collected after 60 min of ozonolysis. To the samples collected after 300 min, 0-80 mmol/100g of oleic acid was added with the intervals of around 10 mmol/100g. Both oleic and nonanal spiked samples were then shaken vigorously for 2 min and were analyzed for the concentration of both nonanal and oleic acid by GC/FID. The results obtained for each time point were plotted against the actual added nonanal or oleic acid and linear regression was performed for each plot.

6.2.8 Extraction of Ozonides

In order to determine test the hypothesis that free aldehydes and acids are not formed from ozonide compounds as a result of the derivatization step, ozonides were extracted from a reaction mixture formed by the ozonolysis of oleic acid in heptane. Briefly, around 2 g oleic acid was dissolved in 20 ml heptane and was transferred into a 50 ml glass ozonolysis reactor with magnet stirrer. Ozonolysis was carried out for 90 min by passing ozone at concentration of 50 g/m^3 with a flow rate of 1L/min and temperature maintained at 0 °C. After completion of ozonolysis, the

mixture was transferred into a separating funnel and the lower layer containing the ozonides was collected. The collected viscous layer was then washed with heptane twice and finally dried under a nitrogen stream and stored at -18 °C prior to analysis by ^{1}H-NMR.

6.2.9 ^{1}H-NMR Spectroscopy

A solution of the ozonide sample in deuterated (D6) acetone at a concentration of 15 mg/ml was prepared for ^{1}H-NMR analysis using a 400 MHz Varian Inova 400-MR NMR. The spectrum was obtained at room temperature.

6.3 Results and Discussion

6.3.1 GC Separation

Figure 6-2 (dark line) shows the GC-FID chromatogram of standards of nonanal, undecanal, 10-heptadecenoic acid and oleic acid after derivatization with BF_3 and dilution with heptane to a concentration of 0.3-0.4 mg/ml.

The derivatization products from nonanal, undecanal, 10-heptadecenoic acid and oleic acid were well separated with retention times of 3.06, 4.22, 7.08, and 7.53 min, respectively. For comparison, the GC chromatogram of the FAME of high oleic canola oil ozonolysis mixture is presented in Figure 6-2 (gray line, offset to the right) and it can be seen that this separation is suitable for quantitative measurement of these analytes.

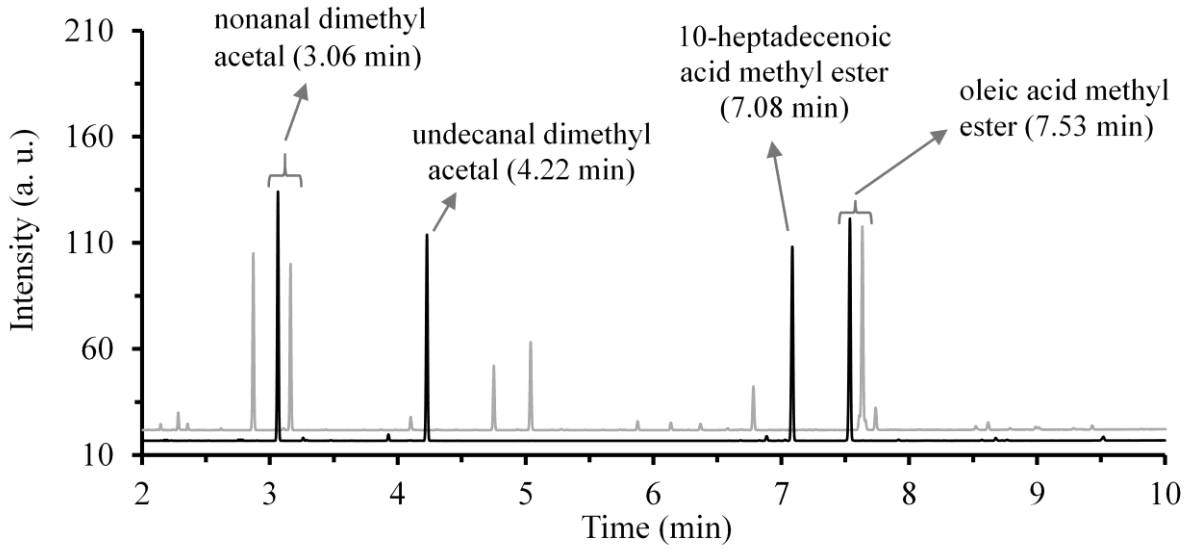

Figure 6-2 GC chromatogram of derivatized nonanal, undecanal, 10-heptadecenoic acid and oleic acid in a heptane solution (dark line) and the ozonolysis sample taken after 120 min ozonolysis of high oleic canola oil fatty acid methyl esters (gray line). The chromatogram of ozonolysis sample has been shifted to the right and up for clarity.

6.3.2 Analysis by Mass Spectroscopy

GC/MS with electron ionization (EI) was performed (data not shown) to identify the products of BF_3/methanol derivatization of nonanal, oleic acid, 10-heptadecenoic acid, and undecanal. The NIST library search showed that the possible derivatization products are nonanal dimethyl acetal, undecanal dimethyl acetal, and methyl esters of 10-heptadecenoic acid and oleic acids. Since the fragmentation in EI is high, the molecular ions of the products were not found in the EI spectrum but in each case an ion representing $[M - CH_3O\cdot]^+$ was observed. In order to confirm the products of derivatization, nonanal, undecanal, 10-heptadecenoic acid, and oleic acid after derivatization were analyzed by flow injection positive ion electrospray ionization (ESI) mass spectrometry. Figure 6-3 shows the ESI (+) mass spectrum of the undecanal and oleic acid after derivatization with BF_3/methanol. The ions at *m/z* 239.200 and *m/z* 319.264 correspond to the

sodium ion adducts of undecanal dimethylacetal ($[C_{13}H_{28}O_2 + Na]^+$) and oleic acid methyl ester ($[C_{19}H_{36}O_2 + Na]^+$), respectively whilst the ion at *m/z* 314.307 is the ammonium ion adduct of oleic acid methyl ester ($[C_{19}H_{36}O_2 + NH_4]^+$). The ion at *m/z* 185.193 ($[C_{12}H_{25}O]^+$) is consistent with the loss of sodium methoxide from the sodium adduct ion of undecanal dimethylacetal (*m/z* 239.2). The results obtained for derivatized nonanal and 10-heptadecenoic acid were analogous to results obtained for derivatized undecanal and oleic acid.

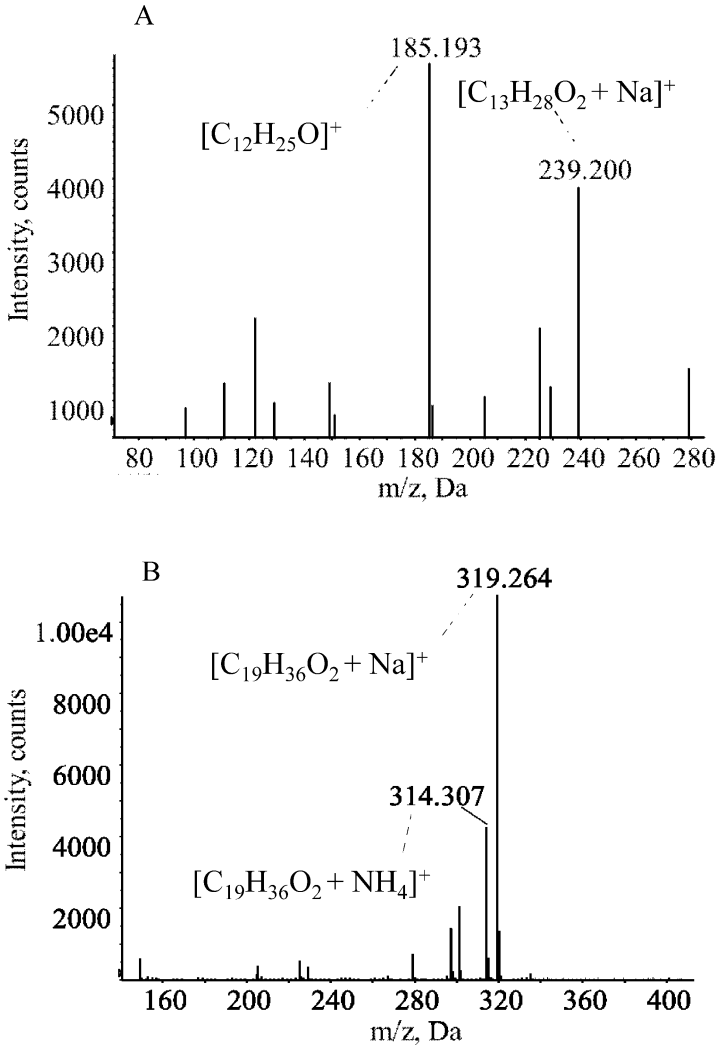

Figure 6-3 Flow injection ESI (+) mass spectrum of products of derivatization of (A) undecanal and (B) oleic acid with BF_3/methanol.

According to the results obtained by GC/MS and ESI mass spectrometry, nonanal dimethyl acetal and undecanal dimethyl acetal were identified as the products of the derivatization of nonanal and undecanal by BF_3/methanol. Similarly, 10-heptadecenoic methyl ester and oleic acid methyl ester were identified as the derivatization products from 10-heptadecenoic acid and oleic acid. Hence, the derivatization reaction can be summarized as given in Figure 6-4.

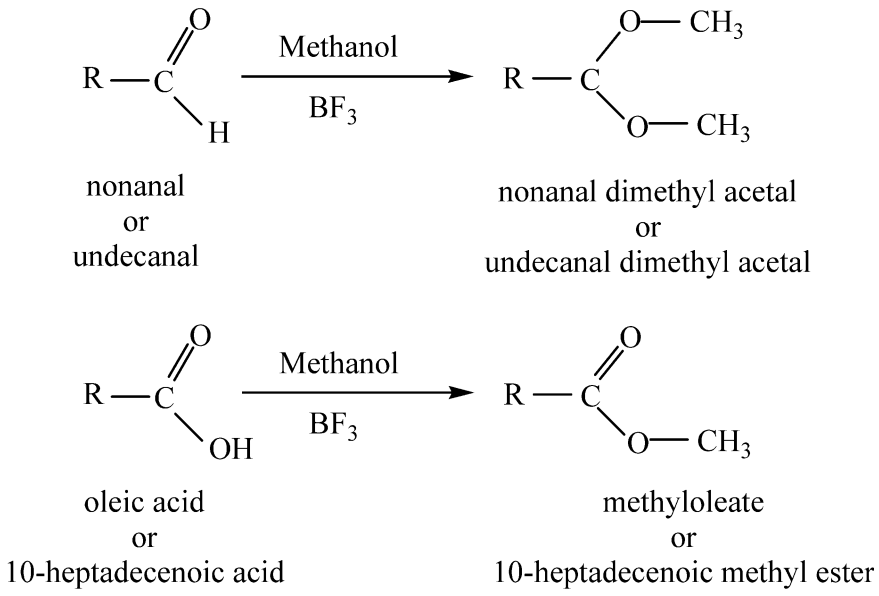

Figure 6-4 The derivatization of aldehydes and acids with methanol.

6.3.3 ^{1}H NMR Spectroscopy

In order to quantify the free aldehydes and acids that are formed as a result of ozonolysis, it is necessary to confirm that during the derivatization step (Figure 6-4), ozonide compounds that are present are not reduced to aldehydes and acids, since this would result in an overestimation in the measurement of free aldehydes and acids. In order to prove this, ozonolysis of oleic acid in heptane was carried out for 90 min and then ozonide compounds, the majority of which become

insoluble in heptane, were separated from the ozonolysis mixture. The extracted material was first analyzed by ^{1}HNMR. As it can be seen in Figure 6-5, resonances at 5.11 and 5.17 ppm were clearly seen in the ^{1}HNMR spectrum, confirming the presence of ozonides [13,14]. Then, a portion of this ozonide sample was derivatized using the above procedures, and analyzed by GC-FID. The duplicate GC-FID results of the dimethyl acetate derivatives indicate that the nonanal concentration is < 2% by weight in the ozonide. Hence, there is not a significant conversion of ozonide to aldehyde during derivatization and it can be assumed that nonanal which is formed during ozonolysis under some reaction conditions (such as in the presence of water) can be quantified via dimethyl acetate derivatives.

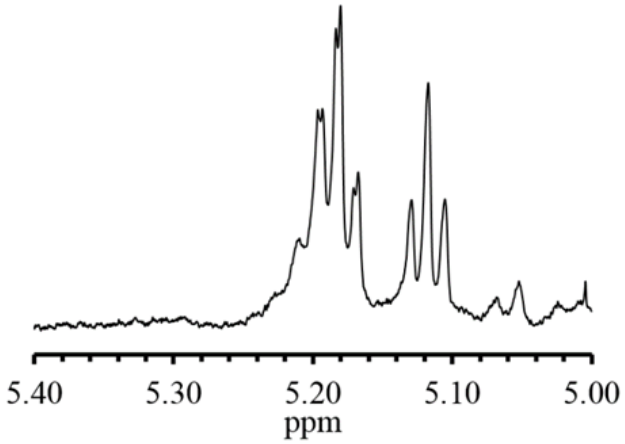

Figure 6-5 HNMR spectrum of extracted materials from ozonolysis mixture of canola oil, resonances at 5.1 and 5.17 refer to ozonide.

6.3.4 Calibration

In order to develop calibration curves, undecanal ($C_{10}H_{21}CHO$) was used as internal standard for nonanal while 10-heptadecenoic acid ($C_{17}H_{32}O_2$) was the internal standard for oleic acid. These were chosen since fatty acids present in vegetable oils commonly contain an even number of carbons whereas fatty acids containing an odd number of carbons are rare. In order to test the formation of undecanal and 10-heptadecenoic acid during the ozonolysis reaction of fatty acids and FAME, a sample was taken from the ozonolysis mixture of the high oleic acid canola oil FAME after 120 min ozonolysis, then derivatized with BF_3/methanol and analyzed by GC-FID. As it can be seen in Figure 6-2, there is no peak related to the undecanal or 10-heptadecenoic acid which indicates that the formation of undecanal and 10-heptadecenoic acid during the ozonolysis reaction is not detectable and hence they are suitable as internal standards.

Figure 6-2 (dark line) shows the chromatogram of a heptane solution of nonanal, undecanal, 10-heptadecenoic acid and oleic acid after derivatization with BF_3/methanol. The peak area of non-derivatized nonanal, undecanal, 10-heptadecenoic acid and oleic acid was not significant indicating that the derivatization reaction is complete within 5 min. Calibration curves of the dimethyl acetal derivative formed from a pure nonanal standard, and the methyl ester derivative formed from an oleic acid standard, are shown in Figure 6-6.

These showed high linearity ($R^2 > 0.998$) and were suitable for the determination of nonanal and oleic acid.

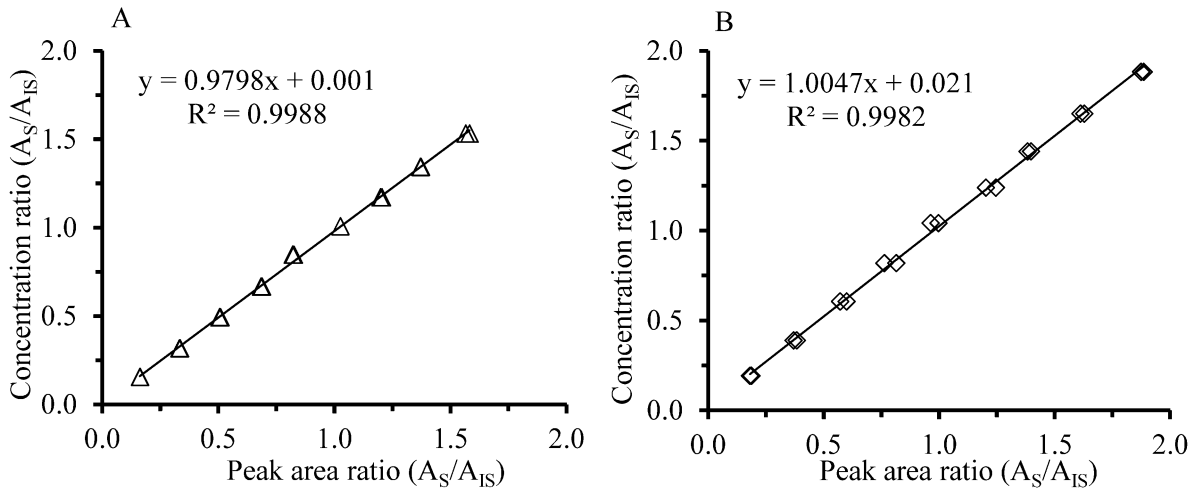

Figure 6-6 Plots of GC-FID peak area ratios of (A) nonanal/undecanal vs. concentration ratios of nonanal/undecanal, (B) oleic acid/10-heptadecenoic acid vs. concentration ratios of oleic acid/10-heptadecenoic acid in standard solutions.

6.3.5 Validation

6.3.5.1 Standard Additions

During the ozonolysis of vegetable oils, ozone reacts with double bonds present in the oil and produces unstable 1, 2, 3-trioxolane, which then decomposed to other intermediates such as zwitterion (carbonyl oxide dipole) and carbonyl fragments. These intermediates participate in further reactions as ozonolysis proceeds to form more stable ozonides, oligomeric peroxides, and aldehydes [10]. Due to the formation of high molecular weight polar products, the viscosity of the ozonolysis mixture greatly increases during the reaction. In order to evaluate recoveries for the extraction of nonanal and oleic acid directly from the ozonolysis reaction mixture, standard additions of nonanal and oleic acid were performed.

Oleic acid (~90%) was ozonized according to the procedure described earlier and the standard addition of nonanal was carried out for a sample collected at the early stage of ozonolysis

(30 min) where the concentration of nonanal from the ozonolysis reaction is relatively low. Also, the standard additions of oleic acid were performed on the sample collected towards the end of ozonolysis process where most of the oleic acid had been consumed. These samples were then derivatized and analyzed by GC-FID. The measured nonanal or oleic acid amounts are plotted against the actual nonanal or oleic acid added to the sample in Figure 6-7. A similar standard addition experiment was also performed using high oleic canola oil in the FAME form, with similar additions of nonanal (after 30min ozonolysis) and oleic acid (after 90 min ozonolysis).

Figure 6-7A shows the measured concentration of nonanal and oleic acid by GC-FID against actual concentration of nonanal added to the ozonolysis of FAME of high oleic acid canola oil collected after 30 min of ozonolysis. As expected, the measured nonanal concentration proportionally increased as nonanal was added to the sample. At the same time, the measured oleic acid decreased because the oleic acid was diluted as nonanal was added to the samples. Figure 6-7B shows the changes in measured oleic acid and nonanal vs. added oleic to the sample collected after 90 min of ozonolysis of fatty acid. The measured oleic acid increased linearly by adding oleic acid while measured nonanal decreased. Similar trends were observed for the oleic acid (~90%) samples collected after 30 and 90 min of ozonolysis and spiked with nonanal and oleic acid respectively (Table 6-1).

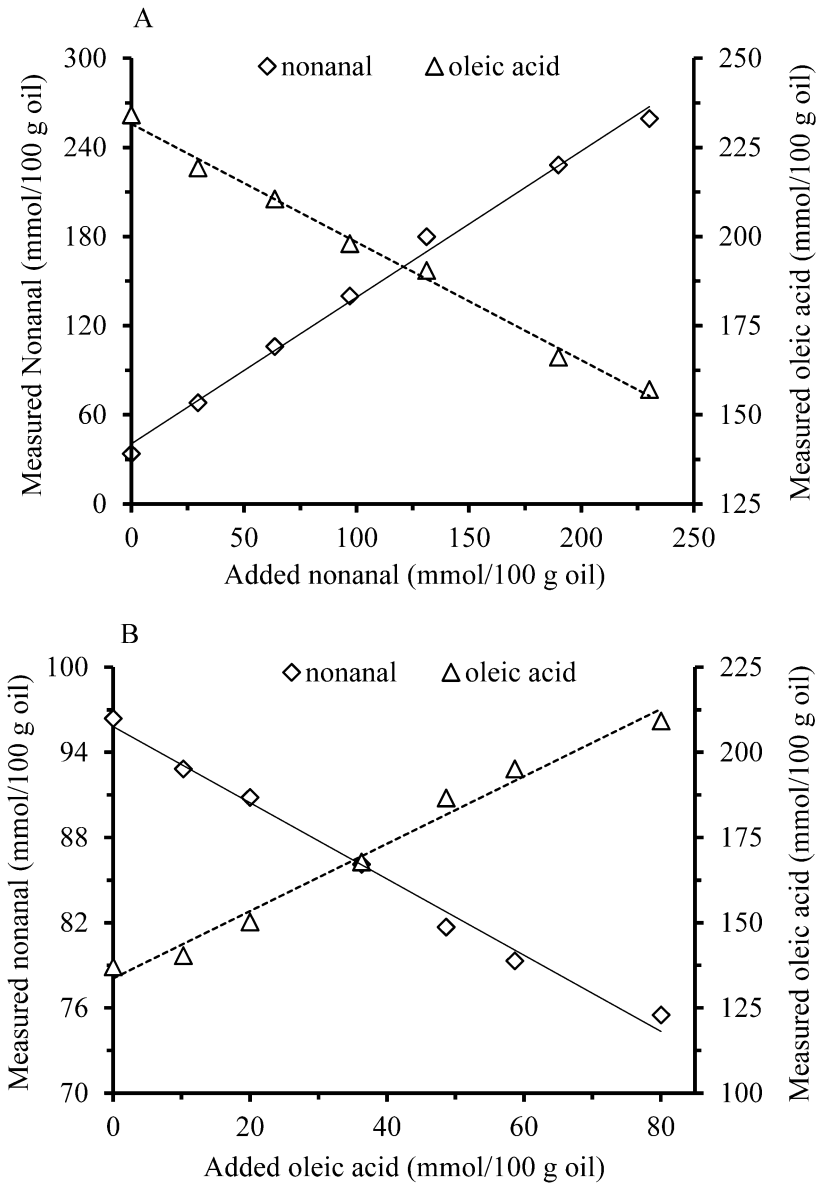

Figure 6-7 Measured nonanal and oleic acid content by GC-FID after derivatization against (A) added nonanal into high oleic acid canola FAME after 30 min of ozonolysis and (B) added oleic acid into high oleic acid canola FAME after 90 min ozonolysis.

A summary of the standard addition results for both free fatty acid and FAME samples are given in Table 6-1.

In both cases, the measured nonanal and oleic acid concentrations following derivatization show good linearity with oleic acid and nonanal additions giving R^2 values of between 0.982-0.996. The slopes obtained by linear regression of plots of measured nonanal vs. added nonanal were similar for free fatty acid and FAME samples and indicate that the recovery of nonanal is 98.5% in both cases. Similarly, the recovery of oleic acid added to the ozonolysis mixtures of FAME and fatty acid collected after 90 min were 98.8% and 101% These recoveries are close to 100% recovery and therefore suitable for the measurement of nonanal and residual oleic in ozonolysis reactions. This data suggests that high recovery of both nonanal and oleic acid is independent of the starting fatty acid form.

Table 6-1 The linear regression results of standard addition of nonanal and oleic acid into the ozonolysis sample taken at the different time of the ozonolysis of FAME of high oleic canola oil and oleic acid fatty acid (~90%).

Oil type	Time	Nonanal changes					Oleic acid changes				
		Slope	Intercept	R^2	SD[c]	CV[d]	Slope	Intercept	R^2	SD[c]	CV[d]
FAME	30 [a]	0.985	37.6	0.999	3.02	2.10	-0.291	203.0	0.996	1.74	1.02
	90 [b]	-0.285	94.6	0.990	0.85	0.99	1.006	118.0	0.987	3.02	2.03
FA	30 [a]	0.985	40.5	0.994	5.40	3.73	-0.331	231.6	0.994	2.46	1.25
	90 [b]	-0.268	95.8	0.990	0.74	0.86	0.988	133.6	0.982	4.14	2.44

[a] Spiked with nonanal
[b] Spiked with oleic acid
[c] Root- mean square error (RMSE)
[d] Coefficient of variation (%)

6.3.5.2 Quantification of Nonanal and Oleic Acids during the Ozonolysis Process

The method was tested to measure nonanal and oleic acid content during the ozonolysis of oleic acid fatty acids (~90%) and FAME from a high oleic acid canola oil. The results are presented in Figure 6-8, which shows the rate of decrease in oleic acid during ozonolysis along with the rate of increase in nonanal concentration.

The ozonolysis of fatty acids and their methyl esters in the presence of water results in the formation of an inhomogeneous mixture of ozonolysis products. Taking representative sample from this mixture without performing separation can be problematic since about 50% of the mixture is water and the polarity of the organic phase changes during the ozonolysis process. In this method, the sample used for the analysis was taken from the organic phase of the ozonolysis mixture. This can reduce the variations due to taking sample from emulsion system.

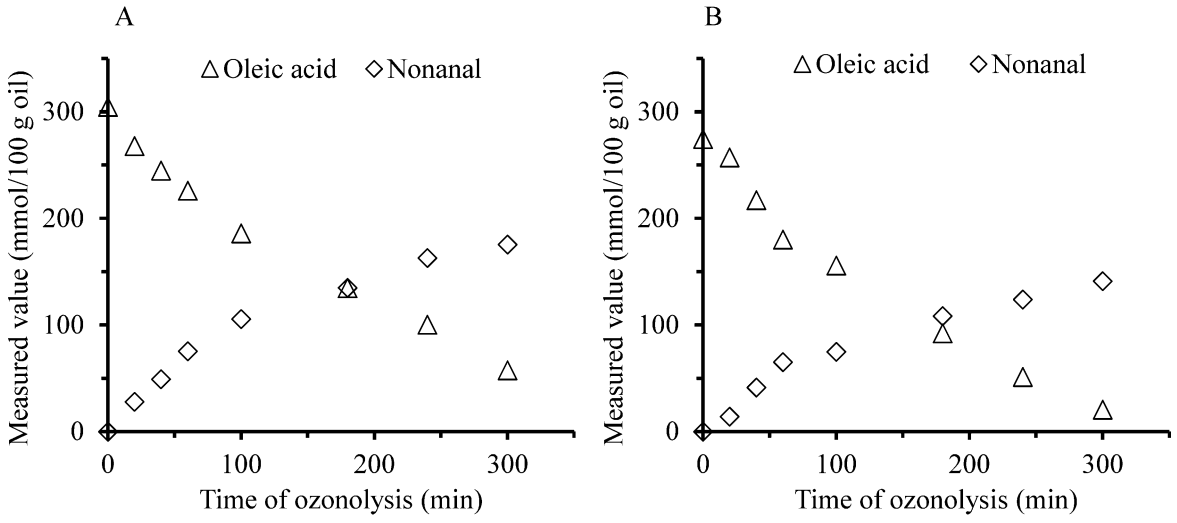

Figure 6-8 Measured nonanal and oleic acid contents during the ozonolysis of (A) fatty acid (oleic acid ~90%) and (B) high oleic acid canola FAME.

Although this method was tested for the ozonolysis of fatty acids and methyl esters in the presence of water, the application of the method is not limited to these conditions. The method has the potential to be used for the ozonolysis of TAGs in the presence of water or organic solvents. In this case, in order to have the representative sample, the mixture of the ozonolysis can be dissolved in a proper solvent to make a homogeneous solution and the results can be reported based on the total ozonolysis mixture. In addition to the measurement of nonanal and oleic acid, the method has the potential to be tested for the measurement of other aldehydes such as hexanal or other carboxylic acids such as nonanoic acid and hexanoic acid during the ozonolysis of vegetable oils and their derivatives.

6.4 Conclusion

The progress of ozonolysis reactions for vegetable oils and their derivatives can be followed by the measurement of oleic acid as one of the major fatty acid in many vegetable oils and nonanal as one of the major formed aldehyde in ozonolysis. In this work, a method was developed for the measurement of these compounds using GC-FID. The results obtained by performing standard additions of nonanal and oleic acid into actual ozonolysis reaction mixtures collected from the ozonolysis of oleic acid and the methyl esters of high oleic canola oil indicate that the method can accurately predict the amounts of added nonanal and oleic acid. In addition, the use of the method was demonstrated by the measurement of nonanal and oleic acid during the ozonolysis of the oleic acid and the methyl esters of high oleic acid canola oil. It should be noted that the total required time for analysis using the method described above, including sampling, derivatization and GC analysis, is under about 30 min total. This is adequate in the context of a reaction running for many hours (see Figure 6-8) but for reaction monitoring and for determination of the reaction end-point with <30 min resolution, a faster method would be desirable.

6.5 References:

[1] Gandini, A., Polymers from renewable resources: A challenge for the future of macromolecular materials, *Macromolecules*. 2008, *41*, 9491-9504.

[2] Mohanty, A. K., Misra, M., Drzal, L. T., Sustainable bio-composites from renewable resources: Opportunities and challenges in the green materials world, *Journal of Polymers and the Environment*. 2002, *10*, 19-26.

[3] McGuire J, H. P., Bond G: Ozonolysis in the production of chiral fine chemicals, in: *Handbook of chiral chemicals* Ed. Ager D, CRC, Taylor & Francis, Boca Raton 2006, pp. 164–185.

[4] Criegee, R., Mechanism of ozonolysis, *Angewandte Chemie International Edition*. 1975, *14*, 745- 752.

[5] Bailey, P. S., The reactions of ozone with organic compounds, *Chemical Reviews*. 1958, *58*, 925-1010.

[6] Fliszar, S., Carles, J., Quantitative investigation of the ozonolysis reaction. VII. Ozonolyses of phenylethylenes in presence of oxygen-18-labeled benzaldehyde, *Journal of the American Chemical Society*. 1969, *91*, 2637-2643.

[7] Petrovic, Z. S., Zhang, W., Javni, I., Structure and properties of polyurethanes prepared from triglyceride polyols by ozonolysis, *Biomacromolecules*. 2005, *6*, 713-719.

[8] Narine, S. S., Kong, X., Bouzidi, L., Sporns, P., Physical properties of polyurethanes produced from polyols from seed oils: I. Elastomers, *Journal of the American Oil Chemists Society*. 2007, *84*, 55-63.

[9] Petrovic, Z. S., Milic, J., Xu, Y., Cvetkovic, I., A chemical route to high molecular weight vegetable oil-based polyhydroxyalkanoate, *Macromolecules*. 2010, *43*, 4120-4125.

[10] Sell, C. S.: Manufacture of fragrance ingredients, in: *Chemistry and the sense of smell*, Wiley, London 2014, pp. 296-356.

[11] Omonov, T. S., Kharraz, E., Curtis, J. M., Ozonolysis of canola oil: A study of product yields and ozonolysis kinetics in different solvent systems, *Journal of the American Oil Chemists Society*. 2011, *88*, 689-705.

[12] Dumont, M. J., Kharraz, E., Qi, H., Production of polyols and mono-ols from 10 North-American vegetable oils by ozonolysis and hydrogenation: A characterization study, *Industrial Crops and Products*. 2013, *49*, 830-836.

[13] Soriano, N. U., Jr., Migo, V. P., Matsumura, M., Ozonation of sunflower oil: spectroscopic monitoring of the degree of unsaturation, *Journal of the American Oil Chemists Society*. 2003, *80*, 997-1001.

[14] Sadowska, J., Johansson, B., Johannessen, E., Friman, R., Bronlarz-Press, L., Rosenholm, J. B., Characterization of ozonated vegetable oils by spectroscopic and chromatographic methods, *Chemistry and Physics of Lipids*. 2008, *151*, 85-91.

CHAPTER 7

Synthesis of Novel Polyol with High Hydroxyl Value from Flaxseed and Canola Oils[6]

7.1 Introduction

Polyols are building blocks for certain polymeric materials including polyurethanes and polyester. The majority of polyols being used in polymer industries are petrochemical-based. However, due to the depletion of petroleum and natural gas resources which are non-renewable and their contribution to the accumulation of greenhouse gases in the atmosphere, there is an increasing interest in finding renewable raw materials to replace these chemicals [1,2]. Vegetable oils are one of the renewable sources for synthesizing chemical platforms for the production of polymers [3-6]. Vegetable oils can be transformed into more chemically reactive polyols by the introduction of hydroxyl functional groups at the positions of double bond [7]. Several routes have been developed to synthesize vegetable oil-based polyols such as ozonolysis [8-10], hydroformylation [11-13], transesterification with functionalized materials [14-16], and epoxidation followed by ring opening [17-20]. Epoxidation of double bonds and then ring opening by various reagents is the most important route for the production of polyols [21]. The hydroxyl value (OHV) of a polyol which is expressed as the equivalent weight of potassium hydroxide (in

[6] A part of this Chapter was used in a patent application: Curtis, J. M., Omonov, T. S., Kharraz, E., Kong, X., Tavassoli-Kafrani, M. H., "Method for Polyol Synthesis from Triacylglyceride Oils" U.S. Provisional Patent Application 62/183,982, Jun 24, 2015

mg) for one gram sample (mgKOH/g) is one of the key parameters of polyols which partially dictates the properties of produced polymers such as polyurethane (PU) [22]. Polyols with higher OHV form more cross linkages upon the reaction with isocyanate and result in PUs with higher tensile strength and Young's Modulus. In addition to OHV, the type of hydroxyl groups; secondary or primary, position of hydroxyl groups on fatty acids, and the viscosity of the polyols are also important [7].

It is difficult to produce vegetable oil-based polyols with OHV greater than 250 mgKOH/g through an epoxidation and ring opening process. As a results, most of the commercial biobased polyols which are currently available have the OHV lower than 250 mgKOH/g [22]. Since polyols of higher OHV generally have a higher viscosity, the synthesis of vegetable oil-based polyols with both high OHV and relatively low viscosity ($\leq$ 10 Pa s) is especially challenging [22]. Transesterification of vegetable oils with mono alcohols such as methanol, ethanol can significantly decrease the viscosity of the oil. Transesterification of vegetable oils has been widely studied and can be carried out in basic or acidic environment [23]. However, the transesterification of epoxidized oils is more challenging since the oxirane groups formed in epoxidation process must be preserved during the reaction. It has been shown that epoxidized oils can be transesterified by methanol in the presence of sodium methoxide, while the oxirane groups remain intact [24]. In polyol production through epoxidation and ring opening processes, transesterification by diols which have two primary hydroxyl groups (e.g. 1,3-propanediol) has the advantage of introducing a primary hydroxyl group at one end side of fatty acids and higher OHV in polyol compared to transesterification with mono alcohols such as methanol. In vegetable oil-based polyols usually double bonds are located at Δ^9, Δ^{12}, and Δ^{15} positions depending on fatty acid type. The chain length between the ends of fatty acid to the first OH group in fatty acid (dangling chains) is

important in polyurethane production because these chains are inactive and act as plasticizer rather than supporting stress [7]. In polyol preparation through epoxidation and ring-opening, transesterification with monools results in the formation of polyols molecules with one or more hydroxyl groups in middle part and two inactive dangling chains while transesterification with diol can form polyols with only one inactive dangling chain (Figure 7-1).

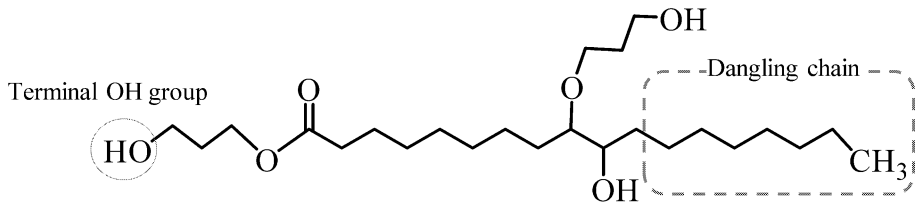

Hydroxylpropyl ester

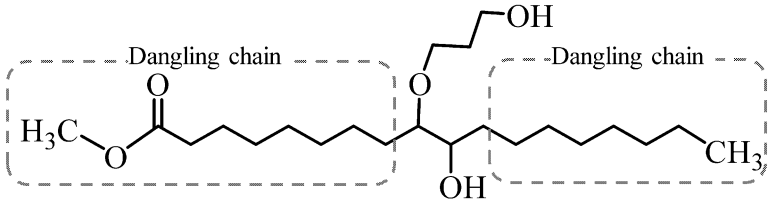

Methyl ester

Figure 7-1 Dangling chains in hydroxylpropyl ester and methyl ester of a fatty acid chain.

This Chapter describes a new route; epoxidation, transesterification with 1,3-propanediol, and ring opening by 1,3-propanediol to produce polyols with high OHV and relatively low viscosity from canola oil and flax oil (route C, Figure 7-2). The transesterification with 1,3-propanediol was optimized for the catalyst concentration, ratio of 1,3-propanediol, and percentage of acetone as a solvent. The new polyols produced through this route were compared to flax oil-based polyols produced by transesterification with methanol before (route A) or after epoxidation (route B) followed by ring opening using 1,3-propanediol.

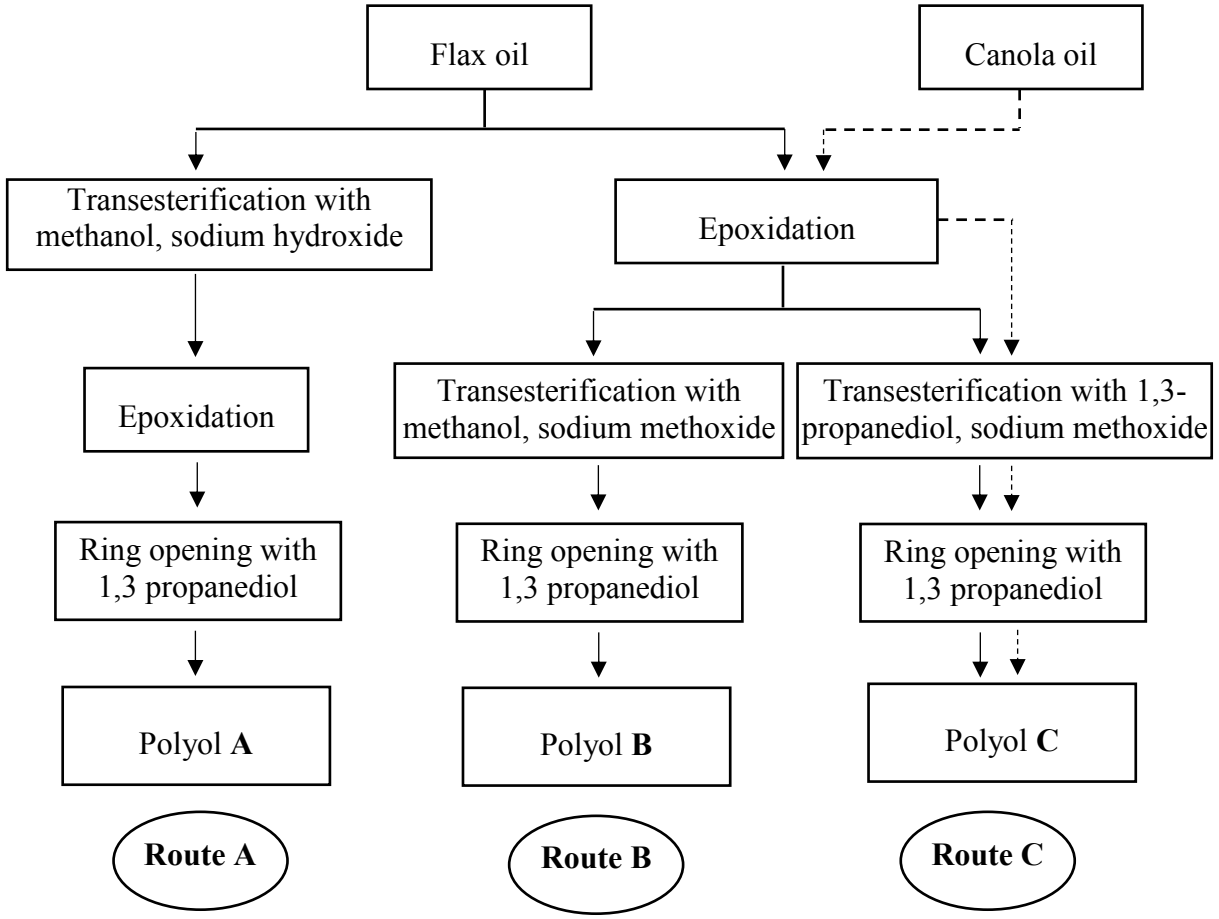

Figure 7-2 Schematic explanation of different routes used in this Chapter for the synthesis of polyol from flax oil (solid line) and canola oil through route C (dashed line).

7.2 Experimental

7.2.1 Materials

Flax oil (NuLin 50) was purchased from Viterra Inc. (SK, Canada) and food grade canola oil (Safeway®) was obtained from a local store. Formic acid (≥85%), hydrogen peroxide (≥35%), and sodium sulfate were provided from Univar (AB. Canada). Analytical grade methanol and ethyl acetate were purchased from Fluka Analytical Sigma-Aldrich (ON, Canada), with 1,3-propanediol

purchased from DuPont Tate and Lyle (USA). Amberlyst 15 in dry form was obtained from the DOW (Philadelphia, USA).

7.2.2 Methyl Esterification of Flax Oil

Flax oil (~1500 g) was transferred into a 6 L glass reactor equipped with a heating/ cooling system and a mechanical stirrer and heated to 60 ± 5°C °C. Sodium hydroxide (~ 8 g) was dissolved in methanol (400 g), heated to 60 ± 5°C °C and then added to the preheated oil. The reaction was performed at temperature 60 ± 5°C and agitation of 300 rpm. After 4 h reaction, the mixture was allowed to cool down to room temperature, then washed with saturated salty water for three times by 1 L salty water each time. Then about 1 L ethyl acetate, 0.25 L HCl (0.5 molar in water), and 1 L salty water was added to the mixture. The mixture was agitated and allowed to separate, then bottom layer was discarded and the remaining organic phase was washed again with salty water. The organic phase was dried by adding ~ 500 g sodium sulfate and then was filtered through Whatman paper filter No. 1. Ethyl acetate was removed using a rotary evaporator under vacuum and the flax fatty acid methyl esters (FAME) was stored under nitrogen gas atmosphere to avoid oxidation.

7.2.3 Epoxidation

Canola oil and flax oil as well as flax FAME were epoxidized by formic acid and hydrogen peroxide. The molar ratios of hydrogen peroxide/formic acid/double bonds were 1.5/0.2/1.0, respectively. About 1000 g of oil or FAME along with hydrogen peroxide (35% w/w in water) were transferred into a 6-L glass reactor equipped with an overhead mechanical stirrer and water heating/cooling system. Temperature was kept at ~25 °C and the mixture was agitated at the speed of ~ 350 rpm. Formic acid (85% w/w) was added to the reactor dropwise while the reaction mixture was agitated. After the completion of adding formic acid, the temperature was increased to 50 ±

5°C gradually at the rate of ~ 10 °C in each 10 min. Due to the exothermic nature of the epoxidation reaction, the temperature of the reaction mixture was controlled by a water cooling/heating system to avoid overheating. The oxirane oxygen content of the reaction mixture was measured and the reaction was stopped when the oxirane oxygen content was at the maximum. After the epoxidation, the mixture was cooled down to room temperature, and ~ 1 L ethyl acetate was added to the mixture then the mixture was washed with saturated salty water by adding ~ 1 L salty water. Washing with salty water was repeated for four times. The trace remaining water was removed by adding ~ 500 g sodium sulfate to the organic phase. The organic phase was filtered through Whatman paper filter No. 1 and then the solvent was removed using rotary evaporator. The resulting epoxidized oil or FAME was stored in a container with closed cap at room temperature.

7.2.4 Optimization of the Transesterification of Epoxidized Flax Oil with 1, 3- Propanediol

In order to optimize transesterification, the reaction was performed at various conditions including three levels of sodium methoxide (0.5, 1.0, and 1.5 wt% of the epoxidized oil) as a catalyst, four levels of 1,3-propanediol (4, 6, 8, and 10 molar ratio to the epoxidized triacylglycerol), and three levels of acetone (20, 30, and 40 wt% of the epoxidized oil) as a solvent. The optimization reaction runs were performed in a 250 ml three necked flat bottom flask which was equipped with a magnetic stirrer and reflux condenser and was placed in an oil bath. In brief, for each run, 50 g epoxidized flax oil was transferred into the reactor flask and heated to ~ 60 ± 5°C. The required amount of acetone, sodium methoxide, and 1,3-propanediol was weighed (± 5%). Sodium methoxide was mixed with acetone for ~2 minutes and then 1,3-propanediol was dissolved in sodium methoxide/acetone mixture and finally the whole mixture was added to the epoxidized flax oil preheated in the flask. All the optimization reaction runs were performed at 60 ± 5°C for 4.0 h. Samples were collected over the course of the reaction as described in Section 7.2.8

and were analyzed for the OHV and epoxidized triacylglycerol (TAG) content using FTIR spectroscopy (Section 7.2.9) and gel permeation chromatography (Section 7.2.10), respectively.

7.2.5 Transesterification of Epoxidized Flax Oil with Methanol

About 400 g epoxidized flax oil was transferred into a 1 L glass reactor equipped with between walls water heating/cooling system, a mechanical stirrer, and a reflux condenser. The epoxidized oil was heated to ~ 60 °C with constant stirring. A solution of 4.0 g sodium methoxide in 120 ml methanol was added to the preheated epoxidized oil in reactor to start the reaction. The reaction was continued for 2 h at 60± 5°C under agitation. After 2 h, the mixture was allowed to cool down to room temperature and then ~ 200 ml ethyl acetate was added to the mixture. The mixture was washed with ~ 0.5 L brine for three times. The organic phase was dried using sodium sulfate (200 g) after filtration through Whatman paper filter No. 1, the solvent was removed using rotary evaporator under vacuum and the product was stored at room temperature.

7.2.6 Synthesis of Polyols from Epoxidized Canola and Flax Oils through the New Route (Transesterification and Hydroxylation with 1, 3-Propanediol)

For the transesterification of the epoxidized oils with 1,3-propanediol, about 4.0 g sodium methoxide was added into ~120 g acetone and then ~ 192 g 1,3-propanediol (~ 6:1 molar ratio to epoxidized TAG) was dissolved into the sodium methoxide/acetone solution. After mixing for about two minutes, the mixture was added to a 400 g epoxidized oil preheated to ~ 60 °C. The transesterification with 1,3-propanediol was performed in the glass reactor described in Section 7.2.5 at the temperature of 60 ± 5°C and agitation at the speed of ~ 300 rpm. The reaction was continued for 4.0 h for the epoxidized flax oil and 5.0 h for the epoxidized canola oil. Then the mixture was cooled to room temperature and sodium methoxide was neutralized by equivalent amount of sulfuric acid (98% wt) which was added slowly to the mixture under agitating. Acetone

was removed using rotary evaporator under vacuum and the product was returned back to the reactor to perform ring opening (hydroxylation) reaction. Prior to the hydroxylation, the OOC of the transesterified epoxidized oil was measured (see Section 7.2.9) and the required amount of 1,3-propanediol for the hydroxylation process was calculated based on ~4.3:1 molar ratio of 1,3-propanediol to oxirane groups. It should be noted that the transesterification reaction was performed using an excess amount of 1,3-propanediol. Hence, the amount of 1,3-propanediol (~ 96g) remaining from the transesterification reaction was subtracted from the total required 1,3-propanediol (based on ~4.3: 1 molar ratio) and then added to the reactor containing the hydroxylpropyl esters. The mixture was heated to 60 ± 5°C and then ~ 60 g Amberlyst 15 (catalyst) was added to the reactor and the reaction was continued for 6.0 h under agitation at the speed of 300 rpm. After hydroxylation, the product was cleaned up using ethyl acetate and brine according to the procedure described for the epoxidation (Section 7.2.3).

7.2.7 Synthesis of Polyols from Epoxidized Flax FAME

For the hydroxylation of the epoxidized FAME, about 400 g of epoxidized flax FAME and 1,3-propanediol (at a molar ratio of ~4.3 to oxirane groups) were added to the 1 L reactor and heated to 60± 5°C. Then ~60 g Amberlyst 15 was added to the mixture and the reaction was continued for 6.0 h. The product was purified by adding ethyl acetate and washing with brine similar to the cleanup procedure described for the epoxidized oil (Section 7.2.3)

7.2.8 Sampling

Over the course of transesterification and hydroxylation reactions, 10 ml aliquots of the reaction mixture were sampled at various time points. Each was transferred into a 40 ml plastic conical tube, then about 5 ml ethyl acetate and 10 ml brine were added to the tube. The tube was shaken vigorously and then centrifuged for 2 min (at 2500 g). The bottom layer was removed and

the oily phase was washed with brine for further three times. The organic phase was dried over sodium sulfate (~1.0g) and filtered and then the solvent was removed by the rotary evaporator.

7.2.9 Hydroxyl Value (OHV) and Oxirane Oxygen Content (OOC) Measurements

Hydroxyl value was determined using the FTIR method described in Chapter 3. The OOC of flax FAME during the epoxidation and the OOC during the hydroxylation process were measured by ASTM method [11]. The OOC of flax and canola oils during the epoxidation was monitored by the ATR-FTIR method (described in Chapter 5).

7.2.10 Gel Permeation Chromatography

Gel permeation chromatography was carried out on a Styragel HR1 column (300 mm × 7.8 mm i. d.) with 5 μm particle size (Styragel HR1, Waters Corporation, USA) coupled with an evaporative light scattering detector (ALLtech ELSD 200, Mandel Scientific Company Inc, Canada) and an isocratic Agilent 1100 pump (Agilent Technologies, CA, USA). Tetrahydrofuran (THF) was used as a mobile phase at flow rate of 0.5 mL/min. The sample (0.5 mg/ml in THF) was injected into the column at the volume of 10 μL. Detector was run at temperature of 60 °C and nitrogen gas flow at 2.5 bar.

7.2.11 Viscosity Measurement of Polyols

An AR 2000 (TA Instrument, DE, USA) TA advanced rheometer with a plate-plate system 25 mm in diameter and a gap of 0.2 mm was used to measure the viscosity of the polyols using a constant shearing rate of 51.6 s^{-1} at temperature of 25 °C.

7.3 Results and Discussion

7.3.1 General Concept

Figure 7-3 shows a schematic illustration of the transesterification reaction of epoxidized oil with 1,3-propanediol which was performed in the presence of sodium methoxide as a catalyst and acetone as a solvent.

Transesterification with methanol is a well-known and widely used reaction to produce methyl esters of fatty acids [23]. However, transesterification of vegetable oil with diols such as ethylene glycol, 1, 2-propanediol, and 1,3-propanediol has been less studied. It is expected that the incorporation of epoxy groups into vegetable oil increases the miscibility of diols in vegetable oils and hence can facilitate transesterification reaction. It has been reported that the oxirane groups remain intact during the methyl esterification of epoxidized soybean oil by sodium methoxide at moderate temperature [24].

Transesterification with 1,3-propanediol introduces a terminal primary hydroxyl group into a fatty acid chain. The primary hydroxyl groups compared to secondary ones are more reactive toward the reaction with isocyanate groups [25] therefore, they are preferred in making polyurethanes from polyols.

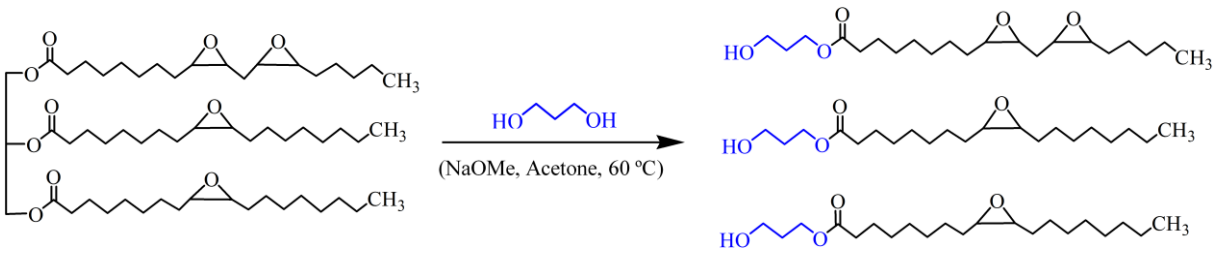

Figure 7-3 Schematic illustration of the transesterification of epoxidized oil with 1,3-propanediol resulting in the formation of hydroxylpropyl esters.

Our first attempt was to perform the transesterification of epoxidized oil with 1,3-propanediol without using solvent, however the reaction did not proceed in the absence of the solvent. Acetone was used as a suitable solvent since it does not contain hydroxyl groups or ester linkages which can participate in the reaction and is a good solvent to dissolve 1,3-propanediol and epoxidized oil. The boiling point of pure acetone is not high (~56 ºC) and therefore easy to remove after the reaction.

7.3.2 Optimization of Transesterification with 1,3-Propanediol

7.3.2.1 Catalyst Concentration

In order to optimize transesterification of epoxidized flax oil with 1,3-propanediol, variables such as percentages of catalyst (three levels) and acetone (three levels), molar ratios of 1,3-propanediol (four levels), and time were studied. It was not feasible to perform full combinations of these variables and for this reason, the reaction was first optimized for the concentration of catalyst while the other variables were kept constant. The transesterification was performed in the presence of three levels of catalyst concentrations (0.5, 1.0, and 1.5 % w/w in epoxidized oil). Sample were collected over the course of the reaction and were analyzed for the OHV and (TAG+ DAG) % after purification using brine and ethyl acetate (Section 7.2.8). The molar ratio of 1,3-propanediol: epoxidized TAG was ~6:1 and the acetone was 30 %wt of the epoxidized oil for all these three levels of catalyst.

As is shown in Figure 7-3, in transesterification reaction with 1,3-propanediol, the fatty acids present in TAG are converted into hydroxylpropyl esters. In order to confirm the formation of hydroxypropyl esters of fatty acids, LC/MS analysis was performed using a Qstar Elite mass spectrometer in positive electrospray ionization (ESI) with time of flight (TOF) mass analyzer. The ions at *m/z* 385.265, 371.284, and 357.299, which correspond to protonated ions of

hydroxypropyl esters of epoxidized linolenic $[C_{21}H_{36}O_6 + H]^+$, linoleic $[C_{21}H_{38}O_5 + H]^+$, and oleic $[C_{21}H_{40}O_4 + H]^+$ acids respectively, were observed in the mass spectra (not shown here), which confirms the formation of hydroxypropyl esters of fatty acid chains.

During the transesterification reaction, the concentration of TAG epoxides decreases and the concentration of hydroxypropyl esters increases. Figure 7-4 shows the GPC trace of samples obtained over the course of the transesterification reaction of epoxidized flax oil with 1,3-propanediol. As expected, the relative peak area of (TAG + DAG) decreases and the relative peak area that corresponds to hydroxypropyl esters of fatty acids increases over the course of the transesterification reaction. It should be noted that in this GPC experiment, MAG (monoacyl glycerol) coelutes with the hydroxypropyl esters. However, due to the large excess of 1,3-propanediol used, only small amounts of MAG are expected to be present by the end of the reaction.

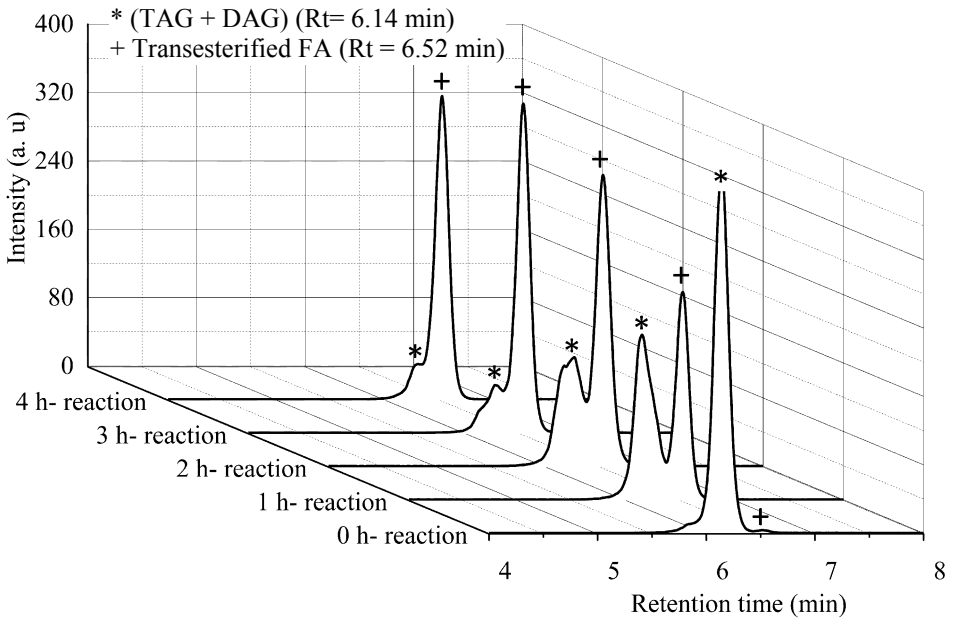

Figure 7-4 GPC trace of epoxidized flax oil over the course of the transesterification reaction with 1,3-propanediol at molar ratio to epoxidized TAG of 6:1. The reactions were carried out in the presence of 1.0% w/w sodium methoxide and 30% wt acetone to epoxidized TAG. The peak with the retention time of 6.14 min (marked with *) is due to (TAG+ DAG) and the peak with retention time of 6.52 min (marked with +) is (hydroxylpropyl ester+ MAG).

In order to monitor the reaction, (hydroxypropyl esters+ MAG) % and OHV were measured. Figure 7-5 represent the changes in the OHV and the (hydroxypropyl esters+ MAG) % during the transesterification reaction performed with 0.5, 1.0, and 1.5% catalyst. At a catalyst concentration of 0.5%, there was no significant change in the measured OHV or esters% during four hours reaction indicating that no reaction occurred. At a catalyst concentration of 1.0%, the OHV increases to ~ 165 mgKOH/g after four hours reaction while the level of (hydroxypropyl esters+ MAG) % increases to ~ 98.2%. By increasing the concentration of catalyst to 1.5%, the OHV and (hydroxypropyl esters+ MAG) % reached to the maximum values of ~155 mgKOH/g and ~ 97.5%, respectively, after ~ 15 min. These results indicate that the concentration of catalyst has a critical impact on the reaction.

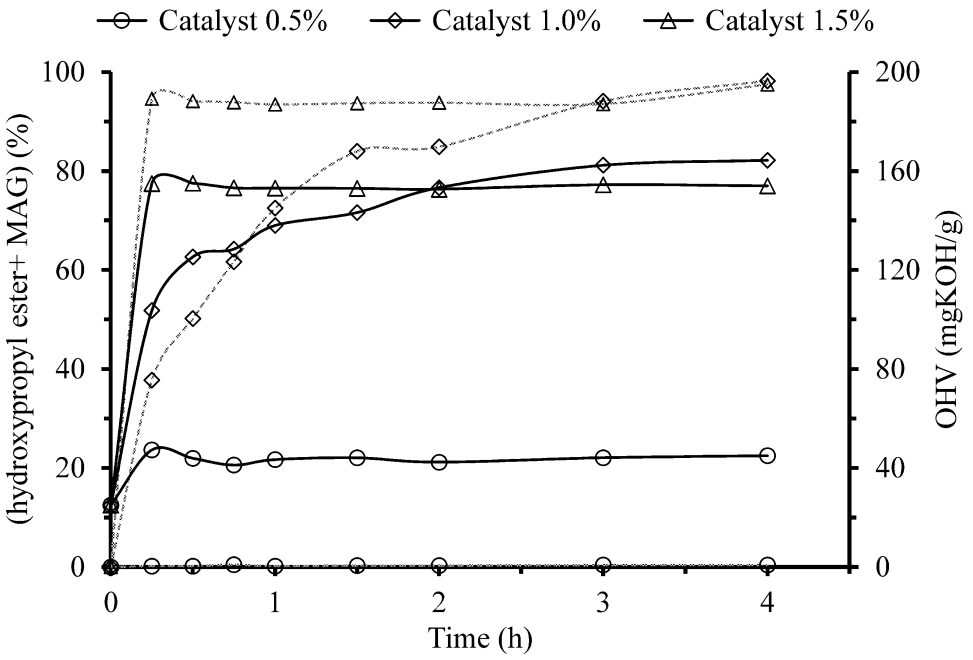

Figure 7-5 Changes in OHV and (hydroxypropyl+ MAG)% of epoxidized flax oil during the transesterification with 1, 3-propanediol (at ratio of 6 to 1 mole TAG) in the presence of 0.5, 1.0, and 1.5%wt of sodium methoxide to the epoxidized oil. Solid line shows OHV and dashed line shows the (hydroxypropyl+ MAG)% changes.

Although, increasing the catalyst concentration from 1.0 to 1.5% increases the rate of reaction, it also results in a product with lower OHV. This can be explained by the composition of sodium methoxide that contains ~ 59% methoxide. The methoxide present in the catalyst leads to the formation of methyl esters of fatty acid. Therefore, a higher concentration of sodium methoxide results in the formation of more methyl esters and consequently a product with lower OHV.

The theoretical OHV of the epoxidized oil after transesterification with 1,3-propanediol can be calculated from the molecular weight of epoxidized TAG (MW_{ETAG}). The $MW_{E\text{-}TAG}$ was estimated 956 g/mole which was calculated from the average molecular weight of the flax oil (MW_{TAG}= ~ 875 g/mole) and the measured oxirane oxygen content (9.2%wt) of the epoxidized oil. In this way, the theoretical increase in OHV during transesterification was determined to be

~154 mgKOH/g. The OHV of the epoxidized oil before transesterification was measured to be ~25 mgKOH/g and after the transesterification, this value became ~ 165 mgKOH/g (at 1.0% catalyst). Therefore, there was ~140 mgKOH/g increment in OHV, which is ~91 % of the theoretical value. A portion of the remaining 9% (~ 6%) can be related to the formation of methyl esters by the methanol present in the catalyst.

7.3.2.2 Ratio of 1,3-Propanediol and Acetone

The concentration of 1.0% (w/w) catalyst was chosen as the optimum concentration for catalyst. Transesterification with 1,3-propanediol at molar ratios of 4, 6, 8, and 10 to epoxidized TAG and acetone at 20, 30, and 40% (w/w) of the epoxidized flax oil in the presence of 1.0% (w/w) sodium methoxide was carried out. The OHV and TAG% were monitored during the reaction for 4 hours. Figure 7-6 shows the OHV of the esterified epoxidized flax oil after 4 hours transesterification using different molar ratios of 1,3-propanediol and percentages of acetone.

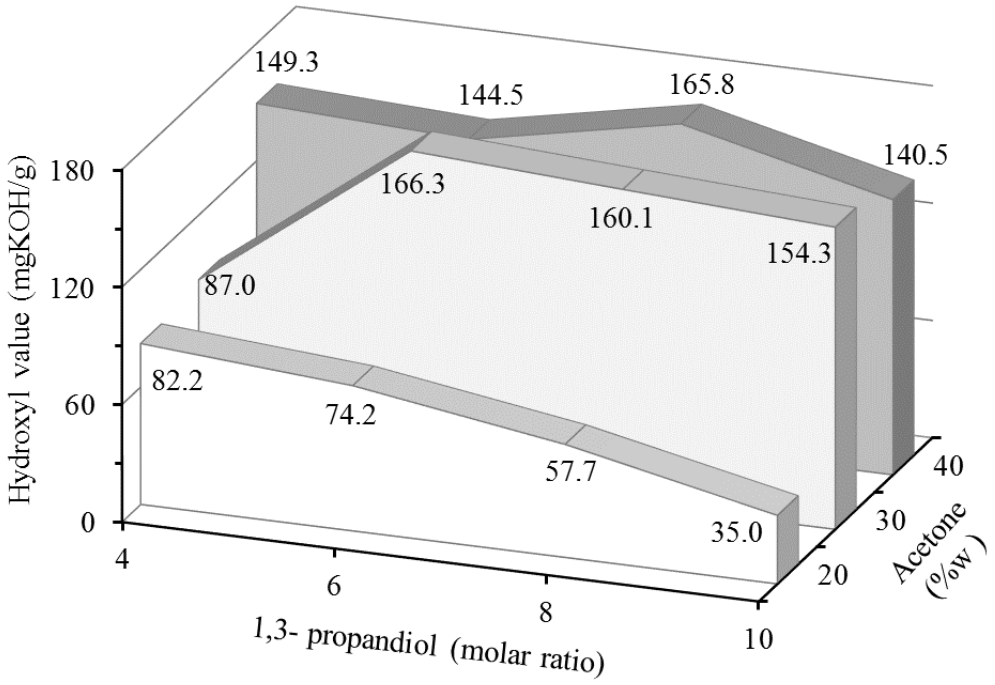

Figure 7-6 Hydroxyl value transesterified epoxidized flax oil after 4 h transesterification with 4, 6, 8, and 10 molar ratios of 1, 3-propanediol to epoxidized TAG and 20, 30, and 40% w/w acetone/epoxidized oil and in the presence of 1.0% w/w sodium methoxide/epoxidized oil.

In initial stages, the reaction is mass-transfer controlled [23] and as transesterification reaction proceeds, the TAG concentration decreases along with a corresponding increase in the concentrations of hydroxypropyl esters and MAG. At the acetone percentages (20-40% of epoxidized oil) studied, the mixture was not homogeneous at the early stage of the reaction but later (i.e. after 20-60 min, depends on the acetone % and ratio of 1,3-propanediol) the mixture became transparent and homogenous. This change in the appearance of the mixture might be explained by the changes in the concentrations of TAG, MAG, and hydroxypropyl esters during the reaction. A higher concentration of the TAG at the early stages of reaction results in a formation of a non-homogenous mixture because 1,3-propanediol is not miscible with the TAG. However,

at the later stages of the reaction, which the concentration of the epoxidized TAG is low and the concentrations of hydroxypropyl esters and MAG are high the mixture become homogeneous since hydroxypropyl esters and MAG compared to the TAG are more miscible with 1, 3-proanediol. Acetone is miscible with both of 1,3-propanediol and TAG hence, facilitates the reaction through the enhancement of mass transfer.

The maximum OHV after 4 h reaction in the presence of 4, 6, and 8 molar ratio of 1,3-propanediol was obtained in the presence of acetone levels of 20, 30, and 40% (w/w), respectively (Figure 7-6). On the other hand, higher molar ratio of 1,3-propanediol to epoxidized TAG requires higher percentage of acetone to epoxidized oil in order to obtain the maximum OHV. At the acetone percentage of 20% (w/w), the reaction was not completed after 4 hour at none of molar ratios of 1,3-propanediol. The acetone percentage of 30% (w/w) was chosen as the best acetone percentage since it gives the maximum OHV of ~ 166 mgKOH/g after 4 h reaction and compared to the 40% acetone requires lower ratio of 1,3-propanediol.

Figure 7-7 shows the changes in OHV and (hydroxypropyl esters+ MAG) % during the transesterification performed with different molar ratios of 1,3-propanediol in the presence of 30% (w/w) acetone and 1.0% catalyst. Among the conditions studied, the best results was obtained with 1,3-propanediol at the molar ratio of 6 (to epoxidized TAG), 30% (w/w) acetone, 1.0% sodium methoxide, and 4 h reaction. The best molar ratio of 1,3-propanediol obtained in this work is similar to the suggested optimum molar ratio of alcohols to TAG in order to achieve maximum conversion of TAG to esters [23].

These results indicate that the ratios of acetone/ 1,3-propaneiol/ epoxidized TAG should be balanced to achieve the maximum conversion of TAG into hydroxypropyl esters.

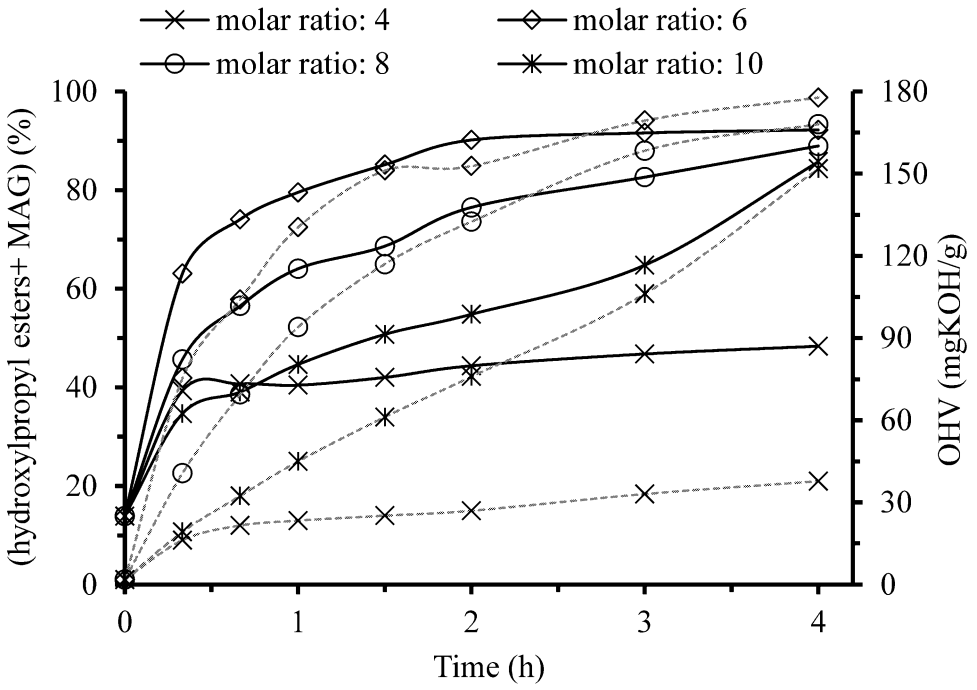

Figure 7-7 Changes in relative concentration of TAG + DAG % (gray dashed line) and OHV ((mgKOH/g) (solid black line)) during the transesterification of epoxidized flax oil with 1,3-propanediol at the molar ratios of 4, 6, 8, and 10 to epoxidized TAG in the presence of 30% (w/w) acetone and 1.0% (w/w) sodium methoxide to the epoxidized

7.3.3 Polyol Synthesis through Different Routes

Flax oil was transformed into polyols through three routes as illustrated in Figure 7-2. These polyols were named polyol **A**, **B**, and **C**. Route **C** was also used to produce polyol from canola oil. In order to compare these routes, the OOC and OHV of the oils and FAME were measured after epoxidation step and after transesterification of the epoxidized oils with 1,3-propanediol (route C) or methanol (route B). Finally, polyols produced through the different routes were analyzed and compared for the OHV, viscosity, dimers/oligomers content, and the average molecular weights of monomers and dimers. In the following sections, the results obtained in each step are described and discussed.

7.3.3.1 Epoxidation

The oxirane oxygen content (OOC) and OHV of flax oil, canola oil, and methyl esters of flax oil after epoxidation are given in Table 7-1. As it was expected, the OOC of epoxidized flax oil (9.23 %) was higher than that of epoxidized canola oil (5.88 %). This is due to the higher degree of unsaturation in flax oil (IV of ~ 211 gI_2/100 g) compare to the canola oil (IV of ~ 119 gI_2/100 g).

Table 7-1 The oxirane oxygen content (OOC), OHV, and yield of OOC of flax oil, flax FAME, and canola oil after epoxidation.

	OHV (mgKOH/g)	OOC (%)	Yield (%) of OOC[d]
E-flax FAME [a]	95.5 ± 3.4	7.20 ± 0.11	61.5 ± 0.94
E-flax oil [b]	25.2 ± 2.2	9.23 ± 0.12	76.8 ± 1.02
E-canola oil [c]	20.4 ± 1.7	5.88 ± 0.10	84.2 ± 1.43

[a] Epoxidized flax FAME, route **A**. (see Figure 7-2)
[b] Epoxidized flax oil, routes **B** and **C**. (Figure 7-2)
[c] Epoxidized canola oil, route **C**. (Figure 7-2)
[d] Yield % = (achieved OOC/theoretical maximum OOC)×100, the maximum OOC is calculated from the iodine value (IV) of the initial oil.

During the epoxidation reaction, side reactions such as ring opening of oxirane groups by water or formic acid can occur which results in a lower OOC% than theoretical maximum value (calculated based on the IV of oils) and formation of hydroxyl groups. Epoxidized flax FAME had significantly lower OOC and higher OHV than those of epoxidized flax oil while both flax oil and flax FAME have similar IV. This results show that FAME compared to oils are more vulnerable to side reactions during the epoxidation.

7.3.3.2 Transesterification

For the polyol synthesis, a portion of epoxidized flax oil was transesterified with 1,3-propanediol (route C) and the second portion was transesterified with methanol in the presence of sodium methoxide as catalyst (route B). Transesterification with 1,3-propanediol was also performed for the epoxidized canola oil.

Table 7-2 shows the OHV, OOC and the percentage of (TAG+DAG) remaining in the epoxidized oils after transesterification. In the transesterification with methanol, the OOC% of epoxidized flax oil slightly decreased (from ~ 9.23 to 9.1%) and its OHV increased (from ~ 25 to 35 mgKOH/g). This is likely due to the ring opening by methanol during the transesterification with methanol.

Unlike transesterification with methanol, transesterification with 1,3-propanediol resulted in a significant decrease in OOC% of epoxidized flax oil from 9.23 to 8.15% (~ 12.0% decrease) and in a case of epoxidized canola oil, from 5.88 to 5.16% (~ 12.2% decrease). This can be explained by the increase in mass due to adding one mole of 1,3-propanediol to each mole of fatty acid. By having the average molecular weight of epoxidized fatty acids present in epoxidized flax and canola oils, theoretical molar mass increments were calculated 12.4% and 12.7 % for epoxidized flax oil and epoxidized canola oil, respectively. These values are close to the percentages of decrease in measured OOC, indicating that the decrease in OOC% is due to the molar mass increment and the oxirane groups in the epoxidized oil are preserved during the transesterification reaction.

Table 7-2 OHV, OOC, and relative percentage of (TAG+ DAG) % of hydroxypropyl esters and methyl esters of the epoxidized oils.

	OHV (mgKOH/g)	OOC %	(TAG + DAG) %
Methyl esters of E-flax oil [a]	35.2 ± 0.5	9.10 ± 0.11	≤1.0
Hydroxypropyl esters of E-flax oil [b]	166.6 ± 1.3	8.15 ± 0.08	≤1.0
Hydroxypropyl esters of E-canola oil [c]	172.2 ± 4.2	5.16 ± 0.13	2.4 ± 0.4

[a] Epoxidized flax oil transesterified with methanol, route B (Figure 7-2)
[b] Epoxidized flax oil transesterified with 1,3-propanediol, route C (Figure 7-2)
[c] Epoxidized canola oil transesterified with 1,3-propanediol, route C (Figure 7-2)

7.3.3.3 Hydroxylation (Oxirane Ring Opening)

Ring opening (hydroxylation) was carried out using 1,3-propanediol in the presence of Amberlyst 15 as a catalyst. After transesterification with methanol (route **B**) and prior to the hydroxylation process, sodium methoxide and methanol remaining from the transesterification reaction should be removed from the mixture. This is because Amberlyst 15, which is used as a catalyst in hydroxylation step, contains acidic chains and sodium methoxide can react with these chains and reduce the catalyst activity. Furthermore, residual methanol can open the oxirane group during the hydroxylation process resulting in the formation of a methyl ether group and a secondary hydroxyl group rather than primary hydroxyl group.

However after transesterification with 1,3-propanediol, the amount of 1,3-propanediol remaining from the transesterification step can still be used for the hydroxylation process. Therefore, after transesterification with 1,3-propanedol, sodium methoxide was neutralized by adding one equivalent of sulfuric acid dropwise into the mixture. Acetone was then removed from the mixture using rotary evaporator. Amberlyst 15 and additional 1,3-propanediol was then added

to the mixture and hydroxylation was performed. This strategy decreases the required amounts of 1,3-propanediol and eliminates a washing step after transesterification step.

It should be noted that in the transesterification reaction, glycerol is produced and can participate in ring opening of oxirane groups during hydroxylation process. However, due to the small ratio of glycerol to 1,3-propanediol, it is expected that only a small percentages of oxirane groups are opened by glycerol in hydroxylation. This low ratio can be explained by the following discussion. After the transesterification reaction, the molar ratio of glycerol to hydroxypropyl ester is 1:3 and in the hydroxylation process the molar ratio of 1,3-propanediol to oxirane groups is ~ 4.3:1. Since each mole of hydroxypropyl esters contains on average more than one mole of oxirane groups, the molar ratio of glycerol to 1,3-propanediol in the hydroxylation process would be less than 1:13.

Acetone was removed and recovered after transesterification and prior to hydroxylation process. The recovery of acetone in the rotary evaporator was ≥ 85% w/w. The hydroxylation process was also performed in the presence of acetone which resulted in the production of polyols with similar OHV, viscosity, and dimer/oligomer content to those produced in the absent of acetone. This proves that residual acetone does not affect the hydroxylation reaction, however removing and recovering acetone before hydroxylation is easier.

Samples were collected over the course of the hydroxylation process every one hour. Then, were washed, cleaned up (see Section 7.2.8), and analyzed for the OHV and OOC%. The hydroxylation reaction was stopped when the OOC reduced to <0.1 % and OHV reached to a plateau state.

7.3.3.4 Polyols Characteristics

Table 7-3 represents the characteristics of the polyol produced from different routes. Polyol produced from flax oil through route C (see Figure 7-2) had the highest OHV (~ 408 mgKOH/g) amongst the polyols. This value for the polyol synthesized through route A and B was ~334 and ~ 361 mgKOH/g, respectively (Table 7-3). Amongst flax oil-based polyols, the polyol produced through route A (i.e. flax oil →transesterification with methanol →epoxidation → hydroxylation) had the lowest OHV which can be related to the lower OOC% after epoxidation.

Table 7-3 Hydroxyl value (OHV), viscosity, relative percentage of monomers, dimers and oligomers and their average molecular weight obtained by GPC of the polyols produced form different routes.

Polyols [a]	OHV (mgKOH/g)	Viscosity (Pa.s)	Monomers		Dimers and oligomers	
			(%)	MW [b]	(%)	MW [b]
Flax oil polyol route A	334 ± 3.2	1.20 ± 0.01	80.3	478	19.7± 0.7	1024
Flax oil polyol route B	361± 6.2	2.17 ± 0.002	79.6	480	20.4 ± 0.9	1100
Flax oil polyol route C	407 ± 4.2	9.62 ± 0.03	57.5	576	42.5± 1.2	1520
Canola oil polyol route C	347± 2.5	1.60 ± 0.001	68.6	566	31.4± 0.6	1200

[a] See Figure 7-2
[b] Estimated Average molecular weight obtained by GPC

It should be noted that the ratio of primary hydroxyl groups to total hydroxyl groups in polyols produced through transesterification with 1,3-propanediol (route **C**) would be higher than that for the other polyols. This is because that a higher amount of 1,3-propanediol is incorporated into the polyol. The OHV measured after the epoxidation reaction is due to the formation of secondary OH groups. The epoxidized flax FAME had a higher OHV (~95.5 mgKOH/g) compared to epoxidized flax (OHV of ~25 mgKOH/g) and canola (~20 mgKOH/g) oils (Table 7-1).

Therefore, the flax FAME polyol produced through route **A** would have the lowest ratio of primary OH to total OH groups.

The viscosities of the polyols were measured and the results are listed in Table 7-3. The viscosity of flax oil-polyol $_{\text{route C}}$ was 9.62 Pa.s that is much higher than the viscosities of other polyols. However, canola oil polyol that was produced through a similar route to flax oil-polyol $_{\text{route C}}$ had a lower viscosity (1.6 Pa.s). The formation of dimers and oligomers in hydroxylation process can results in an increase in the viscosity of polyols. Dimerization and oligomerization can occur during the hydroxylation process when the two hydroxyl groups present in a 1,3-propanediol opens two oxirane groups forming a bridge. In order to investigate the hypothesis that the higher viscosity of flax oil-polyol $_{\text{route C}}$ was due to its higher dimer-oligomer content, gel permeation chromatography (GPC) was performed (Figure 7-8). It was found that the dimer-oligomer content of flax oil-polyol $_{\text{route C}}$ was 42.5% that is higher than the 31.4% dimer-oligomer content of canola oil-polyol (Table 7-3).

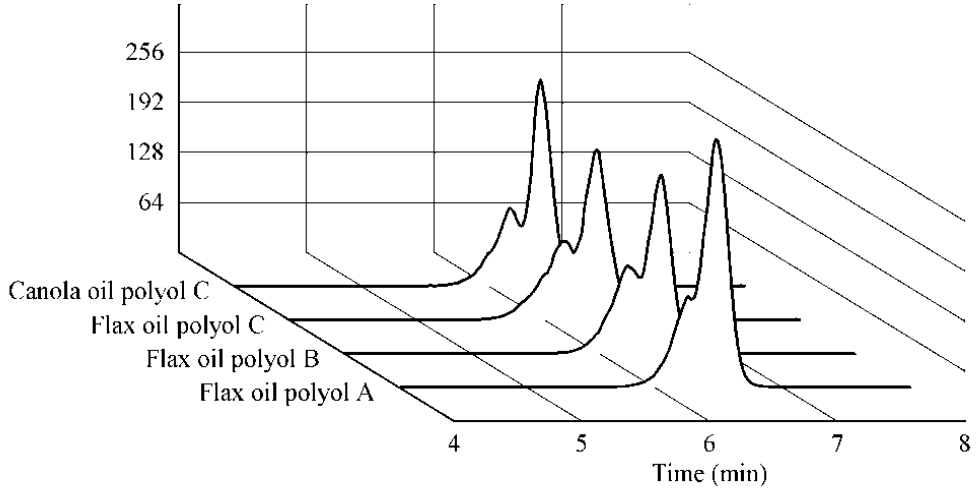

Figure 7-8 The GPC trace of flax oil based polyols produced through different routes and canola oil-based polyol synthesized through route **C** (see Figure 7-2).

In the hydroxylation reaction, the OHV increases through ring opening by 1,3-propanediol, so the molecular mass also increases. The average molecular weight (MW) of the monomers and dimer-oligomer of flax oil-polyol $_{route\ C}$ and canola oil-polyol $_{route\ C}$ prepared through route C were determined by GPC coupled with ELSD (Table 7-3). The average MW of dimer-oligomer of flax oil-polyol $_{route\ C}$ was estimated to be 1520 g/mole, which is higher than that for canola oil-polyol $_{route\ C}$ (average MW of 1200 g/mole). Therefore, the higher viscosity of flax oil-polyol $_{route\ C}$ can be explained by the higher content of dimer-oligomer with a higher average MW. In addition, flax oil-polyol $_{route\ C}$ had higher OHV which results in a greater hydrogen bonding and hence, an increase in viscosity. It is also likely that the flax oil-polyol $_{route\ C}$ compared to canola oil-polyol $_{route\ C}$ contains higher amounts of oligomers with a very high MW. The presence of these oligomers in a polyol, even at low concentrations, can significantly increase the viscosity of the polyol. However, more works are required to confirm the presence of a higher concentration of these oligomers in flax oil-polyol $_{route\ C}$ compared to canola oil-polyol $_{route\ C}$. For example, a GPC with a series of columns can be used to resolve further the peaks.

The transesterification of epoxidized oils with 1,3-propanediol were completed in 4 h and the time required for the hydroxylation reaction (maximum OHV achieved) was 6 h for flax oil-based polyols (route A, B, and C) and 5 h for canola oil-based polyol (route C). Therefore, the total time required for transesterification and ring opening with 1,3-propanediol was 10 h for flax oil polyol $_{route\ C}$ and 9 h in case of canola oil polyol $_{route\ C}$. This time is much shorter than the time required for performing ring opening and transesterification with 1,3-propanediol at the same time in the presence of sulfuric acid, as reported by our group previously [22].

7.4 Conclusion

A new route for producing polyol from vegetable oil was described in this work. The steps of this route can be summarized as: vegetable oil→ epoxidation→ transesterification with 1,3-propanediol→ hydroxylation. In this route, no washing or clean up step is required after transesterification with 1,3-propanediol. Sodium methoxide (transesterification catalyst) is neutralized by adding sulfuric acid to the mixture, and the acetone used in transesterification can be evaporated and recovered prior to hydroxylation. In addition, the excess amounts of 1,3-propanediol remaining from transesterification reaction is used for ring-opening. The new route yields a polyol with high OHV and relatively low viscosity. This in particular, benefits the production of polyols from vegetable oils with a relatively low degree of unsaturation. For these polyols, this process maximizes the OHV that can be achieved. The polyols produced through this method can be used as raw materials for the production of polyurethane polymers, foam, and flame retardant.

7.5 References:

[1] Zieleniewska, M., Leszczynski, M. K., Kuranska, M., Prociak, A., Szczepkowski, L., Krzyowska, M., Ryszkowska, J., Preparation and characterisation of rigid polyurethane foams using a rapeseed oil-based polyol, *Industrial Crops and Products*. 2015, *74*, 887-897.

[2] Pietrzak, K., Kirpluks, M., Cabulis, U., Ryszkowska, J., Effect of the addition of tall oil-based polyols on the thermal and mechanical properties of ureaurethane elastomers, *Polymer Degradation and Stability*. 2014, *108*, 201-211.

[3] Rouilly, A., Rigal, L., Agro-materials: A bibliographic review, *Journal of Macromolecular Science-Polymer Reviews*. 2002, *C42*, 441-479.

[4] Williams, C. K., Hillmyer, M. A., Polymers from renewable resources: A perspective for a special issue of polymer reviews, *Polymer Reviews*. 2008, *48*, 1-10.

[5] Seniha Guner, F., Yagci, Y., Tuncer Erciyes, A., Polymers from triglyceride oils, *Progress in Polymer Science*. 2006, *31*, 633-670.

[6] Meier, M. A. R., Metzger, J. O., Schubert, U. S., Plant oil renewable resources as green alternatives in polymer science, *Chemical Society Reviews*. 2007, *36*, 1788-1802.

[7] Zlatanic, A., Lava, C., Zhang, W., Petrovic, Z. S., Effect of structure on properties of polyols and polyurethanes based on different vegetable oils, *Journal of Polymer Science Part B: Polymer Physics*. 2004, *42*, 809-819.

[8] Dumont, M. J., Kharraz, E., Qi, H., Production of polyols and mono-ols from 10 North-American vegetable oils by ozonolysis and hydrogenation: A characterization study, *Industrial Crops and Products*. 2013, *49*, 830-836.

[9] Petrovic, Z. S., Wan, X., Bilic, O., Zlatanic, A., Hong, J., Javni, I., Ionescu, M., Milic, J., Degruson, D., Polyols and polyurethanes from crude algal oil, *Journal of the American Oil Chemists Society*. 2013, *90*, 1073-1078.

[10] Tran, P., Graiver, D., Narayan, R., Ozone-mediated polyol synthesis from soybean oil, *Journal of the American Oil Chemists Society*. 2005, *82*, 653-659.

[11] Petrovic, Z. S., Guo, A., Javni, I., Cvetkovic, I., Hong, D. P., Polyurethane networks from polyols obtained by hydroformylation of soybean oil, *Polymer International*. 2008, *57*, 275-281.

[12] Petrovic, Z. S., Cvetkovic, I., Hong, D., Wan, X., Zhang, W., Abraham, T. W., Malsam, J., Vegetable oil-based triols from hydroformylated fatty acids and polyurethane elastomers, *European Journal of Lipid Science and Technology*. 2010, *112*, 97-102.

[13] Vanbesien, T., Hapiot, F., Monflier, E., Hydroformylation of vegetable oils and the potential use of hydroformylated fatty acids, *Lipid Technology*. 2013, *25*, 175-178.

[14] Campanella, A., Bonnaillie, L. M., Wool, R. P., Polyurethane foams from soyoil-based polyols, *Journal of Applied Polymer Science*. 2009, *112*, 2567-2578.

[15] Mohammed, I. A., Al-Mulla, E. A. J., Kadar, N. K. A., Ibrahim, M., Structure-property studies of thermoplastic and thermosetting polyurethanes using palm and soya oils-based polyols, *Journal of Oleo Science*. 2013, *62*, 1059-1072.

[16] Tanaka, R., Hirose, S., Hatakeyama, H., Preparation and characterization of polyurethane foams using a palm oil-based polyol, *Bioresource Technology*. 2008, *99*, 3810-3816.

[17] Dai, H., Yang, L., Lin, B., Wang, C., Shi, G., Synthesis and characterization of the different soy-based polyols by ring opening of epoxidized soybean oil with methanol, 1,2-ethanediol and 1,2-propanediol, *Journal of the American Oil Chemists Society*. 2009, *86*, 261-267.

[18] Xu, J., Jiang, J., Li, J., Preparation of polyester polyols from unsaturated fatty acid, *Journal of Applied Polymer Science*. 2012, *126*, 1377-1384.

[19] Ahmad Syafiq, A. H., Aung, M., Luqman Chuah, A., Mek Zah, S., Mohd Hilmi, M., Producing Jatropha oil-based polyol via epoxidation and ring opening, *Industrial Crops and Products*. 2013, *50*, 563-567.

[20] Rojek, P., Prociak, A., Effect of different rapeseed-oil-based polyols on mechanical properties of flexible polyurethane foams, *Journal of Applied Polymer Science*. 2012, *125*, 2936-2945.

[21] Miao, S. D., Wang, P., Su, Z. G., Zhang, S. P., Vegetable-oil-based polymers as future polymeric biomaterials, *Acta Biomaterialia*. 2014, *10*, 1692-1704.

[22] Kong, X., Liu, G., Curtis, J. M., Novel polyurethane produced from canola oil based poly(ether ester) polyols: Synthesis, characterization and properties, *European Polymer Journal*. 2012, *48*, 2097-2106.

[23] Meher, L. C., Sagar, D. V., Naik, S. N., Technical aspects of biodiesel production by transesterification: a review, *Renewable & Sustainable Energy Reviews*. 2006, *10*, 248-268.

[24] Holser, R. A., Transesterification of epoxidized soybean oil to prepare epoxy methyl esters, *Industrial Crops and Products*. 2008, *27*, 130-132.

[25] Ionescu, M.: Polyols from renewable resources-oleochemical polyols, in: *Chemistry and technology of polyols for polyurethanes*, RAPRA Technology, United Kongdom 2005, pp. 435-470.

CHAPTER 8

General Conclusion

The use of efficient and rapid analytical methods for the measurement of critical parameters could facilitate the synthesis and development of polyol products. These methods could reduce the time and labor required for these analyses and could additionally provide useful information about each process step.

In this thesis, Fourier Transform infrared (FTIR) spectroscopy was employed to develop analytical methods for the determination of the critical parameters involved in lipid transformations into polyols. These critical parameters were the hydroxyl value (OHV) of polyols, the moisture content of vegetable oils and oil derivatives, and the changes in the iodine value (IV) and oxirane oxygen content (OOC) of vegetable oils during the epoxidation process. Two FITR methods including split-sample and single sample methods (Chapter 2 and 3), were developed for the determination of OHV of polyols. These methods are based on the stoichiometric reaction of toluenesulfonyl isocyanate with hydroxyl groups (OH) resulting in the formation of a carbamate group. The split-sample FTIR method is based on the measurement of the carbamate absorption in FTIR spectra. Although, this method is not moisture sensitive, it is problematic in terms of the adaptation to an automated version due to the difficulty inherent to the split-sample procedures. This limitation was then solved by the development of a single-sample FTIR method, which is based on the measurement of the absorption of isocyanate groups. Since both OH groups and water can react with toluenesulfonyl isocyanate, it was necessary to compensate the measured OHV for any water present in the polyol sample, so to avoid bias the measured OHV. This was achieved by

measuring the absorption of the CO_2 formed by reaction of water with the toluenesulfonyl isocyanate.

The measurement of the hydroxyl values of some pure alcohols and polyols with various hydroxyl values by these FTIR methods and standard AOCS method showed that both FTIR methods are capable of producing accurate results. These FTIR methods compared to AOCS standard method, are much faster (~10 times), more reproducible, and require a lower amount of the solvents and samples. The single sample FTIR method can be automated by using an FTIR instrument equipped with an autosampler. The automated version, could significantly speed-up the measurement of OHV in laboratories which analyze a large number of samples per day. In addition, by the development of a calibration curve for water, the OHV and water content of polyols could be measured simultaneously. This would be a big advantage for polyol manufacturers, who need to report both the OHV and the water content of their products. The current methods available for the measurement of OHV, which is a routine analysis in polyol synthesis, are time-consuming. Therefore, the rapid FTIR methods developed for the determination of OHV can significantly facilitate the development and synthesis of polyols. These methods can benefit researchers, manufacturers, and laboratories that are working in polyol filed.

The concept of quantifying CO_2 absorptions in FTIR spectra to correct the OHV of polyols for water (Chapter 3) was further investigated in Chapter 4 where a rapid and simple FTIR method for the measurement of the moisture content of hydrophobic systems was developed. This method opens a new way to measure the moisture content of hydrophobic products such as biodiesel, lubricant oils, transformer oils, solvents (for instance, hexane, heptane, 1,4-dioxane) and even foods and pharmaceutical products. The FTIR method, which is amenable to automation, can be used as a complementary method to Karl Fischer (KF) method. The accurate determination of

water by KF method is dependent on the complete solubilization of sample in KF reagents (i.e. a mixture of iodine, sulfur dioxide, a base, and an alcohol). Therefore, KF is more suitable for the measurement of water in hydrophilic samples such as alcohols, which are miscible with KF reagents. In contrast, the FTIR method is more suitable for hydrophobic samples such as oils that do not contain high concentration of hydroxyl groups.

Although in this thesis the method was tested for the moisture contents in the range of ~200-1500 ppm, it is feasible to adapt it for much lower moisture contents. This can be achieved for example, by increasing the pathlength of the transmission cell from 115 μm used in this thesis to ~1000 μm or even larger. In this way, in preliminary experiments it was possible to achieve measurement of water contents as low as ~10ppm in transformer oils.

FTIR spectroscopy was also exploited for the monitoring the epoxidation reaction of vegetable oils (Chapter 5). An attenuated total reflectance (ATR) FTIR was developed to track changes in the iodine (IV) value and the oxirane oxygen content (OOC), as the indicators of the progress of the epoxidation reaction for vegetable oils. This method produces similar results to those obtained by ASTM methods for the measurement of IV and OOC of vegetable oils, but in much shorter time with much lower solvent consumption. The ATR-FTIR method was tested for the monitoring of epoxidation of canola, camelina, and flax oils with IV in the range of ~120-210 $gI_2/100g$, which is representative of many other vegetable oils. This method can be also used to facilitate kinetic studies of the epoxidation reaction that requires the analysis of many samples.

Overall, the results show that the FTIR spectroscopy can be used for the development of rapid and simple methods to determine the critical parameters involved in lipid-based reactions. For example, as shown in this thesis it can assist in the synthesis and in the development of new polyols. In polyol synthesis, a single technique for the measurement of OHV, moisture content,

and monitoring the epoxidation reaction is advantageous since all of these measurements can be performed by a single FTIR instrument equipped with an ATR accessory. This would be beneficial in both a research and an industrial setting.

It was demonstrated that the nonanal and oleic acid in the ozonolysis of fatty acids and their methyl esters can be measured by GC coupled with flame ionization detector (FID) after derivatization by boron trifluoride in methanol (Chapter 6). The products of derivatization of nonanal and oleic acid were analyzed by mass spectrometry and were identified as nonanal dimethyl acetal and methyl oleate, respectively. Although this method was used to measure nonanal and oleic acid, it could be adapted for the measurement of other aldehydes and acids such as hexanal, hexanoic acid, and nonanoic acid, which may form in ozonolysis.

A route for the synthesis of polyols with high OHV and low viscosity was introduced in Chapter 7. In this route, epoxidation of a vegetable oil precedes the transesterification reaction. The epoxidized oil is transesterified with 1,3-propanediol in the presence of sodium methoxide (as a catalyst) and acetone (as a solvent) and then subjected to ring opening of oxirane groups with 1,3-propanediol. Although transesterification with methanol and other monools such as ethanol, propanol, and butanol reduces the viscosity of the final polyols, the transesterification with diols having 2 primary hydroxyl groups, such as 1,3-propanediol, has two other advantages. Firstly, one primary hydroxyl group is introduced to each fatty acid and secondly, the excess amounts of 1,3-propanediol left from the transesterification reaction can be used for the ring opening step.

In summary, this thesis provides some novel analytical methods for the measurement of critical parameters involved in the transformation of vegetable oils into polyols. In particular, the FTIR method developed for the measurement of moisture content provides a foundation for the development of further analytical methods for the measurement of the moisture content of various

materials. This technique was considered sufficiently promising that it was featured on the cover of a major analytical chemistry journal (Analytica Chimica Acta). This thesis also contributes to ongoing developments in the synthesis of vegetable oil-based polyols, a promising area for commercialization.

Thesis Bibliography

[1] Pfister, D. P., Xia, Y., Larock, R. C., Recent advances in vegetable oil-based polyurethanes, *Chemsuschem*. 2011, *4*, 703-717.

[2] Gandini, A., Polymers from renewable resources: A challenge for the future of macromolecular materials, *Macromolecules*. 2008, *41*, 9491-9504.

[3] Nohra, B., Candy, L., Blanco, J. F., Guerin, C., Raoul, Y., Mouloungui, Z., From petrochemical polyurethanes to biobased polyhydroxyurethanes, *Macromolecules*. 2013, *46*, 3771-3792.

[4] Desroches, M., Escouvois, M., Auvergne, R., Caillol, S., Boutevin, B., From vegetable oils to polyurethanes: Synthetic routes to polyols and main industrial products, *Polymer Reviews*. 2012, *52*, 38-79.

[5] Vilela, C., Sousa, A. F., Fonseca, A. C., Serra, A. C., Coelho, J. F. J., Freirea, C. S. R., Silvestrea, A. J. D., The quest for sustainable polyesters insights into the future, *Polymer Chemistry*. 2014, *5*, 3119--3141.

[6] Towards sustainable development, in our common future, ch. 2, http://www.un-documents.net/ocf-02.htm, accessed March 2016.

[7] Rouilly, A., Rigal, L., Agro-materials: A bibliographic review, *Journal of Macromolecular Science-Polymer Reviews*. 2002, *42*, 441-479.

[8] Williams, C. K., Hillmyer, M. A., Polymers from renewable resources: A perspective for a special issue of polymer reviews, *Polymer Reviews*. 2008, *48*, 1-10.

[9] Seniha Guner, F., Yagci, Y., Tuncer Erciyes, A., Polymers from triglyceride oils, *Progress in Polymer Science*. 2006, *31*, 633-670.

[10] Metzger, J. O., Bornscheuer, U., Lipids as renewable resources: current state of chemical and biotechnological conversion and diversification, *Applied Microbiology and Biotechno*logy. 2006, *71*, 13-22.

[11] Miao, S. D., Wang, P., Su, Z. G., Zhang, S. P., Vegetable-oil-based polymers as future polymeric biomaterials, *Acta Biomaterialia*. 2014, *10*, 1692-1704.

[12] Alagi, P., Hong, S. C., Vegetable oil-based polyols for sustainable polyurethanes, *Macromolecular Research*. 2015, *23*, 1079-1086.

[13] Meier, M. A. R., Metzger, J. O., Schubert, U. S., Plant oil renewable resources as green alternatives in polymer science, *Chemical Society Reviews*. 2007, *36*, 1788-1802.

[14] L. Montero de Espinosa, Meier, M. A. R., Plant oils: The perfect renewable resource for polymer science ?, *European Polymer Journal*. 2011, *47*, 837-852.

[15] de Espinosa, L. M., Ronda, J. C., Galia, M., Cadiz, V., A new route to acrylate oils: crosslinking and properties of acrylate triglycerides from high oleic sunflower oil, *Journal of Polymer Science Part a-Polymer Chemistry*. 2009, *47*, 1159-1167.

[16] Montero De Espinosa, L., Ronda, J. C., Galia, M., Cadiz, V., A straightforward strategy for the efficient synthesis of acrylate and phosphine oxide-containing vegetable oils and their crosslinked materials, *Journal of Polymer Science Part a-Polymer Chemistry*. 2009, *47*, 4051-4063.

[17] Bica, I., Anitas, E. M., Averis, L. M. E., Tensions and deformations in composites based on polyurethane elastomer and magnetorheological suspension: Effects of the magnetic field, *Journal of Industrial and Engineering Chemistry*. 2015, *28*, 86-90.

[18] More, A. S., Lebarbé, T., Maisonneuve, L., Gadenne, B., Alfos, C., Cramail, H., Novel fatty acid based di-isocyanates towards the synthesis of thermoplastic polyurethanes, *European Polymer Journal*. 2013, *49*, 823-833.

[19] Zhang, C. Q., Madbouly, S. A., Kessler, M. R., Biobased polyurethanes prepared from different vegetable oils, *Acs Applied Materials & Interfaces*. 2015, *7*, 1226-1233.

[20] Zhang, C. Q., Xia, Y., Chen, R. Q., Huh, S., Johnston, P. A., Kessler, M. R., Soy-castor oil based polyols prepared using a solvent-free and catalyst-free method and polyurethanes therefrom, *Greem Chemistry*. 2013, *15*, 1477-1484.

[21] Lligadas, G., Ronda, J. C., Galia, M., Cadiz, V., Plant oils as platform chemicals for polyurethane synthesis: Current state-of-the-art, *Biomacromolecules*. 2010, *11*, 2825-2835.

[22] Pechar, T. W., Wilkes, G. L., Zhou, B., Luo, N., Characterization of soy-based polyurethane networks prepared with different diisocyanates and their blends with petroleum-based polyols, *Journal of Applied Polymer Science*. 2007, *106*, 2350-2362.

[23] Campanella, A., Bonnaillie, L. M., Wool, R. P., Polyurethane foams from soyoil-based polyols, *Journal of Applied Polymer Science*. 2009, *112*, 2567-2578.

[24] Zlatanic, A., Lava, C., Zhang, W., Petrovic, Z. S., Effect of structure on properties of polyols and polyurethanes based on different vegetable oils, *Journal of Polymer Science Part B: Polymer Physics*. 2004, *42*, 809-819.

[25] Miao, S. D., Zhang, S. P., Su, Z. G., Wang, P., A novel vegetable oil-lactate hybrid monomer for synthesis of highTg polyurethanes, *Journal of Polymer Science Part a-Polymer Chemistry*. 2010, *48*, 243-250.

[26] Aniceto, J. P. S., Portugal, I., Silva, C. M., Biomass-based polyols through oxypropylation reaction, *Chemsuschem*. 2012, *5*, 1358-1368.

[27] Nadji, H., Bruzzese, C., Belgacem, M. N., Benaboura, A., Gandini, A., Oxypropylation of lignins and preparation of rigid polyurethane foams from the ensuing polyols, *Macromolecular Materials and Engineering*. 2005, *290*, 1009-1016.

[28] Hu, S., Luo, X., Li, Y., Polyols and Polyurethanes from the Liquefaction of Lignocellulosic Biomass, *Chemsuschem*. 2014, *7*, 66-72.

[29] Kumar, S., Hablot, E., Moscoso, J. L. G., Obeid, W., Hatcher, P. G., DuQuette, B. M., Graiver, D., Narayan, R., Balan, V., Polyurethanes preparation using proteins obtained from microalgae, *Journal of Materials Science*. 2014, *49*, 7824-7833.

[30] Yu, F., Le, Z., Chen, P., Liu, Y., Lin, X., Ruan, R., Atmospheric pressure liquefaction of dried distillers grains (DDG) and making polyurethane foams from liquefied DDG, *Applied Biochemistry and Biotechnology*. 2008, *148*, 235-243.

[31] Suresh, K. I., Kishanprasad, V. S., Synthesis, structure, and properties of novel polyols from cardanol and developed polyurethanes, *Industrial & Engineering Chemistry Research*. 2005, *44*, 4504-4512.

[32] Gobin, M., Loulergue, P., Audic, J. L., Lemiegre, L., Synthesis and characterisation of bio-based polyester materials from vegetable oil and short to long chain dicarboxylic acids, *Industrial Crops and Products*. 2015, *70*, 213-220.

[33] Mohammed, I. A., Al-Mulla, E. A. J., Kadar, N. K. A., Ibrahim, M., Structure-property studies of thermoplastic and thermosetting polyurethanes using palm and soya oils-based polyols, *Journal of Oleo Science*. 2013, *62*, 1059-1072.

[34] Petrovic, Z. S., Zhang, W., Javni, I., Structure and properties of polyurethanes prepared from triglyceride polyols by ozonolysis, *Biomacromolecules*. 2005, *6*, 713-719.

[35] Kong, X., Narine, S. S., Physical properties of polyurethane plastic sheets produced from polyols from canola oil, *Biomacromolecules*. 2007, *8*, 2203-2209.

[36] Guo, A., Demydov, D., Zhang, W., Petrovic, Z. S., Polyols and polyurethanes from hydroformylation of soybean oil, *Journal of Polymers and the Environment*. 2002, *10*, 49-52.

[37] Caillol, S., Desroches, M., Carlotti, S., Auvergne, R., Boutevin, B., Synthesis of new polyurethanes from vegetable oil by thiol-ene coupling, *Green Materials*. 2013, *1*, 16-26.

[38] Desroches, M., Caillol, S., Lapinte, V., Auvergne, R., Boutevin, B., Synthesis of biobased polyols by thiol-ene coupling from vegetable oils, *Macromolecules*. 2011, *44*, 2489-2500.

[39] Chaudhari, A. B., Tatiya, P. D., Hedaoo, R. K., Kulkarni, R. D., Gite, V. V., Polyurethane prepared from neem oil polyesteramides for self-healing anticorrosive coatings, *Industrial & Engineering Chemistry Research*. 2013, *52*, 10189-10197.

[40] Chaudhari, A., Kuwar, A., Mahulikar, P., Hundiwale, D., Kulkarni, R., Gite, V., Development of anticorrosive two pack polyurethane coatings based on modified fatty amide of Azadirachta indica Juss oil cured at room temperature - a sustainable resource, *Rsc Advances*. 2014, *4*, 17866-17872.

[41] Galià, M., de Espinosa, L. M., Ronda, J. C., Lligadas, G., Cádiz, V., Vegetable oil-based thermosetting polymers, *European Journal of Lipid Science and Technology*. 2010, *112*, 87-96.

[42] Mustata, F., Bicu, I., Cascaval, C. N., Rheological and thermal behaviour of an epoxy resin modified with reactive diluents, *Journal of Polymer Engineering*. 1997, *17*, 491-506.

[43] Rosch, J., Mulhaupt, R., Polymers from renewable resoureces: polyester resins and blends based upon anhydride-cured epoxidized soybean oil, *Polymer Bulletin*. 1993, *31*, 679-685.

[44] Thames, S. F., Yu, H., Cationic UV-cured coatings of epoxide-containing vegetable oils, *Surface & Coatings Technology*. 1999, *115*, 208-214.

[45] Harry-O'Kuru, R. E., Carriere, C. J., Synthesis, rheological characterization, and constitutive Modeling of polyhydroxy triglycerides derived from milkweed oil, *Journal of Agricultural and Food Chemistry*. 2002, *50*, 3214-3221.

[46] Harry-O'kuru, R. E., Holser, R. A., Abbott, T. P., Weisleder, D., Synthesis and characteristics of polyhydroxy triglycerides from milkweed oil, *Industrial Crops and Products*. 2002, *15*, 51-58.

[47] Ionescu, M., Petrovic, Z. S., Wan, X., Ethoxylated soybean polyols for polyurethanes, *Journal of Polymers and the Environment*. 2007, *15*, 237-243.

[48] Lu, Y., Larock, R. C., Soybean-oil-based waterborne polyurethane dispersions: Effects of polyol functionality and hard segment content on properties, *Biomacromolecules*. 2008, *9*, 3332-3340.

[49] Javni, I., Zhang, W., Petrovic, Z. S., Effect of different isocyanates on the properties of soy-based polyurethanes, *Journal of Applied Polymer Science*. 2003, *88*, 2912-2916.

[50] Kong, X., Liu, G., Curtis, J. M., Novel polyurethane produced from canola oil based poly (ether ester) polyols: Synthesis, characterization and properties, *European Polymer Journal*. 2012, *48*, 2097-2106.

[51] Lyon, C. K., Garrett, V. H., Goldblatt, L. A., Rigid urethane foams from blown castor oils *Journal of the American Oil Chemists Society*. 1964, *41*, 23-25.

[52] Petrovic, Z. S., Fajnik, D., Preparation and properties of castor oil-based polyurethanes, *Journal of Applied Polymer Science*. 1984, *29*, 1031-1040.

[53] Schuchardt, U., Sercheli, R., Vargas, R. M., Transesterification of vegetable oils: a review, *Journal of the Brazilian Chemical Society*. 1998, *9*, 199-210.

[54] Hablot, E., Zheng, D., Bouquey, M., Averous, L., Polyurethanes based on castor oil: Kinetics, chemical, mechanical and thermal properties, *Macromolecular Materials and Engineering*. 2008, *293*, 922-929.

[55] Narine, S. S., Kong, X., Bouzidi, L., Sporns, P., Physical properties of polyurethanes produced from polyols from seed oils: I. Elastomers, *Journal of the American Oil Chemists Society*. 2007, *84*, 55-63.

[56] Ionescu, M.: The general characteristics of oligo-polyols, in: Chemistry and technology of polyols for polyurethanes, RAPRA Technology, United Kongdom 2005, pp. 40-47.

[57] Voort, F. R. v. d., Sedman, J., Russin, T., Lipid analysis by vibrational spectroscopy. I, *European Journal of Lipid Science and Technology*. 2001, *103*, 815-825.

[58] Subramanian, A., Rodriguez-Saona, L.: Fourier transform infrared (FTIR) spectroscopy, in: Infrared Spectroscopy for Food Quality Analysis and Control Ed. D. Sun, Academic Press, Amsterdam 2009, pp. 145-178.

[59] Vlachos, N., Skopelitis, Y., Psaroudaki, M., Konstantinidou, V., Chatzilazarou, A., Tegou, E., Applications of Fourier transform-infrared spectroscopy to edible oils, *Analytica Chimica Acta*. 2006, *573*, 459-465.

[60] Mba, O., Adewale, P., Dumont, M.-J., Ngadi, M., Application of near-infrared spectroscopy to characterize binary blends of palm and canola oils, *Industrial Crops and Products*. 2014, *61*, 472-478.

[61] Azizian, H., Kramer, J. K. G., A rapid method for the quantification of fatty acids in fats and oils with emphasis on trans fatty acids using Fourier transform near infrared spectroscopy (FT-NIR), *Lipids*. 2005, *40*, 855-867.

[62] Li, H., van deVoort, F. R., Sedman, J., Ismail, A. A., Rapid determination of cis and trans content, iodine value, and saponification number of edible oils by Fourier transform near-infrared spectroscopy, *Journal of the American Oil Chemists Society*. 1999, *76*, 491-497.

[63] Li, H., van de Voort, F. R., Ismail, A. A., Cox, R., Determination of peroxide value by Fourier transform near-infrared spectroscopy, *Journal of the American Oil Chemists Society*. 2000, *77*, 137-142.

[64] Hendl, O., Howell, J. A., Lowery, J., Jones, W., A rapid and simple method for the determination of iodine values using derivative Fourier transform infrared measurements, *Analytica Chimica Acta*. 2001, *427*, 75-81.

[65] Sedman, J., van de Voort, F. R., Ismail, A. A., Simultaneous determination of iodine value and trans content of fats and oils by single-bounce horizontal attenuated total reflectance Fourier transform infrared spectroscopy, *Journal of the American Oil Chemists Society*. 2000, *77*, 399-403.

[66] Yu, X., van de Voort, F. R., Sedman, J., Determination of peroxide value of edible oils by FTIR spectroscopy with the use of the spectral reconstitution technique, *Talanta*. 2007, *74*, 241-246.

[67] Yu, X., de Voort, F. R. v., Sedman, J., Gao, J.-m., A new direct Fourier transform infrared analysis of free fatty acids in edible oils using spectral reconstitution, *Analytical and bioanalytical chemistry*. 2011, *401*, 315-324.

[68] Xu, L., Zhu, X., Chen, X., Sun, D., Yu, X., Direct FTIR analysis of isolated trans fatty acids in edible oils using disposable polyethylene film, *Food Chemistry*. 2015, *185*, 503-508.

[69] Cerretani, L., Giuliani, A., Maggio, R. M., Bendini, A., Toschi, T. G., Cichelli, A., Rapid FTIR determination of water, phenolics and antioxidant activity of olive oil, *European Journal of Lipid Science and Technology*. 2010, *112*, 1150-1157.

[70] Meng, X., Pan, Q., Ding, Y., Jiang, L., Rapid determination of phospholipid content of vegetable oils by FTIR spectroscopy combined with partial least-square regression, *Food Chemistry*. 2014, *147*, 272-278.

[71] Meng, X., Sedman, J., van de Voort, F. R., Improving the determination of moisture in edible oils by FTIR spectroscopy using acetonitrile extraction, *Food Chemistry*. 2012, *135*, 722-729.

[72] Xiuzhu, Y., Qinghua, L., Daijun, S., Xiaobin, D., Tong, W., Determination of the peroxide value of edible oils by FTIR spectroscopy using polyethylene films, *Analytical Methods*. 2015, *7*, 1727-1731.

[73] Ma, K., vandeVoort, F. R., Sedman, J., Ismail, A. A., Stoichiometric determination of hydroperoxides in fats and oils by Fourier transform infrared spectroscopy, *Journal of the American Oil Chemists Society*. 1997, *74*, 897-906.

[74] Al-Alawi, A., van de Voort, F. R., Sedman, J., A new FTIR method for the analysis of low levels of FFA in refined edible oils, *Spectroscopy Letters*. 2005, *38*, 389-403.

[75] Chalasani, S. R. K., Dewasthale, S., Hablot, E., Shi, X., Graiver, D., Narayan, R., A spectroscopic method for hydroxyl value determination of polyols, *Journal of the American Oil Chemists Society*. 2013, *90*, 1787-1793.

[76] Tena, N., Aparicio, R., Garcia-Gonzalez, D. L., Thermal deterioration of virgin olive oil monitored by ATR-FTIR analysis of trans content, *Journal of Agricultural and Food Chemistry*. 2009, *57*, 9997-10003.

[77] Rohman, A., Man, Y. B. C., Application of FTIR spectroscopy for monitoring the stabilities of selected vegetable oils during thermal oxidation, *International Journal of Food Properties*. 2013, *16*, 1594-1603.

[78] Rohman, A., Man, Y. B. C., The use of Fourier transform mid infrared (FT-MIR) spectroscopy for detection and quantification of adulteration in virgin coconut oil, *Food Chemistry*. 2011, *129*, 583-588.

[79] Srivastava, Y., Semwal, A. D., A study on monitoring of frying performance and oxidative stability of virgin coconut oil (VCO) during continuous/prolonged deep fat frying process using chemical and FTIR spectroscopy, *Journal of Food Science and Technology-Mysore*. 2015, *52*, 984-991.

[80] Dreau, Y. l., Dupuy, N., Gaydou, V., Joachim, J., Kister, J., Study of jojoba oil aging by FTIR, *Analytica Chimica Acta*. 2009, *642*, 163-170.

[81] Quinones-Islas, N., Gabriela Meza-Marquez, O., Osorio-Revilla, G., Gallardo-Velazquez, T., Detection of adulterants in avocado oil by Mid-FTIR spectroscopy and multivariate analysis, *Food Research International*. 2013, *51*, 148-154.

[82] Abdul, R., Riyanto, S., Sasi, A. M., Mohd. Yusof, F., The use of FTIR spectroscopy in combination with chemometrics for the authentication of red fruit (Pandanus conoideus Lam) oil from sunflower and palm oils, *Food Bioscience*. 2014, *7*, 64-70.

[83] Zhang, Q., Liu, C., Sun, Z., Hu, X., Shen, Q., Wu, J., Authentication of edible vegetable oils adulterated with used frying oil by Fourier Transform Infrared Spectroscopy, *Food Chemistry*. 2012, *132*, 1607-1613.

[84] Escuderos, M. E., Olive oil aroma evaluation by Gas chromatographic method: A critical review, *Critical Reviews in Analytical Chemistry*. 2011, *41*, 70-80.

[85] Tao, W., Jina, L., SeongHo, C., HanSeok, K., HongGu, L., Comparative studies on derivatization methods of single or mixed fatty acids, *Food Science and Biotechnology*. 2013, *22*, 1573-1579.

[86] Official Methods and Recommended Practices of the American Oil Chemists' Society (1997), 4th edn. American Oil Chemists' Society, Champaign, 1993, revised (1997).

[87] American Society for Testing and Materials ASTM D4274-11 (2011).

[88] American Society for Testing and Materials ASTM E222-10 (2010).

[89] American Society for Testing and Materials ASTM E1899-08 (2008).

[90] German National Standard DIN 53240-2 (2007).

[91] American Society for Testing and Materials ASTM D6342-12 (2012).

[92] Ferrao, M. F., Godoy, S. C., Gerbase, A. E., Mello, C., Furtado, J. C., Petzhold, C. L., Poppi, R. J., Non-destructive method for determination of hydroxyl value of soybean polyol by LS-SVM using HATR/FT-IR, *Analytica Chimica Acta*. 2007, *595*, 114-119.

[93] Godoy, S. C., Ferrao, M. F., Gerbase, A. E., Determination of the hydroxyl value of soybean polyol by attenuated total reflectance/fourier transform infrared spectroscopy, *Journal of the American Oil Chemists Society*. 2007, *84*, 503-508.

[94] Fuller, M. P., Ritter, G. L., Draper, C. S., Partial Least-Squares quantitative analysis of infrared spectroscopic data. Part I: Algorithm implementation, *Applied Spectroscopy*. 1988, *42*, 217-227.

[95] van de Voort, F. R., Sedman, J., Russin, T., Lipid analysis by vibrational spectroscopy, *European Journal of Lipid Science and Technology*. 2001, *103*, 815-826.

[96] Chemical Online (2011) MB3600-CH20 chemicals analyzer. http://www.chemicalonline.com/doc/mb3600-ch20-chemicals-analyzer-0001. Accessed May 2013.

[97] Anuar, S. T., Zhao, Y. Y., Mugo, S. M., Curtis, J. M., Monitoring the epoxidation of canola oil by non-aqueous reversed phase liquid chromatography/mass spectrometry for process optimization and control, *Journal of the American Oil Chemists Society*. 2012, *89*, 1951-1960.

[98] Curtis, J. M., Liu, G. G., Polyol synthesis from fatty acids and oils. 2012, WO 2012-009801.

[99] Ma, K., van de Voort, F. R., Ismail, A. A., Sedman, J., Quantitative determination of hydroperoxides by Fourier transform infrared spectroscopy with a disposable infrared card, *Journal of the American Oil Chemists Society*. 1998, *75*, 1095-1101.

[100] van de Wort, F. R., Sedman, J., Cocciardi, R., Juneau, S., An automated FTIR method for the routine quantitative determination of moisture in lubricants: An alternative to Karl Fischer titration, *Talanta*. 2007, *72*, 289-295.

[101] Ionescu, M., Petrovic, Z. S., Wan, X., Primary hydroxyl content of soybean polyols, *Journal of the American Oil Chemists Society*. 2008, *85*, 465-473.

[102] van de Voort, F. R., Sedman, J., Yaylayan, V., Laurent, C. S., Determination of acid number and base number in lubricants by Fourier transform infrared spectroscopy, *Applied Spectroscopy*. 2003, *57*, 1425-1431.

[103] Van De Voort, F. R., Sedman, J., Pinchuk, D., An overview of progress and new developments in FTIR lubricant condition monitoring methodology, *Journal of ASTM International*. 2011, *8*, 1-14.

[104] Xiuzhu, Y., Voort, F. R., Sedman, J., Jin-Ming, G., A new direct Fourier transform infrared analysis of free fatty acids in edible oils using spectral reconstitution, *Analytical and bioanalytical chemistry*. 2011, *401*, 315-324.

[105] Hui, L., Voort, F. R. v. d., Ismail, A. A., Cox, R., Determination of peroxide value by Fourier transform near-infrared spectroscopy, *Journal of the American Oil Chemists' Society*. 2000, *77*, 137-142.

[106] Al-Alawi, A., van de Voort, F. R., Sedman, J., Ghetler, A., Automated FTIR analysis of free fatty acids or moisture in edible oils, *Journal of Laboratory Automation*. 2006, *11*, 23-29.

[107] Sonntag, N. O. V.: Analytical methods, in: Bailey's industrial oil and fat products Ed. D. Swern, John Wiley & Sons, New York 1982, pp. 484–487.

[108] Official and Tentative Methods of the American Oil Chemists' Society, Ed. D. Firestone, American Oil Chemists' Society, Champaign 1989.

[109] American Association of Cereal Chemists AACC 14-15A (1995).

[110] Cedergren, A., Luan, L. W., Potentiometric determination of water using spent imidazole-buffered Karl Fischer reagents, *Analytical Chemistry*. 1998, *70*, 2174-2180.

[111] Rosvall, M., Lundmark, L., Cedergren, A., Computer-controlled, coulometric Karl Fischer system for continuous titration of water based on zero current potentiometry, *Analytical Chemistry*. 1998, *70*, 5332-5338.

[112] Cedergren, A., Jonsson, S., Diaphragm-free cell for trace determination of water based on the Karl Fischer reaction using continuous coulometric titration, *Analytical Chemistry*. 1997, *69*, 3100-3108.

[113] Cedergren, A., Jonsson, S., Progress in Karl Fischer coulometry using diaphragm-free cells, *Analytical Chemistry*. 2001, *73*, 5611-5615.

[114] Cedergre.A, Reaction rates between water and Karl-Fischer reagent, *Talanta*. 1974, *21*, 265-271.

[115] Margolis, S. A., Effect of hydrocarbon composition on the measurement of water in oils by coulometric and volumetric Karl Fischer methods, *Analytical Chemistry*. 1998, *70*, 4264-4270.

[116] van de Voort, F. R., Ghetler, A., Garcia-Gonzalez, D. L., Li, Y. D., Perspectives on quantitative mid-FTIR spectroscopy in relation to edible oil and lubricant analysis: evolution and integration of analytical methodologies, *Food Analytical Methods*. 2008, *1*, 153-163.

[117] Man, Y. B. C., Mirghani, M. E. S., Rapid method for determining moisture content in crude palm oil by Fourier transform infrared spectroscopy, *Journal of the American Oil Chemists' Society*. 2000, *77*, 631-637.

[118] A. Rohman, Y. B. C. M., Analysis of water content in soap formulation using Fourier transform infrared (FTIR) spectroscopy, *Journal of Applied Sciences Research*. 2009, *5*, 717-721.

[119] van de Voort, F. R., Sedman, J., Yaylayan, V., Saint Laurent, C., Mucciardi, C.,, Quantitative determination of moisture in lubricants by Fourier transform, *Applied Spectroscopy*. 2004, *58*, 193-198.

[120] Al-Alawi, A., Van De Voort, F. R., Sedman, J., A new Fourier transform infrared method for the determination of moisture in edible oils, *Applied Spectroscopy*. 2005, *59*, 1295-1299.

[121] Xianghe, M., Sedman, J., Voort, F. R. v. d., Improving the determination of moisture in edible oils by FTIR spectroscopy using acetonitrile extraction, *Food Chemistry*. 2012, *135*, 722-729.

[122] Ng, E.-P., Mintova, S., Quantitative moisture measurements in lubricating oils by FTIR spectroscopy combined with solvent extraction approach, *Microchemical Journal*. 2011, *98*, 177-185.

[123] Hadjadj, Y., Fofana, I., van de Voort, F. R., Bussieres, D., Potential of determining moisture content in mineral insulating oil by Fourier transform infrared spectroscopy, *Ieee Electrical Insulation Magazine*. 2016, *32*, 34-39.

[124] Winterfield, C., van de Voort, F. R., Automated Acid and Base Number Determination of Mineral-Based Lubricants by Fourier Transform Infrared Spectroscopy: Commercial Laboratory Evaluation, *JALA*. 2014, *19*, 577-586.

[125] Margolis, S. A., Amperometric measurement of moisture in transformer oil using Karl-Fischer reagents, *Analytical Chemistry*. 1995, *67*, 4239-4246.

[126] Cai, C., Dai, H., Chen, R., Su, C., Xu, X., Zhang, S., Yang, L., Studies on the kinetics of in situ epoxidation of vegetable oils, *European Journal of Lipid Science and Technology*. 2008, *110*, 341-346.

[127] Abdullah, B. M., Salimon, J., Epoxidation of vegetable oils and fatty acids: Catalysts, methods and advantages, *Journal of Applied Sciences*. 2010, *10*, 1545-1553.

[128] American Society for Testing and Materials ASTM D5554-95 (2006).

[129] American Oil Chemists' Society AOCS Cd 1d-92 (2009).

[130] Association of Official Analytical Chemistry AOAC 993.20 (1998).

[131] International Organization for Standardization ISO 3961 (2009). .

[132] International Union of Pure and Applied Chemistry IUPAC 2.205 (1987). .

[133] Association of Official Analytical Chemistry AOAC 28.060 (1984).

[134] Association of Official Analytical Chemistry AOAC 963.22 (1995).

[135] Sedman, J., van de Voort, F. R., Ismail, A. A., Maes, P., Industrial validation of Fourier transform infrared trans and iodine value analyses of fats and oils, *Journal of the American Oil Chemists Society*. 1998, *75*, 33-39.

[136] Talpur, M. Y., Kara, H., Sherazi, S. T. H., Ayyildiz, H. F., Topkafa, M., Arslan, F. N., Naz, S., Durmaz, F., Sirajuddin, Application of multivariate chemometric techniques for simultaneous determination of five parameters of cottonseed oil by single bounce attenuated total reflectance Fourier transform infrared spectroscopy, *Talanta*. 2014, *129*, 473-480.

[137] Adewale, P., Mba, O., Dumont, M.-J., Ngadi, M., Cocciardi, R., Determination of the iodine value and the free fatty acid content of waste animal fat blends using FT-NIR, *Vibrational Spectroscopy*. 2014, *72*, 72-78.

[138] American Society for Testing and Materials ASTM D1652-11 (2011).

[139] American Oil Chemists' Society AOCS Cd 9-57 (2009).

[140] Parreira, T. F., Ferreira, M. M. C., Sales, H. J. S., de Almeida, W. B., Quantitative determination of epoxidized soybean oil using near-infrared spectroscopy and multivariate calibration, *Applied Spectroscopy*. 2002, *56*, 1607-1614.

[141] Goud, V. V., Patwardhan, A. V., Dinda, S., Pradhan, N. C., Kinetics of epoxidation of jatropha oil with peroxyacetic and peroxyformic acid catalysed by acidic ion exchange resin, *Chemical Engineering Science*. 2007, *62*, 4065-4076.

[142] Mohanty, A. K., Misra, M., Drzal, L. T., Sustainable bio-composites from renewable resources: Opportunities and challenges in the green materials world, *Journal of Polymers and the Environment*. 2002, *10*, 19-26.

[143] McGuire J, H. P., Bond G: Ozonolysis in the production of chiral fine chemicals, in: Handbook of chiral chemicals Ed. Ager D, CRC, Taylor & Francis, Boca Raton 2006, pp. 164–185.

[144] Criegee, R., Mechanism of ozonolysis, *Angewandte Chemie International Edition*. 1975, *14*, 745- 752.

[145] Bailey, P. S., The reactions of ozone with organic compounds, *Chemical Reviews*. 1958, *58*, 925-1010.

[146] Fliszar, S., Carles, J., Quantitative investigation of the ozonolysis reaction. VII. Ozonolyses of phenylethylenes in presence of oxygen-18-labeled benzaldehyde, *Journal of the American Chemical Society*. 1969, *91*, 2637-2643.

[147] Petrovic, Z. S., Milic, J., Xu, Y., Cvetkovic, I., A chemical route to high molecular weight vegetable oil-based polyhydroxyalkanoate, *Macromolecules*. 2010, *43*, 4120-4125.

[148] Sell, C. S.: Manufacture of fragrance ingredients, in: Chemistry and the sense of smell, Wiley, London 2014, pp. 296-356.

[149] Omonov, T. S., Kharraz, E., Curtis, J. M., Ozonolysis of canola oil: A study of product yields and ozonolysis kinetics in different solvent systems, *Journal of the American Oil Chemists Society*. 2011, *88*, 689-705.

[150] Dumont, M. J., Kharraz, E., Qi, H., Production of polyols and mono-ols from 10 North-American vegetable oils by ozonolysis and hydrogenation: A characterization study, *Industrial Crops and Products*. 2013, *49*, 830-836.

[151] Soriano, N. U., Jr., Migo, V. P., Matsumura, M., Ozonation of sunflower oil: spectroscopic monitoring of the degree of unsaturation, *Journal of the American Oil Chemists Society*. 2003, *80*, 997-1001.

[152] Sadowska, J., Johansson, B., Johannessen, E., Friman, R., Bronlarz-Press, L., Rosenholm, J. B., Characterization of ozonated vegetable oils by spectroscopic and chromatographic methods, *Chemistry and Physics of Lipids*. 2008, *151*, 85-91.

[153] Zieleniewska, M., Leszczynski, M. K., Kuranska, M., Prociak, A., Szczepkowski, L., Krzyowska, M., Ryszkowska, J., Preparation and characterisation of rigid polyurethane foams using a rapeseed oil-based polyol, *Industrial Crops and Products*. 2015, *74*, 887-897.

[154] Pietrzak, K., Kirpluks, M., Cabulis, U., Ryszkowska, J., Effect of the addition of tall oil-based polyols on the thermal and mechanical properties of ureaurethane elastomers, *Polymer Degradation and Stability*. 2014, *108*, 201-211.

[155] Petrovic, Z. S., Wan, X., Bilic, O., Zlatanic, A., Hong, J., Javni, I., Ionescu, M., Milic, J., Degruson, D., Polyols and polyurethanes from crude algal oil, *Journal of the American Oil Chemists Society*. 2013, *90*, 1073-1078.

[156] Tran, P., Graiver, D., Narayan, R., Ozone-mediated polyol synthesis from soybean oil, *Journal of the American Oil Chemists Society*. 2005, *82*, 653-659.

[157] Petrovic, Z. S., Guo, A., Javni, I., Cvetkovic, I., Hong, D. P., Polyurethane networks from polyols obtained by hydroformylation of soybean oil, *Polymer International*. 2008, *57*, 275-281.

[158] Petrovic, Z. S., Cvetkovic, I., Hong, D., Wan, X., Zhang, W., Abraham, T. W., Malsam, J., Vegetable oil-based triols from hydroformylated fatty acids and polyurethane elastomers, *European Journal of Lipid Science and Technology*. 2010, *112*, 97-102.

[159] Vanbesien, T., Hapiot, F., Monflier, E., Hydroformylation of vegetable oils and the potential use of hydroformylated fatty acids, *Lipid Technology*. 2013, *25*, 175-178.

[160] Tanaka, R., Hirose, S., Hatakeyama, H., Preparation and characterization of polyurethane foams using a palm oil-based polyol, *Bioresource Technology*. 2008, *99*, 3810-3816.

[161] Dai, H., Yang, L., Lin, B., Wang, C., Shi, G., Synthesis and characterization of the different soy-based polyols by ring opening of epoxidized soybean oil with methanol, 1,2-ethanediol and 1,2-propanediol, *Journal of the American Oil Chemists Society*. 2009, *86*, 261-267.

[162] Xu, J., Jiang, J., Li, J., Preparation of polyester polyols from unsaturated fatty acid, *Journal of Applied Polymer Science*. 2012, *126*, 1377-1384.

[163] Ahmad Syafiq, A. H., Aung, M., Luqman Chuah, A., Mek Zah, S., Mohd Hilmi, M., Producing Jatropha oil-based polyol via epoxidation and ring opening, *Industrial Crops and Products*. 2013, *50*, 563-567.

[164] Rojek, P., Prociak, A., Effect of different rapeseed-oil-based polyols on mechanical properties of flexible polyurethane foams, *Journal of Applied Polymer Science*. 2012, *125*, 2936-2945.

[165] Meher, L. C., Sagar, D. V., Naik, S. N., Technical aspects of biodiesel production by transesterification: a review, *Renewable & Sustainable Energy Reviews*. 2006, *10*, 248-268.

[166] Holser, R. A., Transesterification of epoxidized soybean oil to prepare epoxy methyl esters, *Industrial Crops and Products*. 2008, *27*, 130-132.

[167] Ionescu, M.: Polyols from renewable resources-oleochemical polyols, in: Chemistry and technology of polyols for polyurethanes, RAPRA Technology, United Kongdom 2005, pp. 435-470.

[168] Petrovic, Z. S., Polyurethanes from vegetable oils, *Polymer Reviews*. 2008, *48*, 109-155.

[169] Habibi, Y., Lucia, L. A., Rojas, O. J., Cellulose nanocrystals: Chemistry, self-assembly, and applications, *Chemical Reviews*. 2010, *110*, 3479-3500.

[170] Wik, V. M., Aranguren, M. I., Mosiewicki, M. A., Castor oil-based polyurethanes containing cellulose nanocrystals, *Polymer Engineering and Science*. 2011, *51*, 1389-1396.

[171] Marcovich, N. E., Auad, M. L., Bellesi, N. E., Nutt, S. R., Aranguren, M. I., Cellulose micro/nanocrystals reinforced polyurethane, *Journal of Materials Research*. 2006, *21*, 870-881.

[172] Pei, A., Malho, J. M., Ruokolainen, J., Zhou, Q., Berglund, L. A., Strong nanocomposite reinforcement effects in polyurethane elastomer with low volume fraction of cellulose nanocrystals, *Macromolecules*. 2011, *44*, 4422-4427.

[173] Kong, X., Zhao, L., Curtis, J. M., The preparation of polyurethane nanocomposite materials incorporating biobased polyols and reinforced with a low fraction of cellulose nanocrystals. *Carbohydrate Polymers*. (Submitted), 2016.

[174] Curtis, J. M., Kong, X., Zhao, L., Homogenous cellulose nanocrystals - diols suspension and its reinforced polyurethane nanocomposites. 2015, U.S. Provisional Patent Application 62/211,119.

[175] Wu, Q., Henriksson, M., Liu, X., Berglund, L. A., A high strength nanocomposite based on microcrystalline cellulose and polyurethane, *Biomacromolecules*. 2007, *8*, 3687-3692.

[176] Xue, B. L., Wen, J. L., Zhu, M. Q., Sun, R. C., Lignin-based polyurethane film reinforced with cellulose nanocrystals, *Rsc Advances*. 2014, *4*, 36089-36096.

[177] Park, S. H., Oh, K. W., Kim, S. H., Reinforcement effect of cellulose nanowhisker on bio-based polyurethane, *Composites Science and Technology*. 2013, *86*, 82-88.

APPENDIX 1

Polyurethanes with High Mechanical Properties Synthesized from Flax and Canola Oils Polyols

1A.1 Introduction

Polyurethanes can be synthesized from polyols and di-isocyanates through the reaction of hydroxyl groups with isocyanates resulting in the formation of cross linkages and development of a network. PU is used in wide range of applications including flexible and rigid foams, elastomers, coating, adhesives and sealants [1]. Vegetable oil-based polyols are materials with a high renewable content that can be used in making PU. The mechanical and thermal properties of a PU are largely dependent on the structure, hydroxyl value (OHV), and positions of the hydroxyl groups in polyols used for the preparation of the PU [2]. A polyol with a high OHV can lead to the formation of a high amount of crosslinking upon the reaction with isocyanate groups and hence, a PU with enhanced mechanical properties. It has been also reported that the mechanical properties of a PU can be significantly enhanced by the dispersion of a low fraction of cellulose nanocrystals (CNC) into the polymer [3-9]. For example, Young's modulus and tensile strength of castor oil-based PU has been from 472.5 MPa and 27.6 MPa to 682.9 MPa and 31.2 MPa, respectively, by incorporating 1% CNC [4]. Another example is the reinforcement of PU prepared from poly (tetramethylene glycol) by incorporating 0.5, 1.0, and 5.0 % w/w CNC [6]. It has been reported that the incorporation of 5.0% w/w CNC has increased Young's modulus from 8.2 to 44.9 MPa

and tensile strength from 7.5 to 49.8 MPa [6]. This reinforcement effect has been related to the high aspect ratio of CNC and hydrogen bonding interactions between nanocrystals [3] .

In this Chapter, canola and flax oil-based polyols that were synthesized through the routes described in Chapter 7 were used to prepare PU samples. Young's modulus, tensile strength, elongation at break, and glass transition temperatures (T_g) of these PU samples were measured and compared to each other. Additionally, the effect of the incorporation of CNC, at the levels of 0.25 and 0.5% (w/w), on the mechanical properties and T_g of PUs were investigated.

1A.2 Experimental

1A.2.1 Materials

Diphenylmethylene diisocyanate (MDI, Mondur MRS) was supplied by Bayer Corporation (Pittsburgh, PA, USA). Cellulose nanocrystals (with 100-200 nm in length and prepared from softwood by sulfuric acid hydrolysis [10]) dispersed in water (10.2% w/w) were obtained from Alberta Innovates Technologies Futures (Edmonton, AB, Canada).

1A.2.2 Polyol Synthesis

Flax oil was converted to polyol through three routes as described in Chapter 7. These routes were:

A) Flax oil→ fatty acid methyl esters (FAME) of flax→ epoxidation → ring opening by 1,3-propanediol→ flax FAME-polyol **A**,

B) Flax oil → epoxidation → transesterification with methanol → ring opening with 1,3-propanediol → flax FAME- polyol **B**,

C) Flax oil → epoxidation → transesterification with 1,3-propanediol → ring opening with 1,3-propanediol → flax oil- polyol **C**.

Route C) was also used to synthesize polyol from canola oil (canola oil- polyol **C**).

1A.2.3 Incorporation of CNC into Polyols

A suspension of 10.2% w/w CNC in water, as received, was further diluted in a glass flask with water to a final concentration of 5 % (w/w). After mixing for ~5 min, 1,3-propanediol (calculate amount for the final concentration of 5% CNC in 1,3-propanediol after removing water) was added to the suspension and the resulting mixture was vigorously shaken by hand for another 5 min to fully disperse 1,3-propanediol in CNC-in-water dispersion. The water present in the mixture was then removed using a rotary evaporator at 60 ºC under vacuum until the weight of solution reached to a constant weight to yield a dispersion of CNC in 1,3-propanediol (5% w/w) [10].

In the next step, the CNC in 1,3-propanediol dispersion was mixed with polyol using an overhead mechanical stirrer at 350 rpm for about 1 h at 60 ºC. Finally, the 1,3-propanediol was removed to leave a dispersion of CNC in polyol using a wiped film evaporator (WFE) at low pressure (< 0.0001 mbar). The polyol-CNC dispersions produced were sealed and stored in a desiccator to avoid moisture absorption [10].

1A.2.4 Polyurethane Preparation

A NCO/OH ratio of 1.1/1.0 was used to synthesize 15 g of PU from polyol and pMDI. The calculated amounts of polyol and pMDI were weighed in a plastic container and blended thoroughly for about 2 min and then the blend was transferred to a hexagonal plastic mold (12 cm diameter) and placed in a vacuum oven at a temperature of 50 ºC and pressure of 2.66×10^3 Pa. for 8-15 min to remove bubbles. Then, while the blend was still in liquid form, the vacuum was broken by introducing air to the oven to avoid deformation of the PU sample. The PU sample was

allowed to stay at room temperature for about 4 h and before becoming hard, it was cut by ASTM D638 Type V cutter into the pieces needed for tensile strength test. The sample pieces were cured for ~24 h at 50 ºC and post-cured for another 24 h at 100 ºC.

1A.2.5 Characteristics of Polyurethane

1A.2.5.1 Glass Transition Temperature (T_g)

A DSC Q100 (TA Instruments, DE, USA) instrument, equipped with a cooling system was used to perform Modulated Differential Scanning Calorimetry (MDSC) measurement according to the ASTM E1356-03 standard method. To erase the thermal history, samples were heated from 25 to 165 ºC at a rate of 10ºC/min and then cooled down to -20 ºC at a rate of 5 ºC/min. A modulation amplitude of 1 ºC/min and a modulation period of 60 s at a heating rate of 2 ºC/min to 200 ºC were applied to perform MDSC. The heating data of the second heating stage was analyzed.

1A.2.5.2 Mechanical Properties

To measure the mechanical properties, specimens were cut out from PU samples by an ASTM D638 Type V cutter and then tested at room temperature by an Instron (MA, USA) tensile testing machine (model 4202) equipped with a 500 kgf load cell at a cross head speed of 100 mm/min (according to ASTM D638 standard). Five measurements were performed for each sample and averaged.

1A.3 Results and Discussion

Glass transition temperature (T_g) and mechanical properties of PU samples are presented in Table 1A-1. A higher density of cross-linking in a polymeric network results in a higher T_g and Young's modulus [11]. Amongst the PU samples tested, the one incorporating flax- polyol $_{\text{route C}}$

showed the highest T_g (117.6 ºC), tensile strength (80.8 MPa), Young's modulus (2008 MPa) and elongation at break (7.2 %).

As seen in Table 1A-1 canola oil-PU compared to flax oil-PU was found to have a lower T_g, Young's modulus and tensile strength. The higher T_g and mechanical properties of flax oil-PU can be explained by the higher OHV of flax oil-polyol which results in the formation of more highly cross-linked PU.

Table 1A-1 mechanical properties and glass-transition temperature of polyurethanes (PU) produced from different polyols incorporated with cellulose nanocrystal (CNC).

PU sample	Young's modulus (MPa)	Tensile strength (MPa)	Elongation at break (%)	Glass transition (ºC)
Flax FAME - PU $_{\text{route A}}$				
0%- CNC	1860 ± 60	66 ± 4.0	4.5 ± 0.3	92.9 ± 0.3
0.25%- CNC	1960 ± 60	66 ± 2.0	5.5 ± 0.6	94.1 ± 0.1
0.5%- CNC	1950 ± 50	69 ± 1.0	5.1 ± 0.1	94.6 ± 0.1
Flax oil - PU $_{\text{route B}}$				
0%- CNC	1936 ± 25	68.6 ± 0.7	6.3 ± 0.1	107.3 ± 1.58
0.25%- CNC	1854 ± 34	74.4 ± 4.0	6.6 ± 0.4	107.2 ± 1.2
0.5%- CNC	1886 ± 42	69.8 ± 1.5	5.7 ± 0.4	106.0 ± 0.8
Flax oil - PU $_{\text{route C}}$				
0%- CNC	2008 ± 21	80.8 ± 0.1	7.2 ± 0.4	117.6 ± 0.6
0.25%- CNC	1823 ± 25	78.4 ± 0.5	6.6 ± 0.2	118.8 ± 0.8
0.5%- CNC	1748 ± 23	73.4 ± 1.32	6.2 ± 0.1	116.3 ± 0.9
Canola oil - PU $_{\text{route C}}$				
0%- CNC	1770 ± 40	62.0 ± 1.6	5.3 ± 0.2	86.8 ± 1.6
0.25%- CNC	1729 ± 50	59.7 ± 0.2	6.0 ± 0.3	87.0 ± 1.2
0.5%- CNC	1820 ± 34	61.2 ± 0.3	5.7 ± 0.2	87.5 ± 0.8

APPENDIX 1

The chemical structure of Flax FAME polyols is different from flax and canola oil polyols. In fact, the monomers of FAME polyols still contain some methyl ester groups on the fatty acid chain while monomers of flax and canola oils polyols $_{\text{route C}}$ are hydroxypropyl esters, which have a free OH group at their terminus. This free OH group can form a cross-link upon reaction with isocyanate and hence, increase the rigidity of the network. In contrast, due to the absence of OH group at the terminus in FAME polyols, these ends remain free and flexible and can act as a plasticizer. In general, it is believed that the mechanical properties and T_g of PU samples are primarily affected by the density of the crosslinking whereas the position of the OH groups in polyols has less effect [2].

Most of the studies, on the effect of the incorporation of CNC into polymers, have reported that the T_g of the polymers is not affected by the addition of CNC. There are only a few cases in which the T_g of a polymer changed by the addition of CNC into the polymer [3]. In contrast, it has often been reported that the incorporation of CNC into PU improves the mechanical properties of the PU [4-6].

The results presented in this Chapter showed that the mechanical properties and T_g of PUs were not significantly improved ($p < 0.05$) by the incorporation of CNC. Only a small increment was observed for the T_g of Flax FAME - PU $_{\text{route A}}$ containing 0.25 and 0.5% CNC (Table 1A-1). However, the PUs prepared in this study, even in their pure state (no CNC), had very high Young's modulus and tensile strength.

In order to improve the mechanical properties of a PU by CNC, a complete dispersion of CNC into the PU is critical. In this work, the incorporation of CNC into the polyols was performed according to a procedure developed in our lab [10,12]. The efficiency of this procedure in dispersing CNC into canola polyol-based PU was confirmed in other work by a Transmission

Electron Microscopy (TEM) image taken from a cross section of the PU sample. The suspensions of CNC in flax polyols, described in this Chapter, were transparent similar to suspension of CNC in canola polyol and remained clear after 4 weeks consistent with the formation of stable nanodispersion.

1A.4 Conclusion

In this Chapter, PUs were prepared from the polyols produced from canola and flax oil through various routes (Chapter 7). The measurement of some of the mechanical properties and T_g of these PUs showed that the flax polyol produced through the epoxidation, transesterification with 1,3-propanediol, and ring opening by 1,3-propanediol (route **C**) resulted in a PU with the highest mechanical properties and T_g among the polyols. Although, the incorporation of 0.25 and 0.5% CNC into PUs did not improved the mechanical properties of the PUs, the PUs with no CNC had very high mechanical properties. This short study was a preliminary work and further studies can be performed to investigate the effect of incorporation of CNC on the properties of PU. For example, TEM image of the PU nanocomposites can be prepared to evaluate further the dispersion of CNC in PUs. In addition, PU samples can be tested for the abrasion resistance to study the effect of the incorporation of CNC on the abrasion resistance of PU.

1A.5 References

[1] Petrovic, Z. S., Polyurethanes from vegetable oils, *Polymer Reviews*. 2008, *48*, 109-155.

[2] Zlatanic, A., Lava, C., Zhang, W., Petrovic, Z. S., Effect of structure on properties of polyols and polyurethanes based on different vegetable oils, *Journal of Polymer Science Part B: Polymer Physics*. 2004, *42*, 809-819.

[3] Habibi, Y., Lucia, L. A., Rojas, O. J., Cellulose nanocrystals: Chemistry, self-assembly, and applications, *Chemical Reviews*. 2010, *110*, 3479-3500.

[4] Wik, V. M., Aranguren, M. I., Mosiewicki, M. A., Castor oil-based polyurethanes containing cellulose nanocrystals, *Polymer Engineering and Science*. 2011, *51*, 1389-1396.

[5] Marcovich, N. E., Auad, M. L., Bellesi, N. E., Nutt, S. R., Aranguren, M. I., Cellulose micro/nanocrystals reinforced polyurethane, *Journal of Materials Research*. 2006, *21*, 870-881.

[6] Pei, A., Malho, J.-M., Ruokolainen, J., Zhou, Q., Berglund, L. A., Strong nanocomposite reinforcement effects in polyurethane elastomer with low volume fraction of cellulose nanocrystals, *Macromolecules*. 2011, *44*, 4422-4427.

[7] Wu, Q., Henriksson, M., Liu, X., Berglund, L. A., A high strength nanocomposite based on microcrystalline cellulose and polyurethane, *Biomacromolecules*. 2007, *8*, 3687-3692.

[8] Xue, B. L., Wen, J. L., Zhu, M. Q., Sun, R. C., Lignin-based polyurethane film reinforced with cellulose nanocrystals, *Rsc Advances*. 2014, *4*, 36089-36096.

[9] Park, S. H., Oh, K. W., Kim, S. H., Reinforcement effect of cellulose nanowhisker on bio-based polyurethane, *Composites Science and Technology*. 2013, *86*, 82-88.

[10] Kong, X., Zhao, L., Curtis, J. M., The preparation of polyurethane nanocomposite materials incorporating biobased polyols and reinforced with a low fraction of cellulose nanocrystals, *Carbohydrate Polymers*. 2016, *152*, 487-495.

[11] Kong, X., Liu, G., Curtis, J. M., Novel polyurethane produced from canola oil based poly(ether ester) polyols: Synthesis, characterization and properties, *European Polymer Journal*. 2012, *48*, 2097-2106.

[12] Curtis, J. M., Kong, X., Zhao, L., Homogenous cellulose nanocrystals - diols suspension and Its reinforced polyurethane nanocomposites. 2015, U.S. Provisional Patent Application 62/211,119.

APPENDIX 2

Figure 2A-1 Flax (left) and canola (right) oils (at room temperature).

Figure 2A-2 Epoxidized Flax (left) and epoxidized canola (right) oils (at room temperature). Epoxidized canola oil crystalizes after few days.

Figure 2A-3 Polyols produced from flax and canola oils, from left to right: canola oil polyol route **C**, flax oil polyol route **C**, flax polyol route **B**, and flax fame polyol route **A**, See Figure 7-2.

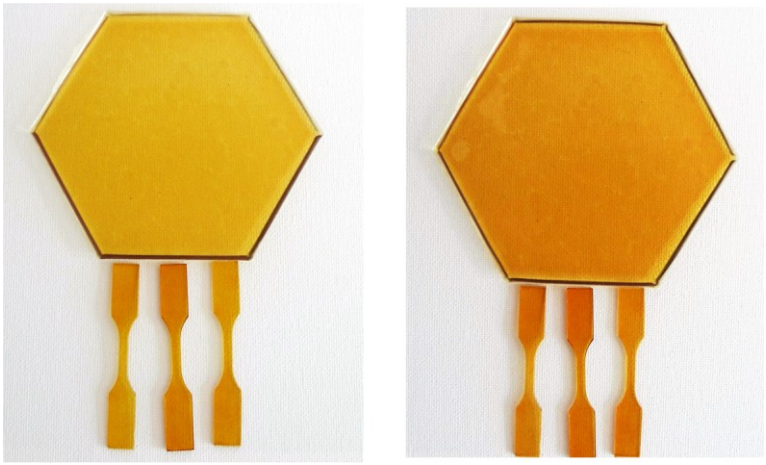

Figure 2A-4 Polyurethanes prepared from flax oil polyol route **C** (left) and canola oil polyol route **C**. Polyurethanes prepared form flax oil polyols routes A and B as well as nanocomposite polyurethanes had similar appearance to these polyurethanes. See Appendix 1.

Figure 2A-5 Ozone generator, image from http://lipid.ualberta.ca

Figure 2A-6 Wiped Film Evaporator (WFE), image from http://lipid.ualberta.ca

Figure 2A-7 Bomem FTIR spectrometer

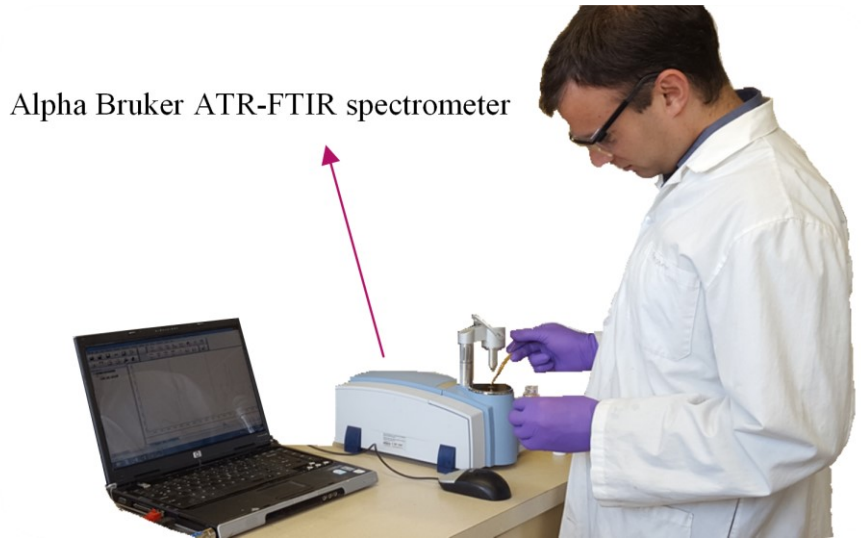

Figure 2A-8 Alpha Bruker ATR-FTIR spectrometer, person in photo: M. Hossein Tavassoli-Kafrani.